UNIVERSITY OF CALGARY

Predicting Water-In-Oil Emulsion Coalescence From Surface Pressure Isotherms

by

Patricia Isabel Urrutia

A THESIS

SUBMITTED TO THE FACULTY OF GRADUATE STUDIES

IN PARTIAL FULFILMENT OF THE REQUIREMENTS FOR THE

DEGREE OF MASTER IN SCIENCE

DEPARTMENT OF CHEMICAL AND PETROLEUM ENGINEERING

CALGARY, ALBERTA

DECEMBER, 2006

UNIVERSITY OF CALGARY

FACULTY OF GRADUATE STUDIES

The undersigned certify that they have read, and recommend to the Faculty of Graduate Studies for acceptance, a thesis entitled " Predicting Water-In-Oil Emulsion Coalescence From Surface Pressure Isotherms " submitted by Patricia I. Urrutia in partial fulfilment of the requirements of the degree of Master in Science.

Supervisor, Dr. H. W. Yarranton
Department of Chemical and Petroleum Engineering

Dr. B. Maini
Department of Chemical and Petroleum Engineering

Dr. M. Husein
Department of Chemical and Petroleum Engineering

Dr. R. Hugo
Department of Mechanical & Manufacturing Engineering

Date

Abstract

Stable water-in-crude oil emulsions are spontaneously formed during oil production when oil and water are stirred together and naturally occurring surfactants such as asphaltenes, resins and clays are also present. The surfactants stabilize these emulsions by forming highly viscous or rigid films at the oil-water interface. For economical and operational reasons, water-in-crude oil emulsions need to be destroyed in order to recover both oil and water phases. To develop more effective emulsion treatments it is necessary to have a better understanding of the factors that affect emulsion stability.

Asphaltenes play an important role in the stability of water-in-oil emulsions because they irreversibly adsorb at surface of the water droplets and form a rigid film (skin). One hypothesis is that the coalescence of these emulsions depends on the compressibility of this asphaltene film. In this work, a new experimental technique was developed to determine the compressibility of asphaltene monolayers from surface pressure isotherms measured with an IT Concept axisymetric drop shape analyzer. Surface isotherms show the relationship between interfacial tension and interfacial area and reflect the compressibility and "phase behavior" of interfacial film.

A droplet of a solution of asphaltenes, *n*-heptane and toluene was formed and aged at the tip of a capillary in an aqueous medium. Then fluid was withdrawn to decrease the surface area of the drop and compress the interfacial film. The compression was done in steps at intervals of approximately 20 seconds and at each step, time, surface pressure,

area and volume data was collected. Surface pressure was plotted versus film ratio, where the film ratio is the fraction of the droplet surface area at a given compression to that of the original drop.

The effects of asphaltene concentration, solvent, and aging time on the film properties were determined. Irreversibly adsorbed films were observed to form rapidly at all asphaltene concentrations and rigid films form least rapidly at intermediate asphaltene concentration (10 kg/m^3). A "phase change" from a compressible film to an almost incompressible film occurred upon compression in most cases. At sufficient compression, the film became completely incompressible and crumpled. The film ratio at which the "phase change" occurs, increases in poorer solvent and as the interface is aged.

The coalescence rates of model emulsions, consisting of asphaltenes, toluene, *n*-heptane, and water, were determined from the change in the mean drop diameter over time. A correlation between the initial coalescence rate and the initial compressibility of the asphaltene film was found. The measured mean droplet diameter of the coalescing emulsion was then predicted over time from the film compressibilities, accounting for aging time and the change film ratio as the emulsion coalesced.

Acknowledgements

I would like to express my sincere gratitude and thanks to my supervisor, Dr. H.W. Yarranton for his excellent guidance, encouragement and valuable advice during my Master's degree program. I also wish to thank Ms. Elaine Stasiuk for her assistance and the great help that she provided during the experimental work.

I would like to thank Dr. Danuta Sztukowski and Ms. Maryam Jafari for teaching me the experimental techniques. I also would like to acknowledge Dr. Alain Cagna for his technical support.

I wish to thank Syncrude Canada Ltd. for providing the bitumen samples for the experimental measurements and for the financial support.

I am thankful to the Department of Chemical and Petroleum Engineering of The University of Calgary for their financial support and to the administrative and technical staff for all their help throughout the duration of my studies.

I am grateful to the Asphaltene and Emulsion Research members at the University of Calgary, and fellow graduate students for their useful suggestions.

Finally, I would like to thank my family and friends for their constant encouragement throughout my postgraduate education.

Table of Contents

Approval Page ii
Abstract iii
Acknowledgements v
Table of Contents vi
List of Tables viii
List of Figures x
List of Symbols xiv

CHAPTER 1- INTRODUCTION 1
1.1 Objectives 3
1.2 Thesis Structure 4

CHAPTER 2- LITERATURE REVIEW 6
2.1 Emulsion Stability 7
2.1.1 Emulsifying Agents 7
2.1.2 Emulsion Stability Mechanisms 9
2.1.3 Emulsion breakdown mechanisms 12
2.1.3.1 Ostwald ripening 12
2.1.3.2 Aggregation 13
2.1.3.3 Sedimentation 13
2.1.3.4 Coalescence 14
2.2 Petroleum Terminology 16
2.2.1 Bitumen Characterization 17
2.2.2 Asphaltenes 21
2.2.2.1 Asphaltene Chemical Composition and Structure 23
2.2.2.2 Asphaltene Molecular Mass 25
2.2.3 Asphaltene Self-Association 27
2.2.4 Asphaltene Surface Activity 28
2.3 Crude Oil Emulsions 30
2.3.1 Asphaltene Film Properties 33
2.4 Chapter Summary 38

CHAPTER 3- EXPERIMENTAL METHODS 40
3.1 Materials 41
3.1.1 Asphaltenes-Solids Precipitation 41
3.1.2 Solids Removal 42
3.2 Surface Pressure Isotherm Experiments 43
3.2.1 Principles of Drop Shape Analysis 44
3.2.2 Preparation of Drop Shape Analyzer 49
3.2.3 Solvent-Water Interfacial Tension 51

3.2.4 Surface Pressure Isotherm Experimental Procedure 53
3.2.5 Comparison with Literature Data 58

CHAPTER 4- INTERFACIAL PROPERTIES EVALUATION BY SURFACE PRESSURE ISOTHERMS 60
4.1 Interfacial Compressibility 60
4.2 Effect of Asphaltene Concentration 66
4.3 Effect of Solvent 70
4.4 Effect of Aging Time 74
4.5 Effect of Temperature 79

CHAPTER 5- COALESCENCE PREDICTION BY INTERFACIAL PROPERTIES 83
5.1 Coalescence Rate of Model Emulsions 83
5.2 Correlation of Coalescence Rate and Interfacial Compressibility 88
5.3 Prediction of Emulsion Coalescence 89

CHAPTER 6- CONCLUSIONS AND RECOMENDATIONS 101
6.1 Thesis Conclusions 101
6.2 Recommendations for Future Work 104

REFERENCES 106

APPENDIX A- DILUTED BITUMEN ISOTHERM RESULTS 115
A.1. Effect of Bitumen Dilution 115
A.2. Effect of Aging Time 118
A.3. Effect of Solvent 119

APPENDIX B- REPRODUCIBILITY ANALYSIS 121
B.1. Interfacial Tension 122
B.2. Phase 1 Compressibility 122
B.3. Phase 2 Compressibility 124
B.4. Phase Change Film Ratio 126
B.5. Crumpling Film Ratio 128

List of Tables

Table 2.1 UNITAR Crude Oil Classification 17

Table 2.2 SARA Analysis of Bitumens (Akbarzadeh et al. 2004a) 19

Table 2.3 Effect of Extraction Method on Asphaltene Properties. (Alboudwarej et al. 2002) 23

Table 2.4 Average molecular weights of asphaltenes by different experimental methods (Moschopedis et al. 1976) 26

Table 2.5 Examples of Emulsions in the Petroleum Industry (Schramm, 1992) 31

Table 3.1 Asphaltene and Solids content of Athabasca Bitumen 43

Table 3.2 Interfacial tensions of solvents against water 50

Table 3.3 Interfacial tensions of different heptol mixtures against water 51

Table 4.1 Interfacial compressibilities, phase change film ratio, and crumpling film ratio for droplets of asphaltenes in toluene surrounded by water at 23°C. 64

Table 4.2 Interfacial compressibilities, phase change film ratio, and crumpling film ratio for droplets of asphaltenes in 25/75 heptol surrounded by water at 23°C. 65

Table 4.3 Interfacial compressibilities, phase change film ratio, and crumpling film ratio for droplets of asphaltenes in 50/50 heptol surrounded by water at 23°C. 66

Table 5.1 Mean Drop Diameters for different aging times and emulsion systems (Sztukowski 2005). 84

Table B.1 Reproducibility analysis for phase 1 compressibility data in pure toluene with a confidential interval of 90%. 122

Table B.2 Reproducibility analysis for phase 1 compressibility data in 25/75 heptol with a confidential interval of 90%. 123

Table B.3 Reproducibility analysis for phase 1 compressibility data in 50/50 heptol with a confidential interval of 90%. 123

Table B.4 Reproducibility analysis for phase 2 compressibility data in pure toluene with a confidential interval of 90%. 124

Table B.5 Reproducibility analysis for phase 2 compressibility data in 25/75 heptol with a confidential interval of 90%. 125

Table B.6 Reproducibility analysis for phase 2 compressibility data in 50/50 heptol with a confidential interval of 90%. 125

Table B.7 Reproducibility analysis for phase change film ratio data in pure toluene with a confidential interval of 90%. 126

Table B.8 Reproducibility analysis for phase change film ratio data in 25/75 heptol with a confidential interval of 90%. 127

Table B.9 Reproducibility analysis for phase change film ratio data in 50/50 heptol with a confidential interval of 90%. 127

Table B.10 Reproducibility analysis for crumpling film ratio data in pure toluene with a confidential interval of 90%. 128

Table B.11 Reproducibility analysis for crumpling film ratio data in 25/75 heptol with a confidential interval of 90%. 129

Table B.12 Reproducibility analysis for crumpling film ratio data in 50/50 heptol with a confidential interval of 90%. 129

List of Figures

Figure 2.1 Surfactants associations in O/W emulsion (Schramm 2005) 8

Figure 2.2 Micellization of surfactant molecules..... 9

Figure 2.3 Illustration of steric stabilization of water droplets due to polymer adsorption..... 10

Figure 2.4 Demulsification mechanisms (Lyklema 2005)..... 12

Figure 2.5 Visual observation of free water and rag layer after 6 hours of settling (Hirasaki et. al. 2006)..... 14

Figure 2.6 Coalescence Mechanism (Heimenz and Rajagopalan 1997)..... 15

Figure 2.7 SARA fractionation scheme 20

Figure 2.8 Hypothetical asphaltene molecule (Strausz et al. 1992)..... 25

Figure 2.9 Before (a) and after (b) deflating an emulsion drop using a micropipette (Yeung et al. 1999).. 34

Figure 2.10 Skin observation after droplet retraction (Taylor 1992)..... 34

Figure 3.1 Drop Shape Analyzer Configuration. 45

Figure 3.2 Drop Shape Analyzer image of a droplet of asphaltene and solvent in distilled water. 46

Figure 3.3 Definition of coordinates for describing a pendant droplet with an axis of symmetry..... 47

Figure 3.4 Comparison of experimental and theoretical heptol-water interfacial tension values at different toluene volume fractions (ϕ)..... 52

Figure 3.5 Image of a droplet of 1 kg/m^3 asphaltenes in toluene surrounded by water at one hour of aging time and 23 °C: (a) before crumpling and (b) after crumpling. 54

Figure 3.6 (a) Interfacial Tension vs. Surface area plot for 1 kg/m^3 of asphaltenes in pure toluene vs. water at 60 minutes of aging time and at 23 °C.. 55

Figure 3.7 Interfacial tension versus time for 1.0 kg/m³ asphaltenes in toluene 57

Figure 3.8 Comparison of different isotherms for 1 kg/m^3 asphaltenes in toluene at time intervals of zero, two and five minutes. 58

Figure 3.9 Comparison of surface pressure isotherms of asphaltene films with similar Zhang et al. (2003) Langmuir trough experiments. 59

Figure 4.1 Detection of low compressibility film formation in semilog coordinates for a) 1 kg/m³ asphaltenes in pure toluene at 10 min of aging time and 23 °C b) 1 kg/m³ asphaltenes in pure toluene at 60 min of aging time and 23 °C. 62

Figure 4.2 Effect of asphaltene concentration on surface pressure isotherms in pure toluene at 60 minute aging time and 23 °C. 67

Figure 4.3 Effect of asphaltene concentration on surface pressure isotherms in 25/75 heptol at 60 minute aging time and 23 °C. 68

Figure 4.4 Effect of asphaltene concentration on surface pressure isotherms in 50/50 heptol at 60 minute aging time and 23 °C. 69

Figure 4.5 Effect of solvent on surface pressure isotherms for 1 kg/m³ asphaltenes after 60 minutes of aging time at 23 °C. 71

Figure 4.6 Effect of solvent on surface pressure isotherms for 10 kg/m³ asphaltenes after 60 minutes of aging time at 23 °C. 72

Figure 4.7 Effect of solvent on surface pressure isotherms for 20 kg/m³ asphaltenes after 60 minutes of aging time at 23 °C. 73

Figure 4.8 Effect of aging time on surface pressure isotherms for 1 kg/m³ asphaltenes on pure toluene at 23 °C. 75

Figure 4.9 Effect of aging time on surface pressure isotherms for 10 kg/m³ asphaltenes on pure toluene at 23 °C. 76

Figure 4.10 Effect of aging time on surface pressure isotherms for 20 kg/m³ asphaltenes on pure toluene at 23 °C. 77

Figure 4.11 Effect of aging on the film ratio at which low compressibility film forms. . 78

Figure 4.12 Effect of temperature on surface pressure isotherms for 1 kg/m³ asphaltenes in a) toluene, b) 25/75 heptol, c) 50/50 heptol over water at both 23 and 60 °C for different aging times..... 80

Figure 4.13 Effect of temperature on surface pressure isotherms for 10 kg/m³ asphaltenes in a) toluene, b) 25/75 heptol over water at both 23 and 60 °C for different aging times 81

Figure 4.14 Effect of temperature on surface pressure isotherms for 20 kg/m³ asphaltenes in toluene over water at both 23 and 60 °C for different aging times. .. 82

Figure 5.1 Effect of aging time on a) the inverse square of the mean drop diameter and b) the calculated rupture rate for emulsions prepared from water and solutions of asphaltenes in toluene at 23 °C 86

Figure 5.2 Effect of aging time and/or solvent on a) the inverse square of the mean drop diameter and b) rupture rate of emulsions prepared from water and solutions of 10 kg/m³ asphaltenes in heptol at 23 °C..... 87

Figure 5.3 Correlation between initial rupture rate (1.5 hours of aging) and initial interfacial compressibility (60 minutes of aging) for 5,10, and 20 kg/m³ asphaltenes in toluene, 25/75 and 50/50 heptol at 23 °C. 89

Figure 5.4 Effect of aging time on the phase transition and crumpling film ratios for 20 kg/m³ asphaltenes in 25/75 heptol at 23 °C. 90

Figure 5.5 Effect of aging time on the Phase 1 and Phase 2 interfacial compressibilities for 20 kg/m³ asphaltenes in 25/75 heptol at 23 °C..... 91

Figure 5.6 Schematic of the procedure to determine the interfacial compressibility and coalescence rate of an emulsion with an irreversibly adsorbed interfacial film. 94

Figure 5.7 Predicted change in interfacial compressibility (a) and mean droplet diameter (b) of a coalescing emulsion prepared from water and a solution of 20 kg/m³ asphaltenes in 25/75 heptol at 23 °C. 96

Figure 5.8 Predicted change in interfacial compressibility (a) and mean droplet diameter (b) of a coalescing emulsion prepared from water and a solution of 20 kg/m³ asphaltenes in toluene, 25/75 heptol and 50/50 heptol at 23 °C. 98

Figure 5.9 Predicted change in interfacial compressibility (a) and mean droplet diameter (b) of a coalescing emulsion prepared from water and a solution of 10 kg/m³ asphaltenes in toluene, 25/75 heptol and 50/50 heptol at 23 °C. 99

Figure 5.10 Predicted change in interfacial compressibility (a) and mean droplet diameter (b) of a coalescing emulsion prepared from water and a solution of 5 kg/m³ asphaltenes in toluene, 25/75 heptol and 50/50 heptol at 23 °C. 100

Figure A.1 Effect of bitumen dilution with pure toluene on surface pressure isotherms after 60 minutes of aging time at 23 °C. 115

Figure A.2 Effect of dilution on bitumen dissolved with 25/75 heptol on surface pressure isotherms after: (a) 60 minutes and (b) 30 minutes of aging time, at 23 °C. 116

Figure A.3 Effect of dilution on bitumen dissolved with 50/50 heptol on surface pressure isotherms after: (a) 60 minutes and (b) 30 minutes of aging time, at 23 °C. 117

Figure A.4 Effect of aging time on surface pressure isotherms for different bitumen to solvent ratios, dissolved in pure toluene at 23 °C: (a) 1:9, (b) 1:7, (c) 1:5, (d) 1:3. 118

Figure A.5 Effect of solvent on surface pressure isotherms for 1:9 bitumen to solvent ratio at 23 °C, after: (a) 60 minutes, (b) 30 minutes and (c) 10 minutes of aging time. 119

Figure A.6 Effect of solvent on surface pressure isotherms for 1:3 bitumen to solvent ratio at 23 °C, after: (a) 60 minutes, (b) 30 minutes and (c) 10 minutes of aging time. 120

List of Symbols

A	interfacial area (mm^2)
A_n	surface area per molecule (m^2/molecule)
b	radius of curvature at the apex of a drop
c_I	interfacial compressibility (m/mN)
C_A	asphaltene molar concentration (mol/m^3)
C	bulk surfactant concentration
g	gravity acceleration (9.8 m/s^2)
q	relative adsorption
R	universal gas constant (8.314 J/mol K)
R_1	radius of curvature in x-z plane
R_2	radius of curvature in y-z plane
t	time (hr)
T	absolute temperature (K)
V	dispersed phase volume

Greek symbols

Γ	excess surfactant interfacial concentration ($mmol/m^2$)
γ	interfacial tension (mN/m)
π	surface pressure (mN/m)
ϕ	volumen fraction
Γ_m	Monolayer surface coverage ($mmol/m^2$)
γ^{id}	ideal interfacial tension (mN/m)
Δp	pressure difference between phases (N/m^2)
θ	angle between R_2 and z-axis (°)
ρ	fluid density (kg/m^3)
ω	rupture frequency ($1/\mu m^2$ h)

Subscripts

‘o’	pure or initial
‘1’	component 1
‘2’	component 2
‘12’	component 1 versus component 2
‘A’	dispersed phase
‘B’	continuous phase
‘n’	n^{th} iteration

Abbreviations

‘IFT’	interfacial tension
‘PR’	phase transition
‘CR’	crumpling point

CHAPTER 1- INTRODUCTION

At present, light oil reservoirs are depleting and a need for producing alternative energy sources such as heavy oil or bitumen has emerged to overcome this energy deficit. One potential problem during bitumen production is the formation of water-in-crude oil emulsions. For example, they can be formed during the Clark Hot Water Extraction (CHWE) process to recover bitumen from oil sands.

Water-in-heavy oil emulsions are stable dispersions of water droplets in a continuous oil phase, stabilized by naturally occurring emulsifiers present in the heavy oil. These emulsions are undesirable in the oil industry due to high costs incurred in transportation, corrosion, and operational demands, among other problems. Therefore, emulsions must be treated to separate oil and water phases. Since dewatering of stable water-in-oil emulsions is a continuous challenge to the oil industry, it is necessary to have an understanding of the factors that contribute to emulsion stability in order to design more effective treatments.

Heavy oil contains heavy molecular weight fractions that have surface-active characteristics. It is generally believed that these surface active compounds adsorb in the oil/water interface and form rigid films surrounding the dispersed water droplets and protecting them from coalescence (Freer and Radke 2004; Gafonova and Yarranton 2001; Jones et al. 1978; Kumar et al. 2001; Taylor 1992; Yarranton et al. 2000b; Zhang et al.

2003a). There is strong evidence that asphaltenes are the primary component of these interfacial films (McLean and Kilpatrick 1997; Sun et al. 2003; Taylor et al. 2002).

Asphaltenes are defined as a solubility class, that is, the oil fraction that is soluble in toluene and insoluble in *n*-alkanes, such *n*-pentane or *n*-heptane. They are a complex mixture of polyaromatic compounds, large aliphatic chains with functional groups including heteroatoms such as nitrogen, sulphur, and oxygen. Asphaltenes irreversibly adsorb at the oil/water interface in monolayers (Zhang et al. 2003, Lopetinsky et al. 2005, Sztukowski et al. 2003) where they are confined and self-associate, resulting in a viscoelastic network structure (Agrawala and Yarranton 2001; Spiecker et al. 2003; Sztukowski et al. 2003).

It has been speculated that emulsion stability is related to the properties of these asphaltenic films (Freer and Radke 2004; Gafonova and Yarranton 2001; Jones et al. 1978; Kumar et al. 2001; Taylor 1992; Yarranton et al. 2000b; Zhang et al. 2003a). The rheological properties of the films have been investigated using elasticity measurements (Freer et al. 2003; Jafari 2005; Sztukowski 2005) and surface pressure isotherms (Jones et al.1978; Nordli et al. 1991; Zhang et al. 2003). A surface pressure isotherm shows the relationship between interfacial tension and interfacial area of an asphaltene monolayer undergoing compression. Surface pressure isotherms indicate what type of interfacial phase is present at the interface and, as well be shown in this work, can be used to measure the compressibility of the interfacial film.

One possible explanation of water-in-crude oil emulsion stability is that the coalescence of these emulsions depends on the compressibility of the asphaltene interfacial film. As coalescence occurs in an emulsion, the total interfacial area decreases and an irreversibly adsorbed interfacial film is compressed. Since the adsorbed material cannot desorb, the film compressibility will decrease as the area decreases. As the interface becomes less compressible, there will likely be a greater resistance to coalescence. For example, a lower compressibility interface will likely inhibit droplet deformation and the potential for water bridging between droplets.

It seems likely that there is a link between the coalescence of water-in-oil emulsions and film compressibility when asphaltenes are adsorbed in the interface. However, it has not been evaluated yet. This thesis attempts to relate both concepts and to provide more insight about film formation mechanisms and properties.

1.1 Objectives

To understand how asphaltenes adsorb in the oil/water interface and inhibit emulsion coalescence, this research was divided into two main objectives:

1. To investigate the interfacial properties of asphaltenic films at the oil/water interface using surface pressure isotherms.
2. To predict emulsion coalescence from interfacial properties (i.e. interfacial compressibility).

The specific objectives of this work are the following:

- To develop a new experimental technique to measure surface pressure-film ratio isotherms of an asphaltene monolayer using an IT concept axisymetric drop shape analyzer.
- To measure the effect of asphaltene concentration, temperature, aging time and solvent chemistry on asphaltenic films by surface pressure isotherms.
- To determine the relationship between the film compressibility and emulsion coalescence rates.

1.2 Thesis Structure

This thesis was distributed into six chapters. Chapter 2 presents the fundamental concepts involved in water-in-oil emulsions within the context of their formation in the petroleum industry and focused on an asphaltene perspective. First, basic emulsion stability principles, including information about emulsification processes, surfactants, and the most important emulsion breakdown mechanisms are discussed. Second, the definition and characterization techniques, chemical composition, structure, and behavior of asphaltenes are reviewed. Finally, detailed information on water-in-crude oil emulsions is addressed explaining the main factors that contribute to their stability.

Chapter 3 describes the experimental approach followed to accomplish the thesis objectives. The techniques, instruments and reagents used to extract asphaltenes, to measure their interfacial properties and to build surface pressure isotherms are provided in this chapter.

Chapter 4 presents the interfacial properties of asphaltenic films obtained using surface pressure isotherms. The effects of asphaltene concentration, aging time, solvent ratios and temperature on film formation and properties are evaluated.

Chapter 5 presents emulsion coalescence predictions based on film compressibility accounting for aging time and film ratio change. The methodology followed for construction of the prediction model is given as well.

Chapter 6 summarizes the conclusions of this study and suggests recommendations for further research.

CHAPTER 2- LITERATURE REVIEW

Emulsions are dispersions of two immiscible liquid phases that result from vigorous mixing. They are thermodynamically unstable because they have an excess of interfacial energy due to the large interfacial area. Therefore, a phase separation is naturally favoured or spontaneous. However, emulsions can be stabilized by the addition of surface-active agents or emulsifiers. Surface-active agents concentrate at the interface between the phases and can form a barrier to droplet contact and coalescence.

There are several types of emulsions and they are classified based on which liquid forms the continuous phase:

- Water-in-oil (W/O) emulsions consisting of water droplets dispersed in oil.
- Oil-in-water (O/W) emulsions consisting of oil droplets dispersed in water.
- Complex emulsions; for example, water-oil-water (W/O/W), consisting of water droplets dispersed in oil droplets that are in turn dispersed in water.

Emulsions are found in daily life and many are useful. They are used to transport water-insoluble substances and are encountered in a broad range of industrial products, including food, cosmetics, pharmaceuticals, paints, and lubricants. On the other hand, some emulsions are undesirable. For example, this thesis is concerned with oilfield water-in-oil emulsions. These emulsions cause a variety of operational problems in almost all phases of oil production and must be broken into separate bulk phases.

This chapter reviews general mechanisms of emulsion stability, petroleum chemistry with a focus on surface-active components, and previous work on the stability of oilfield emulsions.

2.1 Emulsion Stability

2.1.1 Emulsifying Agents

A surfactant or surface-active agent is a chemical compound that has a polar (hydrophilic) and nonpolar (lipophilic) molecular structure, e.g., short-chain fatty acids. This double nature provides the compound with an affinity for both polar and nonpolar media. In emulsions, surfactants tend to adsorb at the interface between the two phases, so that the polar part of the molecule resides in the aqueous phase and the non-polar part in the organic phase.

When a surfactant adsorbs on the interface the interfacial tension between the two phases decreases. The reduced interfacial tension depends on the concentration of the surfactant according to the Gibbs' isotherm:

$$\Gamma = -\frac{1}{RT}\frac{\partial \gamma}{\partial \ln C} \qquad \textbf{Eq. 2.1}$$

where Γ is the excess interfacial concentration of surfactant (mmol/m^2), R the gas constant, T the absolute temperature, C the bulk surfactant concentration, and γ the interfacial tension (mN/m).

Most surfactants also have the ability to form micelles. Micelles are molecular aggregates of surfactants in an aqueous phase, Figure 2.1. The hydrophobic parts of the surfactants are concentrated towards the center of the aggregate while the hydrophilic parts reside on the surface. The specific concentration at which micellization occurs is known as the critical micelle concentration (cmc). Below the cmc, surfactants are monomers in solution and interfacial tension follows the Gibbs's isotherm. Above the cmc, the surface tension and the free surfactant concentration become constant because all the additional surfactant molecules aggregate to form the micelle, Figure 2.2. In general, only free surfactant adsorbs at the interface and micelles do not directly affect emulsion stability.

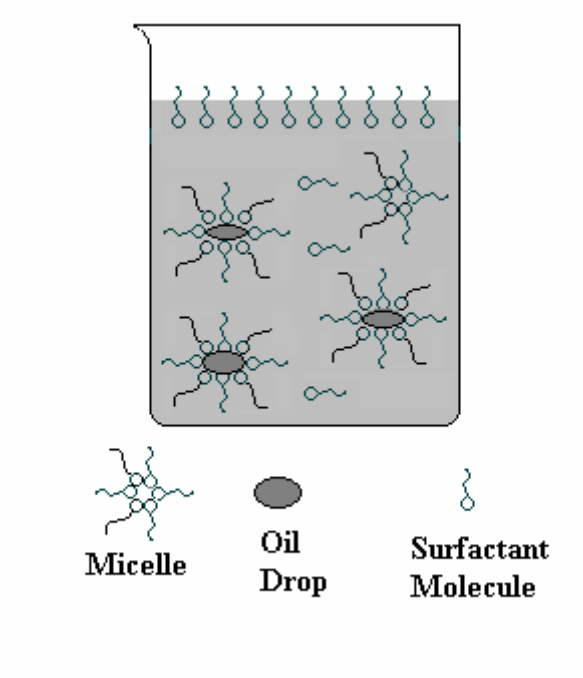

Figure 2.1 Surfactants associations in O/W emulsion (Schramm 2005)

Surfactants can also aggregate in an organic phase in the form of reverse micelles. In this case, surfactant molecules aggregate with an opposite configuration of that found in an aqueous phase. The aggregates tend to be small and form according to step-wise aggregation kinetics rather than a micellization phase formation. These small aggregates may retain their surface activity and contribute to emulsion stability (Sztukowski 2005). Biwettable solid particles can also adsorb on interfaces and stabilize emulsions.

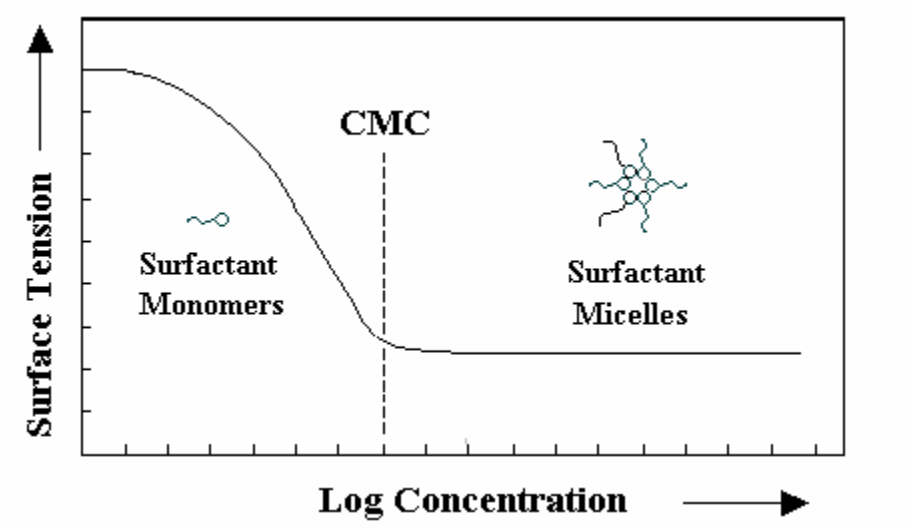

Figure 2.2 Micellization of surfactant molecules

2.1.2 Emulsion Stability Mechanisms

Adsorbed surfactants or solid particles stabilize emulsions via two main mechanisms: steric stabilization and electrostatic stabilization. Steric stabilization arises from a physical barrier to contact and coalescence. For example, high-molecular-weight polymers can adsorb on the surface of the dispersed phase droplets and extend significantly into the continuous phase, providing a volume restriction or a physical

barrier for particle interactions (Hiemenz and Rajagopalan 1997). As polymer coated particles approach, the polymers are forced into close proximity and repulsive forces arise, keeping particles apart from each other, Figure 2.3. Surface-active solid particles such as clays have also been shown to sterically stabilize emulsions (Alboudwarej et al. 2002).

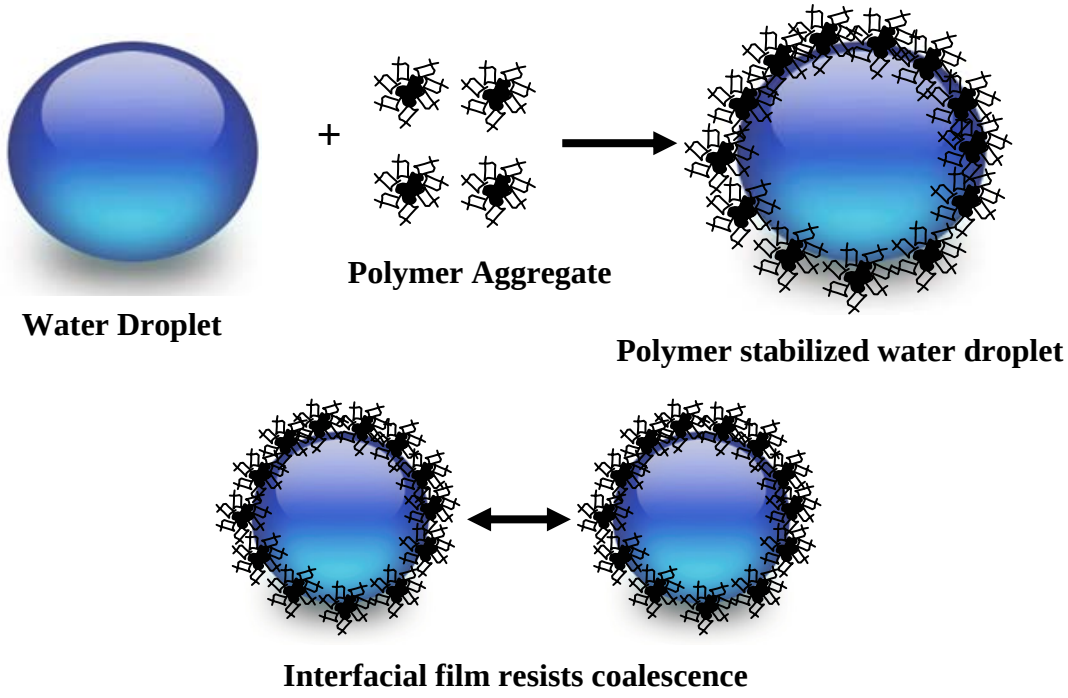

Figure 2.3 Illustration of steric stabilization of water droplets due to polymer adsorption.

Electrostatic stabilization is based on the mutual repulsive forces that are generated when electrical charged surfaces approach each other. In an electrostatically stabilized emulsion, an ionic or ionisable surfactant forms a charged layer at the interface. For an oil-in-water emulsion, this layer is neutralized by counter ions in the continuous phase. The charged surface and the counter ions are termed a double layer. If the counter ions

are diffuse (thick double layer), the disperse phase droplets act as charged spheres as they approach each other. If the repulsive forces are strong enough, the droplets are repelled before they can make contact and coalesce, and the emulsion is stable (Schramm 2005).

In general, electrostatic stabilization is significant only for oil-in-water emulsions since the electric double-layer thickness is much greater in water than in oil. Stable water-in-oil emulsions result from the encapsulating effect of rigid films formed on the water droplets by solid particles or high molecular weight molecules (*e.g.*, asphaltenes) (Schramm 1992). Both electrostatic and steric forces can prevent aggregation or coalescence and hence stabilize emulsions.

Other variables that influence emulsion stability are the:

- Size distribution of droplets
    - Emulsion droplet diameters usually range between 0.2 and 50 μm. The stability of an emulsion is inversely proportional to the size of the droplets.
- Bulk phase properties
    - Viscosity, density, pH, and dielectric constant all affect the collision rate between droplets (Lyklema 2005; Schramm 1992)

2.1.3 Emulsion breakdown mechanisms

Destabilizing or breaking an emulsion is the process in which the emulsion is separated into its component phases. Demulsification mechanisms include: Ostwald ripening, aggregation/flocculation, sedimentation, and coalescence, Figure 2.4 (Lyklema 2005).

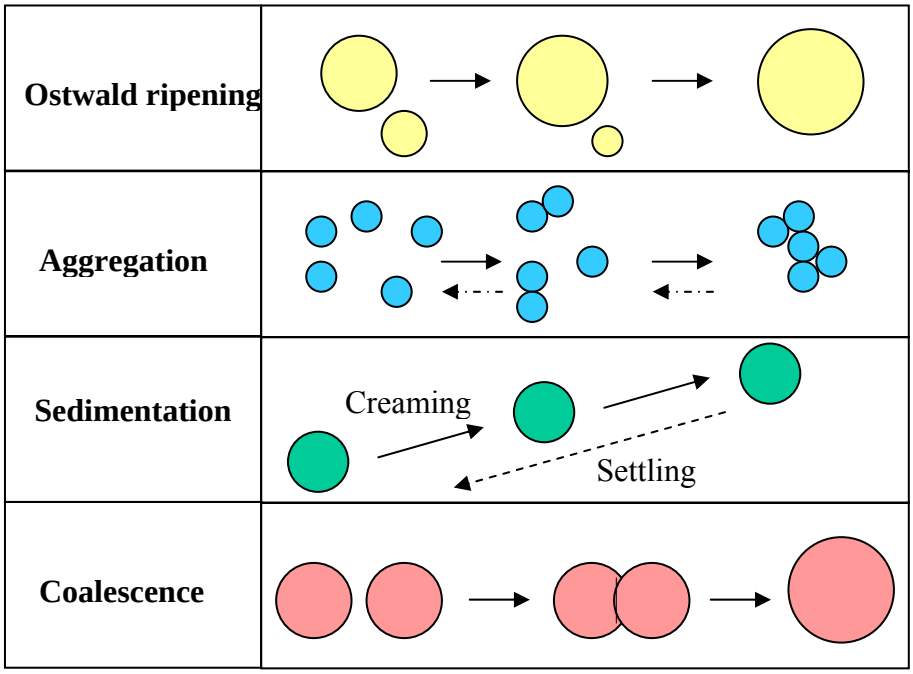

Figure 2.4 Demulsification mechanisms (Lyklema 2005)

2.1.3.1 Ostwald ripening

In a polydisperse emulsion, Ostwald ripening involves mass transfer through the continuous phase between droplets of different sizes. The concentration of the dispersed phase molecules at the outside surface of the drop is inversely proportional to its radius of

curvature (Yarranton and Masliyah 1997). Hence, smaller droplets have a higher concentration of molecules than large droplets. The existence of a concentration gradient promotes diffusion from small to large droplets, resulting in the shrinkage of small droplets and growth of larger ones. Ostwald ripening is a slow process that leads to an eventual disappearance of small drops. Although phase separation is achieved in the long term, Ostwald ripening is usually not relevant to oilfield emulsions.

2.1.3.2 Aggregation

Flocculation occurs when droplets are attracted together but remain separated by a thin film of continuous phase. The droplets are attracted to each other mostly by van der Waals forces, but there is sufficient electrostatic or steric repulsion to prevent close contact. Alternatively, polymer molecules at low concentrations can bond droplets together in a process called bridging flocculation, by adsorbing on more than one particle and forming a bridge that holds particles in a single unit. Flocculation increases the probability of coalescence and accelerates sedimentation.

2.1.3.3 Sedimentation

Sedimentation describes the rise (*i.e.,* creaming) or settling of droplets under the action of gravitational forces, depending on the density difference between phases. In the absence of other forces, the emulsion separates into layers, a cream or sediment layer and a continuous phase layer. Sedimentation brings droplets together and increases the probability of coalescence.

An example of emulsion sedimentation is observed in Figure 2.5, after separating a water/oil emulsion for 6 hours. In this case, water droplets have settled through the continuous oil phase to form a sediment. Some of the sediment has coalesced and formed a free water phase. Some has not yet coalesced and has formed a “rag” layer.

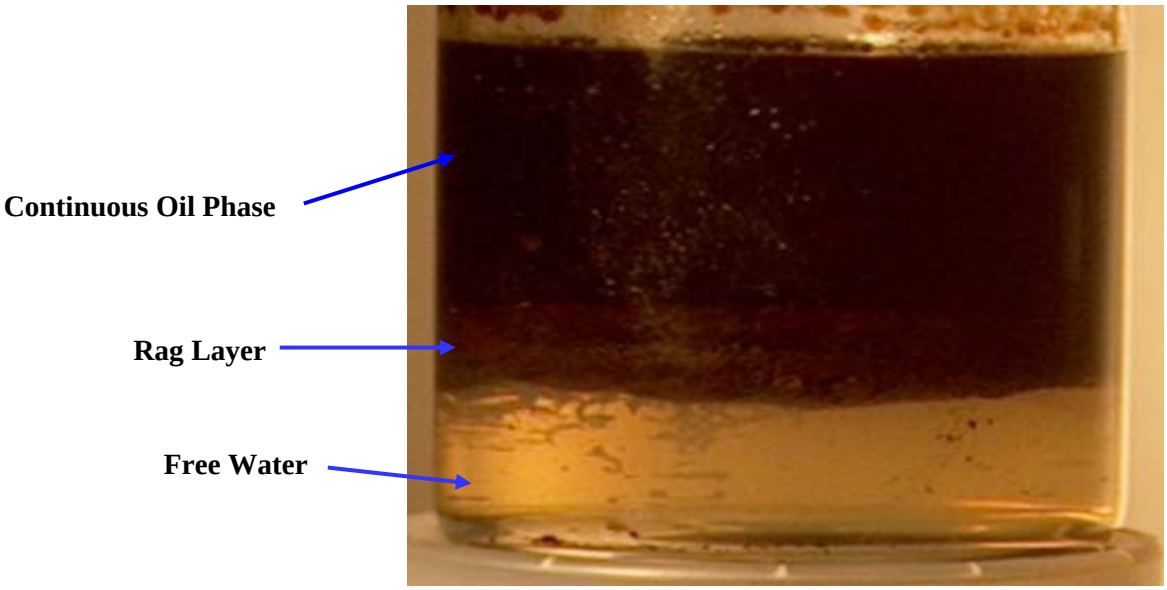

Figure 2.5 Visual observation of free water and rag layer after 6 hours of settling (Hirasaki et al. 2006).

2.1.3.4 Coalescence

The process in which two droplets become a single larger drop due to film rupture is called coalescence. The mechanism involves four steps as presented in Figure 2.6 (Heimenz and Rajagopalan 1997). Two droplets approach each other (1), and as the

separation distance decreases the fluid between them drains out. Hence, the droplets are compressed towards each other, leading to the formation of a planar region (2). Due to the local increase in surface area, the surfactant layer that was covering the interface is spread more thinly, leaving some unprotected surface area free to create a bridge between the droplets (3). Once bridging occurs coalescence follows almost instantly (4). Coalescence leads to a reduction of the total interfacial area. If there is an irreversibly adsorbed film of surfactant on the interface, compression of the film does not occurs. Therefore, film compression is relevant to emulsion stability (Jones et al. 1978).

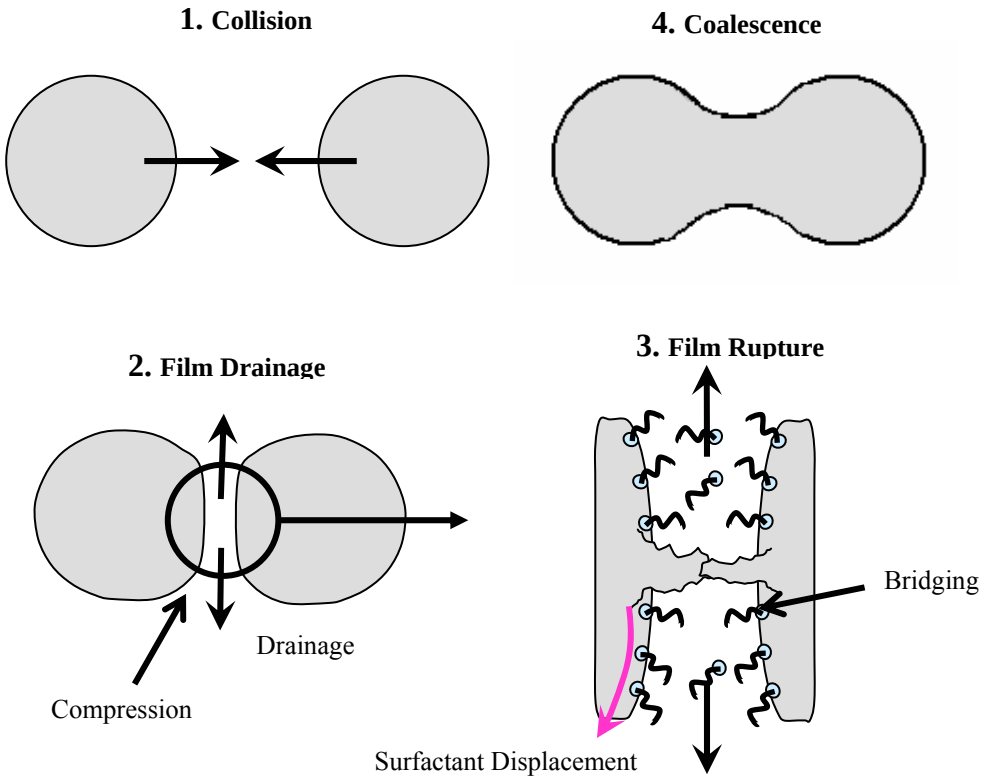

Figure 2.6 Coalescence Mechanism (Heimenz and Rajagopalan 1997)

The factors favouring emulsion breakdown are:

- Increasing temperature decreases emulsion viscosity and increases the Brownian motion of droplets less than 2 μm in diameter and hence accelerates the rate of particle collisions.
- Increasing residence time allows the different emulsion breakdown mechanisms to take place.
- Adding demulsifiers promotes flocculation or replaces the stabilizing film at the interface with a weak film.
- Reducing shear or agitation during emulsification contributes to an increase in droplet size and as a consequence to an increase in the frequency of collisions, aggregation, settling and coalescence.

2.2 Petroleum Terminology

Crude oil or petroleum is defined as a mixture of liquid, gaseous and solid hydrocarbon materials with additional amounts of oxygen, nitrogen, sulphur and metals (Speight 1999). Petroleum components vary in a wide range of boiling points, physical properties and proportions. A conventional crude oil has the following characteristics:

- the appearance can range from a thin, colourless liquid to a thick, very viscous black oil.
- the specific gravity at 15.6 °C ranges from 0.80 to 0.95 (45 to 17° API).

There are other types of crude oils that are more difficult to recover due to their higher viscosity. UNITAR establishes a definition for these oils, based on API gravity and viscosity under reservoir conditions:

Table 2.1 UNITAR Crude Oil Classification

	Viscosity mPa.s	Density g/m^3	API Gravity
Heavy Oil	10^2-10^5	0.934-1.0	20-10
Bitumen	$>10^5$	>1.00	<10

Source:(Gray 1994). Density and API gravity are reported at a standard temperature of 15.6 °C.

2.2.1 Bitumen Characterization

Bitumen or "extra heavy oil" is a mixture of solid and semi-solid hydrocarbons composed mainly of heavy molecular weight components. In general, crude oils can be characterized in terms of chemical composition, boiling point, and solubility fractions (Speight 1999). Chemical composition and boiling point characterization is only applicable for a small fraction of a bitumen. Hence, solubility fractionation is the most commonly used characterization option for heavy oil bitumens.

Solubility fraction analysis known as "SARA" (termed for the initials of each fraction) segregates the bitumen according to their polarity and polarizability with solvents, in four general fractions: saturates, aromatics, resins and asphaltenes. The saturate fraction consists of nonpolar material including linear, branched, and cyclic saturated hydrocarbons (Fan et al. 2002). Aromatics contain a variety of aromatic compounds with saturated groups attached. Resins are a highly complex mixture of heterocycles (*e.g.*, fluorenones, cyclic sulfides, carbazoles, quinolines) and carboxylic acids (Hepler 1989).

The asphaltenes are the highest molecular weight fraction and contain the most polar compounds with a heteroatom content and higher concentration of aromatic carbon (Gray 1994).

A standard procedure for SARA fractionation, ASTM D2007-03, starts with the precipitation of asphaltenes from the bitumen with the addition of a paraffinic solvent (*i.e., n*-heptane or *n*-pentane) in a solvent to bitumen ratio of 40:1 (cm^3/g). The non-asphaltic oil or maltenes, is further separated into saturates, aromatics and resins by clay-gel adsorption chromatography. The complete separation scheme is shown in Figure 2.7. An Attapulgite clay-packed column adsorbs the resins and a silica gel packed column separates the aromatics from the saturate fraction. The saturate material is not adsorbed on either the clay or silica gel under the conditions specified. The resins are recovered from the clay with a 50/50 mixture of toluene and pentane. The aromatics are separated by Soxhlet extraction of the silica gel in hot toluene. Table 2.2 provides SARA analysis results for different bitumens (Akbarzadeh et al. 2004a).

Table 2.2 SARA Analysis of Bitumens (Akbarzadeh et al. 2004a)

	Saturates (wt %)	Aromatics (wt %)	Resins (wt %)	Asphaltenes (wt %)
Western Canadian				
Athabasca	16.3	39.8	28.5	14.7
Cold Lake	19.4	38.1	26.7	15.5
International				
Venezuela	15.4	44.4	25.0	15.2
Russia	25.0	31.1	37.1	6.8
Indonesia	23.2	33.9	38.2	4.7

Note that asphaltenes obtained with this technique coprecipitate with non-asphaltenic solids (Hepler 1989; Mitchell and Speight 1973); however, solids-free asphaltenes are required for any property measurement. To remove non-asphaltenic solids, asphaltenes are redissolved in toluene and centrifuged afterwards. The solids appear as sediments in the bottom of the centrifuge tubes and the supernatant solution is decanted to recover the solids-free asphaltenes. A detailed procedure is provided in Chapter 3.

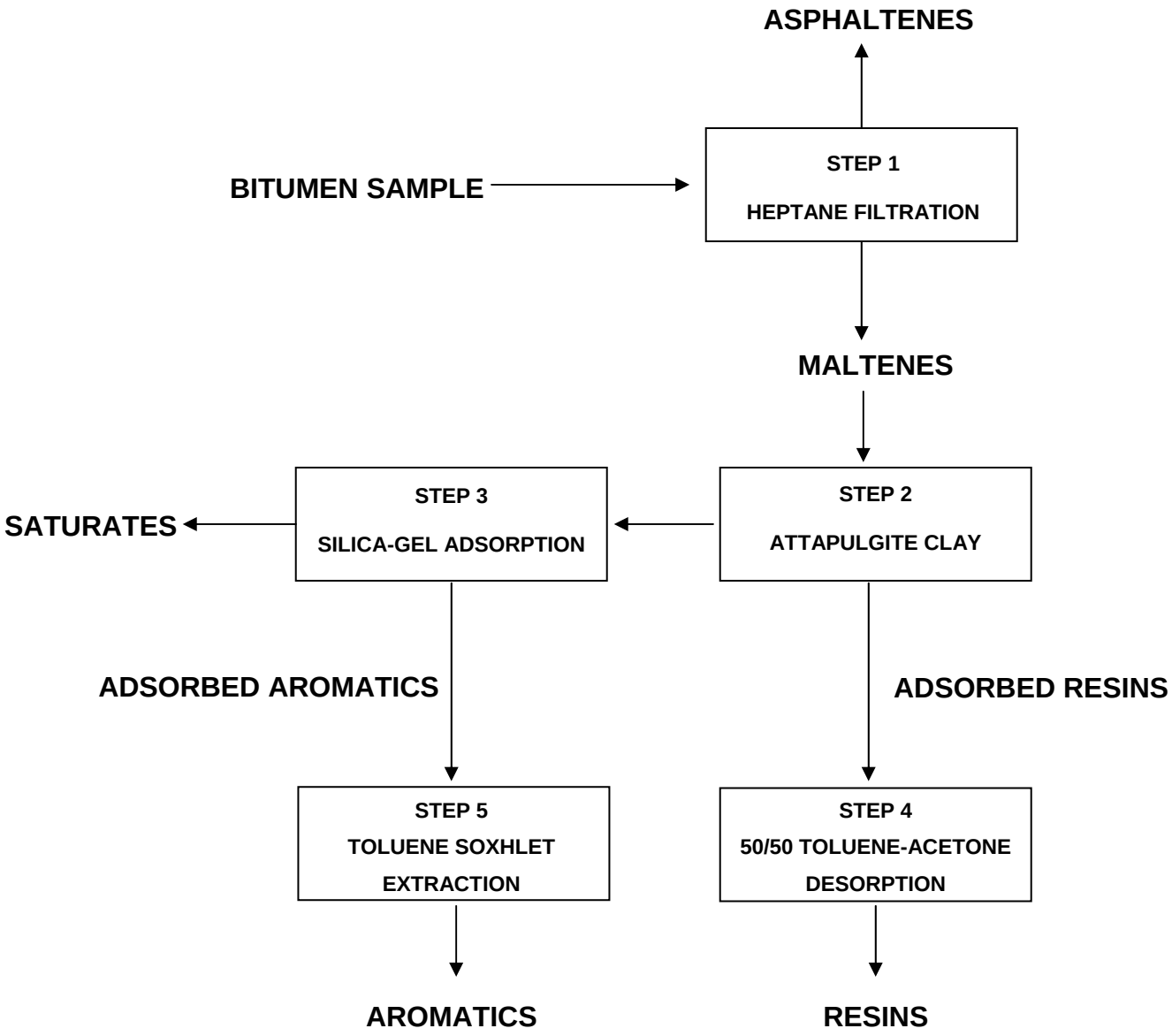

Figure 2.7 SARA fractionation scheme

2.2.2 Asphaltenes

Asphaltenes are dark brown to black solids extracted from heavy oil or bitumen, which have high molecular mass, no definite melting point and decompose leaving a carbonaceous residue when heated above 300-400 °C (Speight 1978). Asphaltenes are a mixture of complex molecules that consist of condensed aromatic rings with alkyl and alicyclic constituents. They also contain heteroatoms (nitrogen, oxygen and sulphur) and metals. The density of asphaltenes has been reported as 1132 to 1193 kg/m³ (Akbarzadeh et al. 2004a).

An operational definition of "asphaltenes" based on a standard separation scheme is the crude oil constituents soluble in toluene (or benzene) but insoluble in excess amounts (greater than 40 volumes) of a paraffinic solvent such as *n*-heptane or *n*-pentane (Gray 1994). The yield and properties of the asphaltenes depend on the choice of solvent (Speight et al. 1985). A comparison of different asphaltene elemental compositions as a function of the precipitation solvent is presented in Table 2.3. As seen in this table, the H/C ratios from the *n*-heptane extracted asphaltenes are lower than the corresponding values of the *n*-pentane extracted asphaltenes. Likewise, the N/C, O/C and S/C ratios are higher in asphaltenes extracted with *n*-heptane, which indicates a higher heteroatom content in these asphaltenes (Speight 1978).

In general, *n*-heptane is preferred as the separation solvent for asphaltene extraction because asphaltene properties are consistent with solvent carbon numbers of C_7 and up.

n-Pentane is used to extract asphaltenes when maltenes preparation is necessary for further SARA analysis (Alboudwarej et al. 2002).

Table 2.3 Elemental compositions of asphaltenes precipitated by different solvents (Speight 1978)

Source	Precipitation Medium	Composition (% weight)					Atomic Ratios			
		C	H	N	O	S	H/C	N/C	O/C	S/C
Canada	*n*-pentane	79.5	8.0	1.2	3.8	7.5	1.21	0.013	0.036	0.035
	n-heptane	78.4	7.6	1.4	4.6	8.0	1.16	0.015	0.044	0.038
Iran	*n*-pentane	83.8	7.5	1.4	2.3	5.0	1.07	0.014	0.021	0.022
	n-heptane	84.2	7.0	1.6	1.4	5.8	1.00	0.016	0.012	0.026
Iraq	*n*-pentane	81.7	7.9	0.8	1.1	8.5	1.16	0.008	0.010	0.039
	n-heptane	80.7	7.1	0.9	1.5	9.8	1.06	0.010	0.014	0.046
Kuwait	*n*-pentane	82.4	7.9	0.9	1.4	7.4	1.14	0.009	0.014	0.034
	n-heptane	82.0	7.3	1.0	1.9	7.8	1.07	0.010	0.017	0.036

Separation procedures also define the asphaltene quality and yields. Factors such as contact time, solvent composition, solvent-to-bitumen ratio, temperature and level of washing may cause property variations in asphaltenes. Alboudwarej et al. (2002) found that increasing the amount of washing in asphaltene extraction, increases density and molar mass as well as decreases solubility. This is likely related to the removal of resins from the asphaltenes and further asphaltene self-association. Table 2.4 compares the effect of asphaltenes extraction methods on asphaltene properties.

Table 2.3 Effect of Extraction Method on Asphaltene Properties. (Alboudwarej et al. 2002)

Asphaltene sample	Yield[a] (%)	Solids[b] (%)	Density[c] (Kg/m^3)	Molar mass[d] (g/mol)
ASTM D4124	9.3	5.7	1215	9200
IP 143	8.7	5.6	1203	8300
Speight	9.2	5.6	1190	6300
Soxhlet	9.8	5.3	1192	9100

[a]Mass percent of bitumen (with solids). [b]Mass percent of asphaltene. [c]Solid-free asphaltene. [d]Molar mass at 10 kg/m^3.

2.2.2.1 Asphaltene Chemical Composition and Structure

The "solubility class" definition of asphaltenes implies a broad variety of components that are subject to variations depending on the crude source. H/C ratios are approximately constant in different asphaltenes, 1.15 ± 0.05. However, oxygen and sulphur contents may vary from 0.3 to 4.9% and from 0.3 to 10.3%, respectively. The nitrogen content ranges from 0.6 to 3.3% (Speight 1978).

Structural units found in the asphaltene molecule include carboxylic acids, thiophenes, fluorenes, cyclic sulfides, alkanes, alkyl benzenes, alkyl naphthalenes and biphenyls, alkyl anthracenes and phenanthrenes. Strausz et al. (1999) reported that asphaltenes contain functional groups such as –OH, –COOH and –NHO–. According to Strausz et al. (1992), the structural units are randomly distributed along the molecule and represent the 50-67 %wt of the asphaltene. The rest of the molecule is made up of larger, polycondensed aromatic and heteroatomic systems.

Asphaltenes tend to self-associate, that is, they form aggregates (Agrawala and Yarranton 2001; Spiecker et al. 2003; Sztukowski et al. 2003). In addition, resins appear to participate in the self-association; hydrogen bond interactions between asphaltenes and resins have been demonstrated (Murgich et al. 1999; Speight et al. 1985). Therefore, the isolation of pure asphaltenes and the determination of its molecular structure has been a research challenge since the late 1930s. Physical methods such as infrared spectroscopy (IR), nuclear magnetic resonance spectroscopy (NMR), and X-ray diffraction (XRD), are commonly used to structurally characterize asphaltenes. Chemical methods involve oxidation, and hydrogenation, among others.

One of the most accepted structural models was proposed by Strausz and coworkers in 1992, which was developed considering data from different asphaltene sources: oil sands, conventional light and heavy oil. This hypothetical model molecule has a two-dimensional structure, an elemental formula of $C_{420}\,H_{496}\,N_6\,S_{14}\,O_4V$ an H/C atomic ratio of 1.18 and a molecular weight of 6191 Daltons. The weight percentage composition is: C, 81; H, 8.0; S, 7.3; N, 1.4; O, 1.0 and V, 0.8 (Strausz et al. 1992). Figure 2.8 shows a diagram of this asphaltene molecular model.

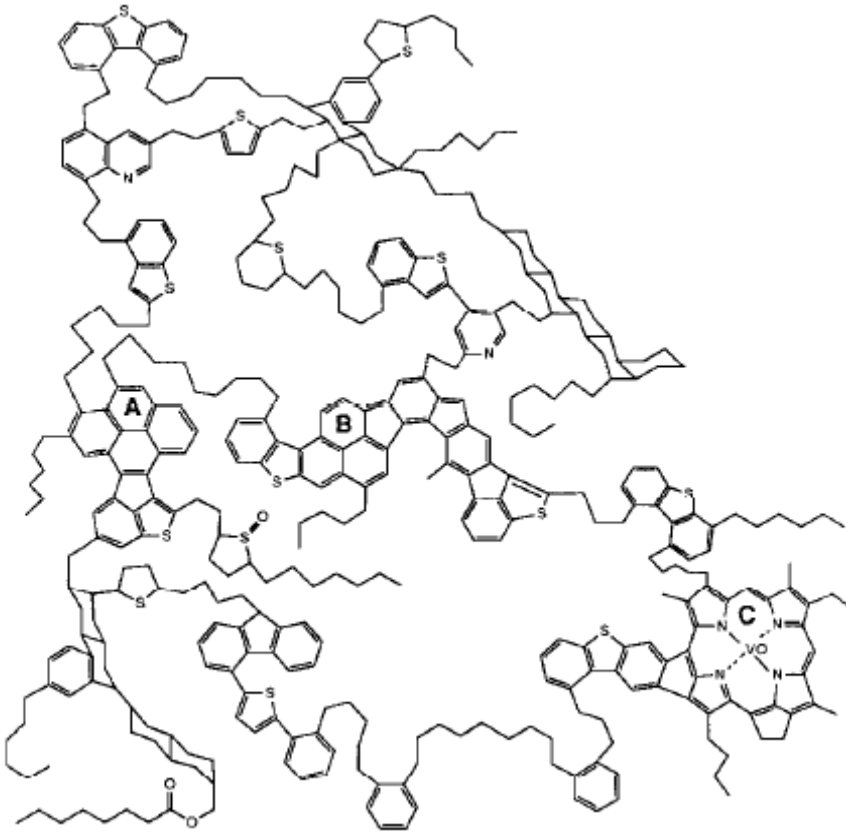

Figure 2.8 Hypothetical asphaltene molecule. (Strausz et al. 1992)

2.2.2.2 Asphaltene Molecular Mass

Asphaltene self-association has led to a wide range of reported molar masses for different experimental techniques (Table 2.5). However, consistent molecular mass values were measured by vapour pressure osmometry (Peramanu et al. 1999; Speight et al. 1985; Yarranton et al. 2000a; Yarranton and Masliyah 1996b).

Table 2.4 Average molecular weights of asphaltenes by different experimental methods (Moschopedis et al. 1976)

Method	Molecular Weight
Ultracentrifugation	≤ 300000
Osmotic pressure	80000
Ultrafiltration	80000-140000
Boiling point elevation	2500-4000
Freezing point depression	600-6000
Vapor pressure osmometry	1000-8000
Viscosity	900-2000
Light scattering	1000-4000

Vapour pressure osmometry (VPO) is the most extensively used "relative" method; it requires calibration with a material with a known molecular mass. The method is based on the difference in vapour pressure caused by the addition of a small amount of solute to a pure solvent (Yarranton et al. 2000a). Although VPO provides a reasonably accurate number average molar mass, still asphaltene molecular masses determined by this technique vary considerably since they are highly dependent on the solvent, solute concentration and temperature. Even at low concentrations, asphaltene association occurs (Yarranton 2005). Measured molecular masses normally increase with an increase in the solute concentration for solvents with high dielectric constants (Peramanu et al. 1999). Yarranton et al., (2000) found that the molar mass decreases as the temperature and the polarity of the solvent increase. They also found that the molar mass of *n*-heptane extracted asphaltenes is higher than that of the *n*-pentane extracted asphaltenes.

Speight et al. (1985) found asphaltene molar masses ranging from 1200 to 2700 g/mol with absolute errors of 30% or more. Yarranton et al. (2000) obtained average molar masses ranging from 1000 to 10000 g/mol for Athabasca asphaltenes dissolved in toluene at temperatures between 50 and 90 °C. The lower limit is expected to approach the monomer molar mass.

2.2.3 Asphaltene Self-Association

The nature and mechanisms of asphaltene association and the size of asphaltene aggregates are still widely debated. However, there are two main views of asphaltene association: colloidal aggregates or polymer like macromolecules.

The colloidal model, first proposed by Nellensteyn (1938) and Pfeiffer and Saal (1940), is based on asphaltene/resins interactions. According to Yen (1974), asphaltene particles are stacks of polycondensed polynuclear aromatic systems attracted by π-π interaction. The asphaltene stacks are kept in solution as a colloidal dispersion, stabilized by a layer of resins. Asphaltene precipitation occurs when the layer of resins is desorbed or disrupted.

The other competing model, known as the thermodynamic model, assumes that asphaltenes self-associate analogously to polymerization to form macromolecules that are in solution with the rest of the oil. Resins are believed to participate in the self-association but do not act as dispersants. Since asphaltene aggregates are considered to be macromolecules, asphaltene precipitation is modeled as a conventional phase transition.

Recently, several groups have had success modeling asphaltene precipitation using regular solution theory or EOS (Equation of State) approaches (Akbarzadeh et al. 2004b; Ting et al. 2003; Wang and Buckley 2001).

Evdokimov et al. (2003) concluded from NMR relaxation studies, that the molecular aggregation in crude oil solutions is a stepwise process, where aggregates of two, three or more are consecutively formed, as the asphaltene concentration increases. Agrawala and Yarranton (2001) modeled asphaltene association in a manner analogous to linear polymerization. By VPO measurements, they found that an average aggregate consists of two to six asphaltene monomers (3000 to 10000 g/mol). They proposed that asphaltene molecules may contain multiple actives sites (functional groups) capable of linking with other molecules. The aggregate may associate through π-π, acid-base, and/or hydrogen bonding. The molecules with multiple active sites act as propagators whereas the molecules with a single active site act as terminators in a polymerization-like reaction. This model is successful in explaining asphaltene molar mass measurements at different solvents and temperatures; and steric stabilization of water-in-oil emulsions by asphaltenes (Yarranton 2005).

2.2.4 Asphaltene Surface Activity

It was mentioned previously that asphaltenes consist of a mixture of a large number of chemical compounds, each of them having different chemical properties. The long alkyl chains and the polyaromatic skeletons are hydrophobic while the heteroatoms are hydrophilic. This mixed nature leads to a surface-active molecule, which adsorbs at an

oil-water interface, oriented with the hydrophilic groups towards the aqueous phase and the hydrophobic structure immersed in the oil phase.

Research on determining the surface activity of asphaltenes was conducted by Rogacheva et al. (1980). They confirmed that diluted solutions of asphaltenes in toluene lowered surface tension of pure toluene by 6.0 mN/m and a critical micelle concentration (cmc) was observed. Results also indicated a dependence of surface tension on asphaltene concentration, proving that the higher the asphaltene concentration the lower the surface tension. Sheu et al. (1992) performed interfacial tension measurements of asphaltene/toluene solutions against an aqueous phase as a function of asphaltene concentration in the oil phase. As a result, for different asphaltene concentrations, interfacial tension decreased monotonically with time. Likewise, Yarranton et al. (2000) evaluated the effect of asphaltenes on the interfacial tension of similar systems, obtaining results that were consistent with Sheu's work and also demonstrating that there is no evidence of critical micelle concentration within the system.

Sztukowski et al. (2003) showed that asphaltenes adsorb on the interface as a "monolayer" of self-associated molecules. Vapour pressure osmometry and gravimetric studies revealed a constant molecular surface coverage (moles of asphaltenes per interfacial area), indicating a monolayer adsorption even at asphaltene concentrations above 40 %wt. They concluded that the higher molar mass aggregates simply extend more into the continuous phase.

Zhang et al. (2003) also observed that asphaltenes can form a monolayer at the oil-water interface. A further study conducted by the same authors in (2005b) showed that asphaltenes are capable of forming an interfacial film or "skin" at the oil-water interface as colloidal particles as well as macromolecules. In addition, asphaltenes appeared to have a higher surface activity upon an increase in the concentration of a non-solvent (*e.g.*, *n*-heptane), which corresponds to the threshold of asphaltene solubility in solution (Kumar et al. 2001).

Note that resins are structurally similar to asphaltenes but have lower molar mass. They contain a largely hydrophobic hydrocarbon structure and hydrophilic heteroatoms, and consequently are surface-active molecules as well.

2.3 Crude Oil Emulsions

Crude oil emulsions are found in almost every phase of oil production and processing, where they may be desirable or undesirable (Table 2.6). The most produced oilfield emulsion is water-in-oil, which may contain not only water and oil, but also solid particles and sometimes gas (Schramm, 1992). The undesirable emulsions must be broken and the dispersed water removed to meet crude specifications and to reduce problems such as corrosion, high pressure in pipelines and catalyst poisoning.

Table 2.5 Examples of Emulsions in the Petroleum Industry (Schramm, 1992)

Occurrence	Type
Undesirable Emulsions	
Well-head emulsions	W/O
Fuel oil emulsions (marine)	W/O
Oil sand flotation process, froth	W/O or O/W
Oil spill mousse emulsions	W/O
Tanker bilge emulsions	O/W
Desirable Emulsions	
Heavy oil pipeline emulsion	O/W
Oil sand flotation process, slurry	O/W
Emulsion drilling fluid, oil-emulsion mud	O/W
Asphalt emulsion	O/W
Enhanced oil recovery in situ emulsions	O/W

Although emulsion stabilization mechanisms are still under investigation, it is generally believed that the stability of water-in-oil emulsions depends mainly on a rigid protective film encapsulating the water droplets (Freer and Radke 2004; Gafonova and Yarranton 2001; Jones et al. 1978; Kumar et al. 2001; Taylor 1992; Yarranton et al. 2000b; Zhang et al. 2003a). The interfacial film is characterized as an insoluble and highly viscous material that has viscoelastic properties. These films reduce interfacial tension as well as increase the interfacial viscosity of emulsions (Freer et al. 2003; Kokal 2005; Xia et al. 2004; Yeung et al. 1999). Highly viscous interfacial films retard the rate of water droplets collisions by providing a mechanical barrier to coalescence.

The protective skin is believed to consist of a mixture of naturally occurring emulsifiers in the crude oil, such as asphaltenes and resins, solids, waxes and organic acids and bases (Kokal 2005). There is strong evidence that asphaltenes are the primary component of stabilizing interfacial films (McLean and Kilpatrick 1997; Sun et al. 2003; Taylor et al. 2002). According to Sun and coworkers, surface-active fractions containing large condensed ring aromatic compounds that have large conjugated structures (*e.g.,* asphaltenes) play a more important role in film forming and film rigidity than fractions with smaller molecules. Many researchers have shown that model water-in-oil emulsions consisting of asphaltene and solvents are very stable (McLean and Kilpatrick 1997; Taylor et al. 2002). McLean and Kilpatrick reported that model oils (mixtures of *n*-heptane, toluene and asphaltenes) with asphaltene contents as low as 0.5% are sufficient to form emulsions which are actually more stable, in some cases, than those formed from their respective whole crudes.

Zaki et al. (2000) demonstrated that resins alone are not capable of stabilizing emulsions. Moreover, resins reduce emulsion stability, as indicated by Gafonova and Yarranton (2001). They found that resins appear to act as a good solvent (*e.g.*, toluene) for asphaltene and, at sufficient high concentrations, are able to replace them on the interface and allow faster coalescence. In agreement with Gafonova and Yarranton's results, Spiecker et al. (2003), speculated that the addition of resins to asphaltenes reduced the aggregate size by disrupting the π-π and polar bonding interactions between asphaltene monomers. The smaller aggregates were expected to be less effective emulsion stabilizers.

Sztukowski et al. (2003) showed that native clays contribute to emulsion stability but that asphaltenes must be present on the interface as well. So it appears that while other oil constituents can increase or reduce emulsion stability, asphaltenes or part of the asphaltenes are a necessary component of stable water/oil emulsions.

2.3.1 Asphaltene Film Properties

Asphaltenic crude oils form viscoelastic network structures (i.e., skins) at the oil/water interface (Aske et al. 2002; Bauget et al. 2001; Freer et al. 2003; Nordli et al. 1991). Freer et al. (2003) studied interfacial elasticity of crude oil droplets immersed in brine. Their results indicate that the interface behaves elastically and that the interfacial elasticity increases as the asphaltene concentration increases. Moreover, interfacial elasticity grows slowly in time even when the rigid skin is not visible macroscopically.

Yeung and coworkers (1999) studied the interfacial surface rigidity; they performed experiments on interfacial structure through area reduction of microsized water droplets immersed in diluted bitumen. They observed that as the droplet was deflated and its area compressed, the surface crumples abruptly, revealing a rigid cortical structure. Figure 2.9 (a) and (b) shows the initial and final steps of droplet compression respectively. The crumpling of the droplet results from the high resistance to surface deformation and such resistance is manifested as surface viscosity. Similar behaviour was found for asphaltene in solvents (Jafari 2005). Taylor (1992) also observed rigid skins during the retraction of pendant crude oil drops (Figure 2.10).

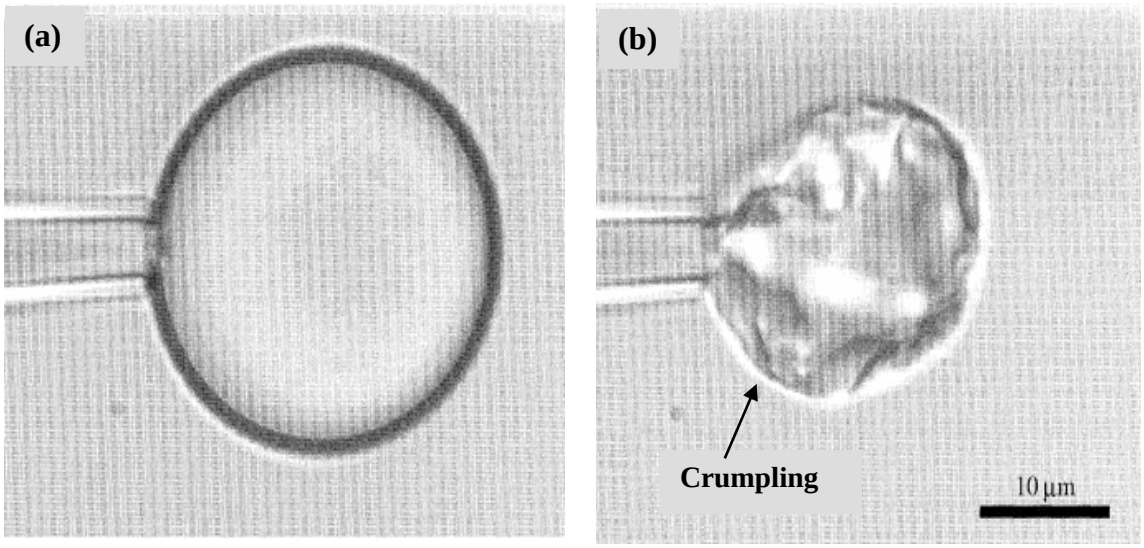

Figure 2.9 Before (a) and after (b) deflating an emulsion drop using a micropipette. The outside layer is made of 0.1% of bitumen. A skin is revealed as the droplet area is reduced (Yeung et al. 1999)

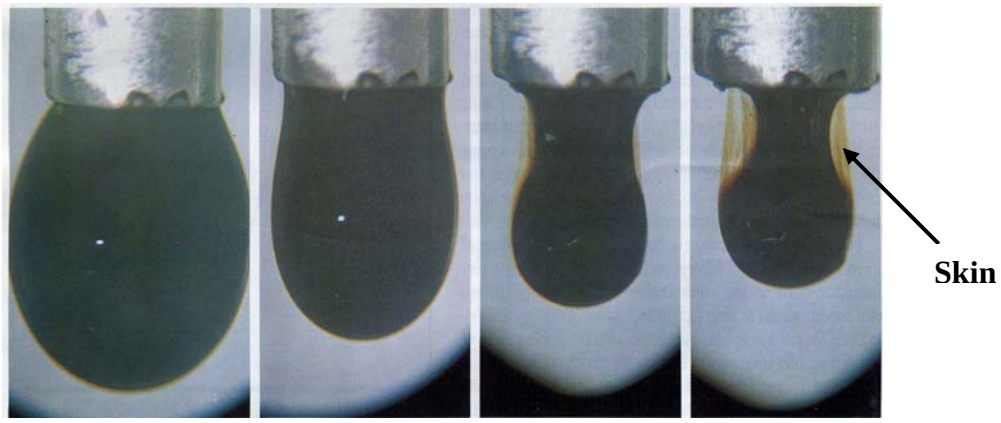

Figure 2.10 Skin observation after droplet retraction (Taylor 1992)

Mechanical properties of films were also evaluated by Jones et al. (1978). They measured film pressure during expansion and compression of an oil/water interface using a Langmuir-type oil/water interfacial film balance. Variation of crude type, pH, temperature, interfacial age, and rate of interfacial compression was taken into account. They found that a variety of film behaviour, from incompressible relaxing to compressible relaxing occurs. The dynamics of the film relaxation process dictates the extent of the barrier to stability.

Film rigidity appears to increase as the interfacial area decreases. Nordli et al. (1991) studied the interfacial properties of the surface-active fractions of different North Sea crude oils at both 293.7 and 313K, using a Langmuir Balance. A film phase change was observed while compressing the interfacial area. The film forming components showed an initial gas state condition. As the area was compressed, the film entered a liquid expanded condition until a film fracture was observed at very small interfacial areas.

Film formation and film properties are driven by several factors such as temperature, solvent chemistry, resin content, asphaltenes concentration, aging time, which allows asphaltenes to adsorb and form cohesive films at the oil-water interface. The type of solvent determines the degree of asphaltene aggregation and the proximity to asphaltene solubility limit (Aske et al. 2002; Gafonova and Yarranton 2001; McLean and Kilpatrick 1997). The addition of a poor solvent (*i.e.*, *n*-heptane) was found to increase the emulsion stability until asphaltene precipitation (Gafonova and Yarranton 2001). In poor solvents, the asphaltenes are more difficult to displace from the interface and make the emulsion

more stable. However, above the solubility limit, approximately 50% (by volume) of *n*-heptane, the precipitated asphaltenes aggregate are large non surface-active particles that do not participate in stabilizing emulsions. Hence, the concentration of surface-active asphaltenes at the interface is reduced and gradually the emulsion becomes less stable. Similar behaviour was found by McLean and Kilpatrick (1997). They determined that at lower solvent aromaticities (e.g., less than 20% of toluene), asphaltenes certainly precipitate out of solution in the form or aggregates which are too large to adsorb at the interface. Zhang et al.'s (2003) surface pressure measurements indicate that more rigid asphaltene films are formed in poorer solvents.

The aging time of an oil/water interface affects the stability of the emulsion. The longer the interfacial contact, the greater the stability (Aske et al. 2002; Jones et al. 1978; Nordli et al. 1991; Sun et al. 2003; Taylor et al. 2002; Taylor 1992). The increment in stability may be related to the aging of the interfacial film. Taylor (1992) considers film formation as an "aging process" that results from the irreversible adsorption of asphaltenes at the interface. Jones et al. (1978) indicated that films develop greater resistance to compression with interfacial age. This incompressibility reflects the time dependency of surfactant adsorption along with molecular reconfiguration at the interface. A decrease in film compressibility with time was also found by Nordli et al. (1991). Sun et al. (2003) showed from interfacial relaxation experiments that the dilatational viscoelasticity of the interface may increase by the enrichment of surface active fractions into the interface over time. Also for samples of higher molecular weights, the dilatational moduli increased with increasing aging time.

The kinetics of interfacial asphaltene adsorption seems to be time dependent, providing a possible explanation for the change in film rigidity over time. Studies have shown that an initial diffusion of asphaltenes takes place towards the interface, followed by a long interfacial reorganization of molecules in a network structure at higher aging times, which is no longer diffusion controlled but instead is a reaction-like process (Bauget et al. 2001; Jeribi et al. 2002; Nordli et al. 1991; Sheu et al. 1992; Sztukowski et al. 2003; Taylor et al. 2002). Sheu et al. (1992) studied the interfacial properties of asphaltenes by measuring the dynamic interfacial surface tension of asphaltene/toluene solutions against an aqueous phase. They observed a reaction-like process, believed to be initiated by molecular packing, as the system approached equilibrium. Jeribi et al. (2002) evaluated asphaltene adsorption at the air-oil and water-oil interfaces. They observed a rapid diffusion stage and a slow molecule rearrangement, which they attributed to the progressive building of multilayers. However, the changes may reflect rearrangement of self-assembled asphaltenes within a single layer of aggregates. They also found the asphaltene adsorption faster in water-oil interfaces as well as in good asphaltene solvents.

Generally at higher temperatures the bulk viscosity decreases resulting in a faster film drainage rate and enhanced droplet coalescence. Temperature influences the rate of build-up of interfacial films by changing the adsorption rate and the film molecular structure. Nordli et al. (1991) found that the monolayers become more close-packed or condensed at elevated temperatures. They believed that, upon elevating the temperature, the film structural restrictions are relaxed and the film is able to pack more closely. However, as

noted by Jones and coworkers, a temperature increment may not change the physical properties of the interfacial film.

Asphaltene concentration also influences the behaviour of interfacial films. Several researchers described that at low asphaltene concentrations, rigid films were observed at very short times (Gafonova and Yarranton 2001; Taylor et al. 2002; Yarranton et al. 2000b). Taylor and coworkers used a thin liquid film-pressure balance technique (TLF-PBT) to determine the interaction between water droplets within a water-in-bitumen emulsion based on disjoining pressure isotherms. They reported that a protective skin appeared within a few minutes for more dilute asphaltene solutions whereas for more concentrated solutions it appeared after more than an hour of contact between the water and oil phases. Similarly, Gafonova and Yarranton (2001) indicated that the stability of the emulsions decreased as asphaltene surface coverage increased. They speculated that at low asphaltene concentrations there was low asphaltene surface coverage, and the molecules attached to the interface at several sites, which consequently may make the interface more rigid and the emulsion more stable.

2.4 Chapter Summary

The formation of oilfield water-in-oil emulsions during oil production is a costly problem, both in terms of capital and operating costs. They result from the mixing of water and oil and are stabilized by naturally occurring emulsifiers present in the crude oil, such as asphaltenes, and native solids. These compounds are believed to be the main

constituents of interfacial films, which encapsulate water droplets in an oilfield emulsion, inhibiting coalescence.

Asphaltenes are a surface-active material that adsorbs in a monolayer in the water/oil interface. The adsorption process is diffusion controlled initially and it undergoes a gradual rearrangement over time to form a cross-linked network or rigid “skin”. The skin has high interfacial viscosity and high interfacial elasticity. During interfacial area compression, the interfacial film increases its resistance to deformation and becomes more rigid until it “crumples”. Film rigidity depends on several factors including the asphaltene concentration, the aging time, the temperature and the resin content.

Many researchers have attributed crude oil emulsion stability to the properties of the asphaltene film. For coalescence to take place it is essential to have a weak, flexible interfacial film that can be compressed enough to allow bridging between drops. However, as yet, no direct link between film properties and emulsion stability has been established.

CHAPTER 3- EXPERIMENTAL METHODS

The purpose of this work is to evaluate asphaltenic film properties and relate them to water-in-oil emulsion stability, specifically to emulsion coalescence rates. This chapter is intended to explain the experimental procedures for the measurement of the rheological properties of interfacial films through the aid of surface pressure-film ratio isotherms. Surface pressure isotherms were obtained by compressing a prepared asphaltene monolayer at a hydrocarbon/water interface and measuring surface area and interfacial tension using drop shape analysis. Surface pressure and film ratio values were calculated and plotted using the collected data. The impact on surface pressure of variables such as solvent composition, asphaltene concentration, temperature and interface age was evaluated. Surface pressure isotherms were also measured for bitumen diluted with mixtures of *n*-heptane and toluene.

The asphaltenes employed in this research were extracted in a two-step procedure. The first step consisted in the precipitation of the asphaltenes from the bitumen followed by a second separation stage in which, the non-asphaltene solids present in the asphaltenes, were removed to ensure the purity of the sample and avoid other possible surface effects in the measurements. These solids include fine clays, ash, and some adsorbed hydrocarbons and are insoluble in toluene (Yarranton et al. 2000b). The materials, instrumentation, and techniques to extract asphaltenes and determine interfacial tensions and surface area are described in detail below.

3.1 Materials

Asphaltenes were recovered from an Athabasca Coker-feed bitumen sample provided by Syncrude Canada Ltd. OMNISOLV *n*-heptane (99.99 % pure) and OMNISOLV toluene (99.38 % pure) were purchased from Van Waters & Rogers Ltd. (VWR) and mixed in different solution ratios. The solvents are combined with asphaltenes to perform surface pressure isotherm experiments. Reverse Osmosis water is supplied by the University of Calgary water plant facilities and is also used in the interfacial measurements.

For simplicity, different solutions of *n*-heptane and toluene are described as A/B heptol, where A and B are the volume fractions of *n*-heptane and toluene in the mixture, respectively.

3.1.1 Asphaltenes-Solids Precipitation

In order to extract asphaltenes from the bitumen, *n*-heptane was added in a 40:1 (cm^3/g) solvent-to-bitumen ratio to an Athabasca bitumen sample and was sonicated for 45-60 minutes to obtain a homogeneous mixing. The solution was left to settle for a period of 24 hours of contact time with the solvent. Then the solution was filtered using a Whatman #2, 24 cm filter paper, keeping a 25% of this solution unfiltered for further dilution. *n*-Heptane was used in a 4:1 (cm^3/g) solvent-to-bitumen ratio to dilute the unfiltered solution and was sonicated for a period of 45-60 minutes and left to rest overnight. This supernatant was then decanted using the same filter paper and was set to dry for four days. The obtained product is labelled "C_7 –Asphaltenes Solids-Unwashed". The average asphaltene yield was 16.9 %.

3.1.2 Solids Removal

For solids removal, a centrifugation technique was employed due to its efficient results and short experimental time compared to other techniques (Sztukowski 2005). To separate solids from asphaltenes, two grams of "C_7-Asphaltenes Solids–Unwashed" were dissolved with 200 cm^3 of pure toluene and sonicated for 15 minutes. The mixture was left to stand for one hour and sonicated again for 10 minutes. Later on, it was centrifuged for six minutes at a constant speed of 4000 rpm. After centrifuging, two distinctive phases were observed, a solid phase collected at the bottom of the centrifuge tubes and a supernatant solution. The supernatant was poured off and was allowed to dry for two days. The obtained product was deemed "C_7-Asphaltenes-Solids Free-Unwashed". Note, some fine free solids may remain in the supernatant after this procedure. All isotherm experiments were performed with "solid-free" asphaltenes. Table 3.1 summarizes the solids and asphaltene content encountered in Athabasca bitumen.

Table 3.1 Asphaltene and Solids content of Athabasca Bitumen

Component	Athabasca Bitumen
Asphaltene-Solids	16.9*
Asphaltenes (fraction of Asphaltene-solids)	95.0
Solids (fraction of Asphaltene-solids)	5.0
Solids (fraction of bitumen)	0.87

* Asphaltene yield from bitumen (mass fraction).

3.2 Surface Pressure Isotherm Experiments

A surface pressure isotherm is a plot of the variation of surface pressure versus interfacial area or film ratio. The film ratio is the ratio of the surface area at any compression state over the initial area (A/A_0). Surface pressure (π) is the difference between the solvent (or solvent mixture) interfacial tension (γ_0) and that of a mixture of the solvent(s) and surface-active agents (*e.g.*, asphaltenes) (γ):

$$\pi = \gamma_o - \gamma \qquad \textbf{Eq. 3.1}$$

In this investigation, interfacial tension and surface area were measured in a stepwise manner for a hydrocarbon drop consisting of asphaltene, toluene and *n*-heptane immersed in an aqueous phase. At each step, fluid from the drop was withdrawn to compress the oil/water interface. Surface pressure isotherms were measured at different asphaltene concentrations, solvent ratios and interface aging times at both 23 and 60 °C on the interface.

3.2.1 Principles of Drop Shape Analysis

An IT Concept Drop Shape Analyzer was used to measure interfacial tension and surface area of a mixture of asphaltenes, toluene and *n*-heptane against water. The interfacial tension between the two fluids was determined via digital processing of the shape of a drop. An apparatus configuration is shown in Figure 3.1. The measurement procedure was as follows: a drop of a less dense fluid (*e.g.*, hydrocarbon solution) was formed on the tip of a stainless steel u-shaped needle inside a glass cuvette filled with a denser fluid (*e.g.*, water). The hydrocarbon was injected or withdrawn from the droplet using a DC motor drive attached to a high precision micrometer syringe. A light source provided illumination to the cuvette and a CCD camera in conjunction with magnifying telecentric lenses photographed the drop and sent the captured image to a personal computer for digital processing using analysis and control software. The whole setup was placed on an anti-vibration optical bench. For measurements at non-ambient temperatures, the cuvette was placed in a thermostated holder located between the light source and the camera. The temperature of the holder was controlled by a circulating water bath.

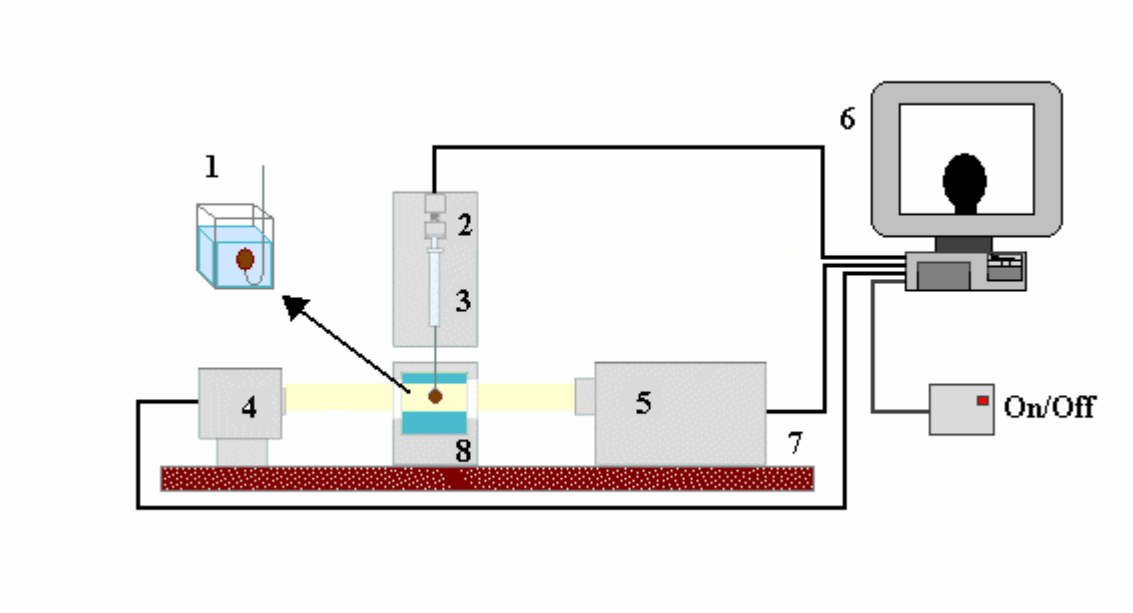

Figure 3.1 Drop Shape Analyzer Configuration: 1.u-shaped needle and cuvette, 2. DC motor drive, 3. syringe, 4. light source, 5. CCD camera and telecentric lenses, 6. PC with analysis and control software, 7. optical bench and 8. thermostated holder.

The shape of a drop is determined by the balance between gravity and surface forces. In the absence of gravity, the drop would have a spherical shape since this geometry will have the smallest area per volume possible. In the presence of gravity, the drop shape becomes elongated. Figure 3.2 shows a real image of a droplet of asphaltenes and heptol with water as a continuous phase.

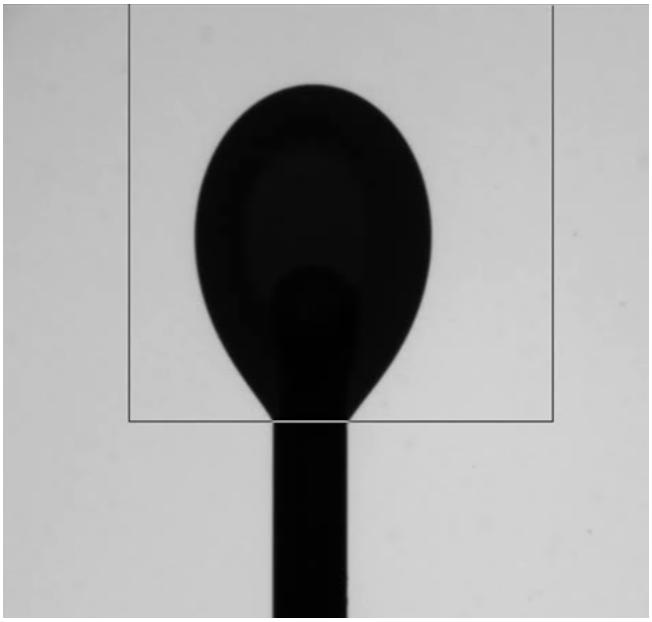

Figure 3.2 Drop Shape Analyzer image of a droplet of asphaltene and solvent in distilled water.

In general, to calculate the shape of a droplet we begin with the Laplace equation. This equation states that the interfacial pressure (Δp) of a drop or bubble is related to its interfacial tension (γ) and radii of curvature R_1 and R_2:

$$\Delta p = p_A - p_B = \gamma\left(\frac{1}{R_1} + \frac{1}{R_2}\right) \qquad \textbf{Eq. 3.2}$$

The profile and description of the radii of curvature for an axisymmetric pendant droplet are shown in Figure 3.3. In this figure, the origin of the coordinate system O is situated at the apex of the droplet. P is a point in the surface of the drop. R_1 is the radius of curvature in the x-z plane. R_2 is the radius of curvature in the y-z plane and θ is the angle between

R_2 and the z-axis. The coordinates of P in the x-z plane are (X,Z). ρ_A and ρ_B are the densities of drop and the surrounding media, respectively.

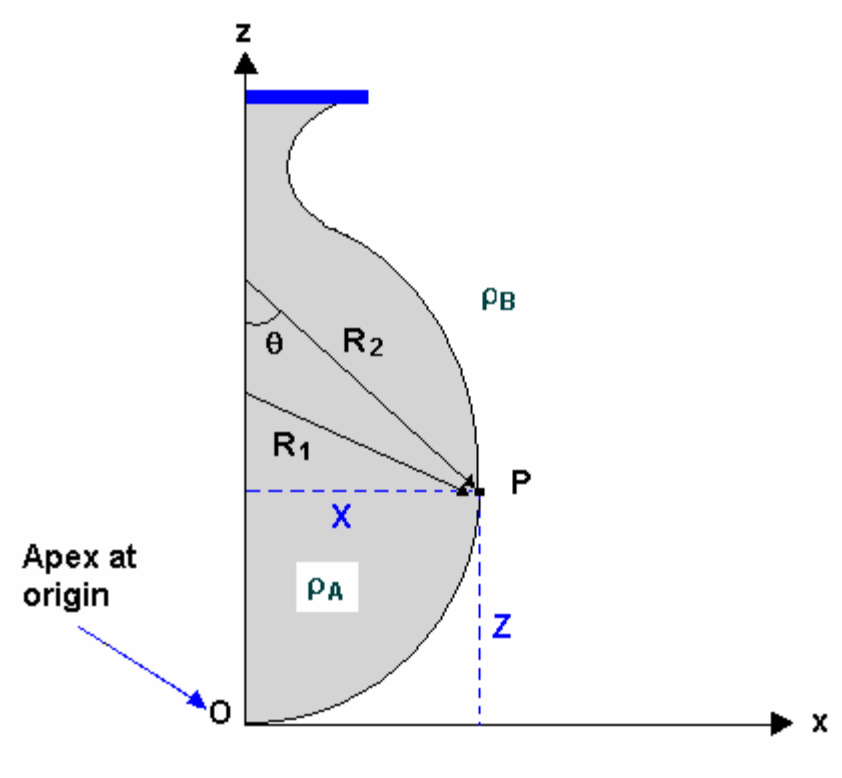

Figure 3.3 Definition of coordinates for describing a pendant droplet with an axis of symmetry.

When accounting for droplet symmetry, R_1 and R_2 must be equal at the apex. The value of the radius at this point is defined as b. Therefore, at the apex Equation 3.2 becomes:

$$\Delta p_{apex} = \frac{2\gamma}{b} \qquad \textbf{Eq. 3.3}$$

At point P, Δp equals the difference between the pressures in each of the phases and is given by:

$$\Delta p_p = \Delta p_{apex} + \Delta \rho g z = \frac{2\gamma}{b} + \Delta \rho g z \qquad \textbf{Eq. 3.4}$$

where g is the gravity, $\Delta\rho$ is the difference between the densities of the drop and the surrounding media. Equations 3.2, and 3.4 are combined to obtain:

$$\left(\frac{1}{R_2} + \frac{1}{R_1}\right) = \frac{2}{b} + \frac{\Delta \rho g z}{\gamma} \qquad \textbf{Eq. 3.5}$$

Now, based on analytical geometry, R_2 can be expressed as:

$$R_2 = \frac{x}{\sin\theta} \qquad \textbf{Eq. 3.6}$$

R_1 is given by:

$$\frac{1}{R_1} = \frac{\dfrac{d^2 z}{dx^2}}{\left[1 + \left(\dfrac{dz}{dx}\right)^2\right]^{\frac{3}{2}}} \qquad \textbf{Eq. 3.7}$$

R_1 and R_2 are calculated from Equations 3.6 and 3.7 and then the value of γ that best fits this data is determined. The Drop Shape Analyzer software applies the same approach but uses curvilinear coordinates. As indicated in Equation 3.5, fluid densities and local gravity are the only required input data besides the drop image.

The densities of toluene, *n*-heptane and water at 23 °C used in this work were taken from the CRC Handbook (1984), whereas densities at 60 °C were found in (Yaws 1999). A

density of 1.19 kg/m^3 was used for Athabasca extracted asphaltenes based on the results obtained by Alboudwarej et al. (2002). The total density of the asphaltene-solvent mixture was calculated by assuming ideal mixing.

3.2.2 Preparation of Drop Shape Analyzer

Prior to an experiment, the syringe, u-shaped needle and cuvette were rigorously cleaned to remove any trace of contaminants that may compromise the validity of the results. The cleaning procedure consisted of repeating the following steps two or three times:

1. Three flushes of the syringe, needle and cuvette with a solution of equal parts of *n*-heptane and 2-propanol.
2. Three flushes with pure 2-propanol.
3. Rinsing with excess distilled water at 60 °C.
4. Three flushes with toluene.

Each time a new solvent was used, the syringe, needle and cuvette were vacuum dried.

Note that to measure a true interfacial tension value; it is important that there is no net diffusion between the two liquid phases. Therefore, prior to executing any experiment, two droplets of each phase were deposited into the other one. The phases were left for one and a half hours to reach a saturation condition.

Finally, the calculation mode of the IT Concept software must be chosen before an experiment. The calculation mode command defines the number of iterations per second

used in an interfacial tension measurement; therefore, it allows the user to specify the degree of accuracy as well as the speed of a particular calculation. Three calculation algorithms are available: normal, precise, and high precise modes. Normal mode performs up to 10 iterations per second but is the least accurate. High precise and precise modes are useful for higher accuracy, performing up to 20 and 15 iterations per second respectively. A normal calculation mode was chosen for the isotherm experiments since asphaltene adsorption was evaluated under dynamic conditions and interfacial tension measurements were performed at a fast pace.

To confirm the accuracy of the instrument, interfacial tensions of pure solvents over water were measured at 23 °C and compared to literature values. Table 3.2 shows the comparison between results obtained by the drop shape analyzer and the corresponding literature values. The measured values were found to be within 2.7% of the literature values.

Table 3.2 Interfacial tensions of solvents against water

Solvent	Interfacial Tension (mN/m)	
	Experimental Values at 23 °C	Literature Values at 25 °C
toluene	35.1	35.8[a], 35.4[b]
n-heptane	49.7	50.1[a]

[a] (Li and Fu 1992) [b](Backes et al. 1990)

3.2.3 Solvent-Water Interfacial Tension

To calculate surface pressure it was necessary to obtain the interfacial tension of the pure solvent mixtures over water. Note that the interfacial tension between water and a solution of hydrocarbon solvents depends on the interfacial area coverage of each of the solute fluids, which are not necessarily the same as the bulk phase compositions (Yeung et al. 1998). Therefore, experimental interfacial tension measurements of toluene-*n*-heptane mixtures at different solvent ratios were performed at both 23 and 60°C against water. Results in terms of toluene volume fractions (ϕ) are presented in Table 3.3.

Table 3.3 Interfacial tensions of different heptol mixtures against water

Toluene volume fraction (ϕ)	1	0.75	0.50	0.25	0
Interfacial Tension 23°C	35.1	35.5	38.9	42.9	49.7
Interfacial Tension 60°C	35.8	36.1	39.3	42.9	48.6

As an additional check to the above experimental results, heptol-water interfacial tensions were modelled applying Handa and Mukerjee's equation (Yarranton and Masliyah 1996a) for a system of mutually insoluble organic and aqueous phases:

$$\gamma^{id} = \gamma_2^0 - RT\Gamma_m \ln\{1 + (q_{12} - 1)x_1\} \qquad \textbf{Eq. 3.8}$$

where γ^{id} is the ideal interfacial tension of the organic mixture over water, γ_2^0 is the interfacial tension of pure component 2 against water, R is the universal gas constant, T is the absolute temperature, Γ_m is the monolayer surface coverage, x_1 is the molar fraction of

component 1 and q_{12} is the relative adsorption ratio of component 1 versus component 2 and is given by the expression:

$$q_{12} = \exp\left\{\frac{\gamma_2^0 - \gamma_1^0}{RT\Gamma_m}\right\} \qquad \textbf{Eq. 3.9}$$

Here, it is assumed that the surface is ideal and that all constituents have the same surface coverage per molecule (Γ_m) of 0.00415 mmol/m^2 as suggested by Yarranton and Masliyah (1996a). The predicted interfacial tension data from the ideal model were plotted against the experimental data in Figure 3.4. As can be seen in the plot, the model fits the data to within 1 mN/m.

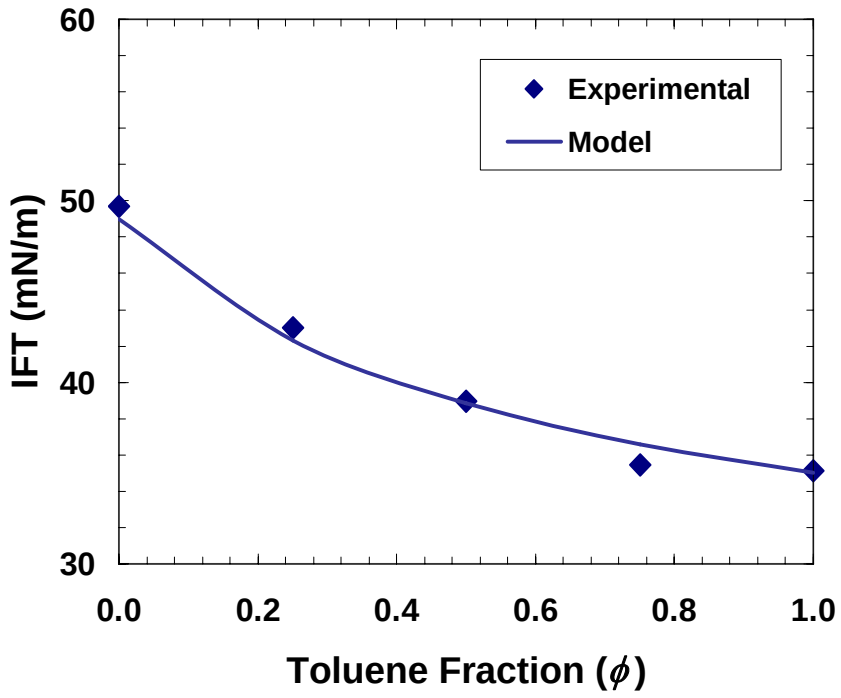

Figure 3.4 Comparison of experimental and theoretical heptol-water interfacial tension values at different toluene volume fractions (ϕ).

3.2.4 Surface Pressure Isotherm Experimental Procedure

The experiments began with the preparation of asphaltene-solvent solutions. The necessary mass of asphaltenes was dissolved in a heptol mixture to prepare asphaltene concentrations of 1, 10 and 20 kg/m^3. Heptol mixtures with toluene volume fractions (ϕ) of 1, 0.50 and 0.25 were used. The solutions were then sonicated for five minutes to ensure complete asphaltene dissolution and homogeneity.

Another set of isotherm experiments were performed using diluted bitumen as the organic phase instead of asphaltenes-solvent solutions. Athabasca bitumen was dissolved in heptol mixtures at heptol/bitumen ratios of 9:1, 7:1, 5:1 and 3:1. The dissolved bitumen was shaken on a sonicator for 10 minutes for complete mixing.

A droplet of the asphaltene-solvent (or bitumen-solvent) solution was formed at the tip of a capillary, immersed in distilled water. The droplet was allowed to age at times varying from 10 minutes to 8 hours before compressing the oil/water interface. The initial drop diameter was approximately 1.2 mm. The compression was performed in consecutive steps by retracting the drop into the capillary at a reverse speed of the drive motor of the Drop Shape Analyzer apparatus. After each step, the interfacial tension and droplet surface area were measured. Data was collected until visual crumpling of the droplet was observed. Figures 3.5 (a) and (b) are images of a droplet before and after crumpling, respectively. The skin remaining after fluid retraction is clearly visible at the edges of the droplet in Figure 3.5 (b).

At least two runs were performed to ensure repeatability. Figure 3.6(a) shows a typical raw data set of interfacial tension (IFT) vs. surface area. The corresponding surface pressure isotherm is plotted in Figure 3.6(b).

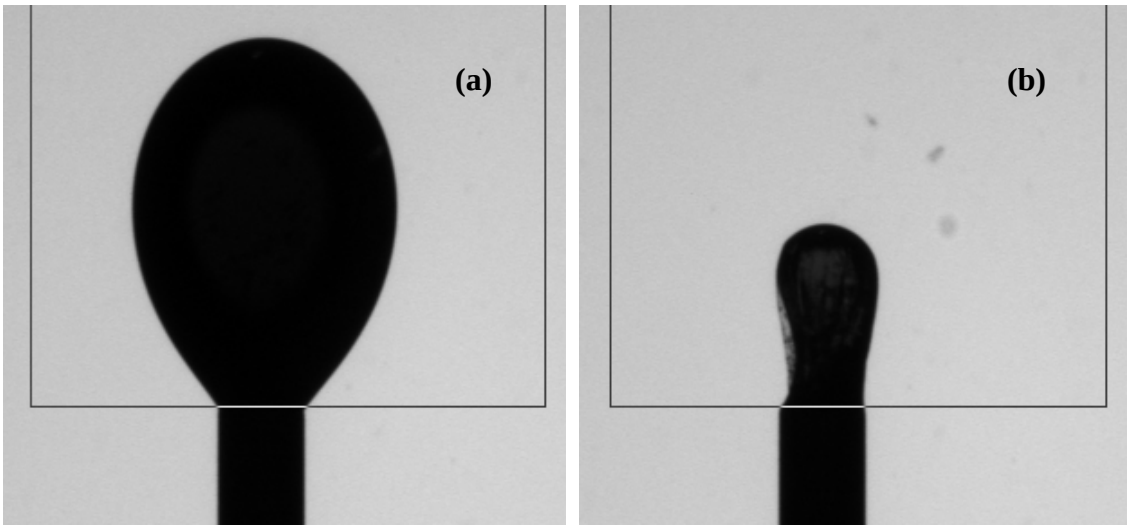

Figure 3.5 Image of a droplet of 1 kg/m^3 asphaltenes in toluene surrounded by water at one hour of aging time and 23 °C: (a) before crumpling and (b) after crumpling.

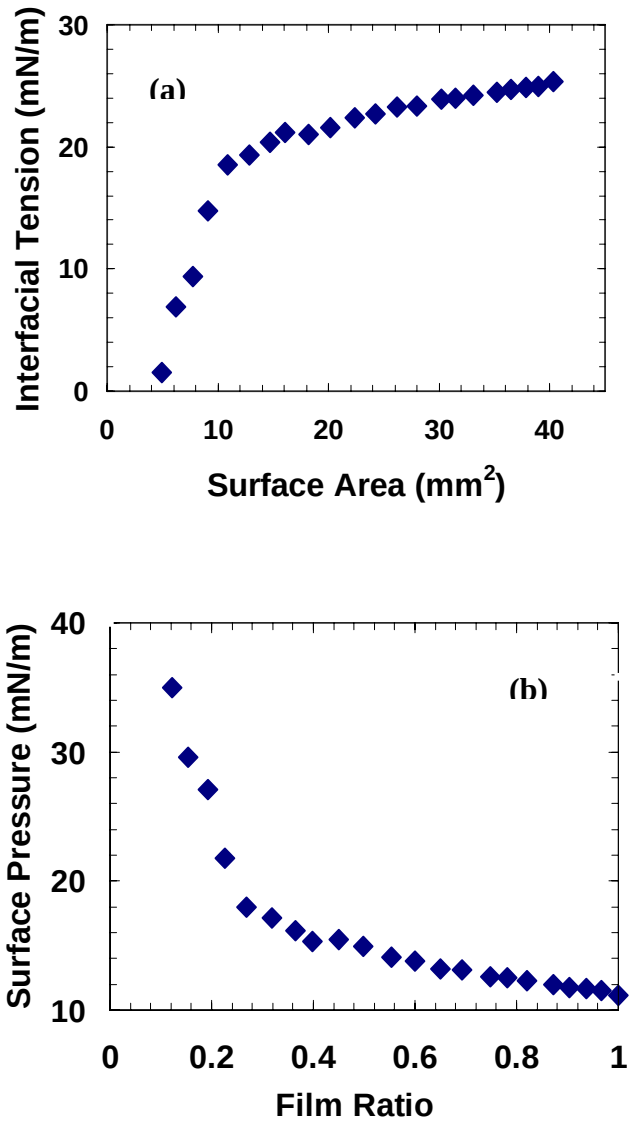

Figure 3.6 (a) Interfacial Tension vs. Surface area plot for 1 kg/m^3 of asphaltenes in pure toluene vs. water at 60 minutes of aging time and at 23 °C. (b) Surface Pressure Isotherm for obtained from the same data.

One experimental parameter that required consideration was the time interval between compression steps. Consider Figure 3.7, a plot of the interfacial tension (IFT) of 1.0 kg/m³ asphaltenes in toluene at 23°C. The rapid initial decrease in IFT over several minutes is a result of asphaltenes diffusing from the bulk phase to the interface. The subsequent slow decrease in IFT over several hours indicates that there is a replacement of some of the adsorbed asphaltene components with more surface-active asphaltene components or that there is a slow structural rearrangement on the interface. The slow dynamics suggest that short compression steps may not provide an equilibrium measurement because asphaltenes may still be diffusing during the measurement in response to the compression. Although the dynamic condition of the surface pressure is not a thermodynamic property (Horvath-Szabo et al. 2005), it is a measure of the time-dependent film properties and may be more relevant to emulsion stability over finite times. An equilibrium surface pressure can be obtained if sufficient time is allowed between steps.

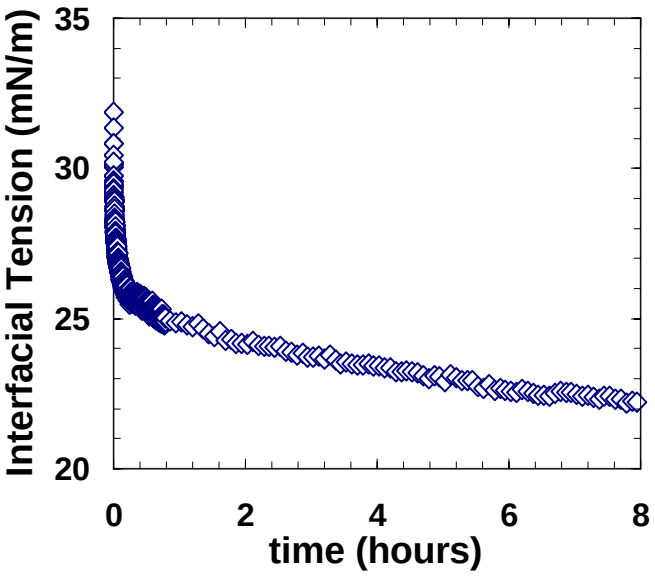

Figure 3.7 Interfacial tension versus time for 1.0 kg/m³ asphaltenes in toluene

To assess the effect of the time interval between successive compression steps, surface pressure isotherms were obtained at step intervals of 0.5, 2 and 5 minutes. The results for a system of 1 kg/m^3 of asphaltenes in pure toluene aged for 60 minutes are shown in Figure 3.8. The variation in surface pressure among the three interval scenarios is small except at low film ratios, suggesting that after 30 seconds there is little asphaltene diffusion to the bulk phase as a result of compression except at low film ratios. Consequently, there was some scatter in the data at low film ratios. However, for convenience all of the experiments were conducted with the minimum step interval of approximately 30 seconds.

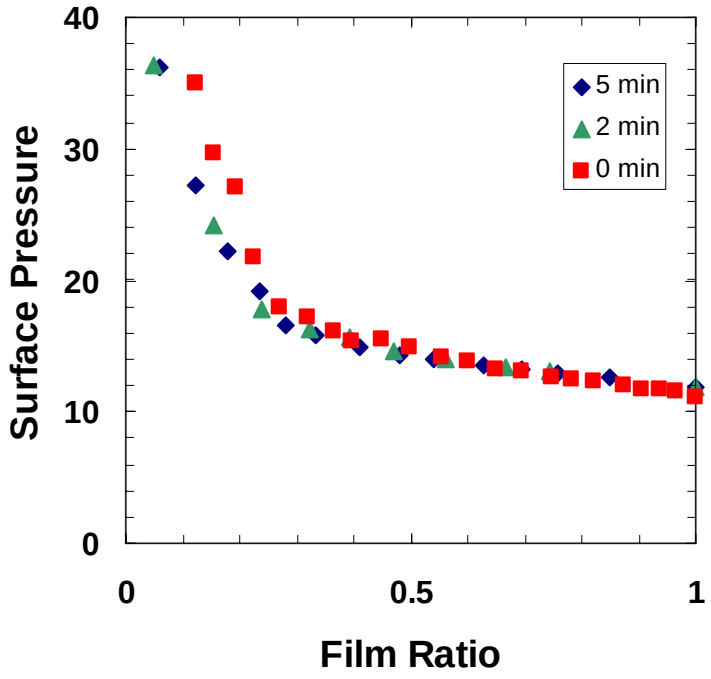

Figure 3.8 Comparison of different isotherms for 1 kg/m^3 asphaltenes in toluene at time intervals of zero, two and five minutes.

3.2.5 Comparison with Literature Data

To confirm the validity of the technique, the surface pressure isotherm shown in Figure 3.6(b) was compared with Langmuir trough experiments conducted by Zhang et al. (2003b) also using Athabasca asphaltenes (Figure 3.9). To make the comparison, the data must be plotted versus area per molecule. The measured droplet surface areas were converted to an area per molecule as follows. The area per molecule for an undisturbed drop in a given solvent at 23°C was determined from the Gibbs adsorption isotherm:

$$A_n = \frac{RT}{d\gamma / d\ln C_A} \qquad \textbf{Eq. 3.10}$$

where A_n is the surface area per molecule on the interface, R is the universal gas constant, T is temperature, and C_A is the asphaltene molar concentration. Since asphaltenes self-associate and their effective molar mass depends on concentration, the molar asphaltene concentration was used rather than the asphaltene mass concentration, as recommended by (Sztukowski et al. 2003). The calculated area per molecule was assumed to apply at the initial condition of the surface pressure isotherm; hence, the area at any film ratio is given by $A_n*(A/Ao)$. The results compare well with Zhang et al.'s, as shown in Figure 3.9.

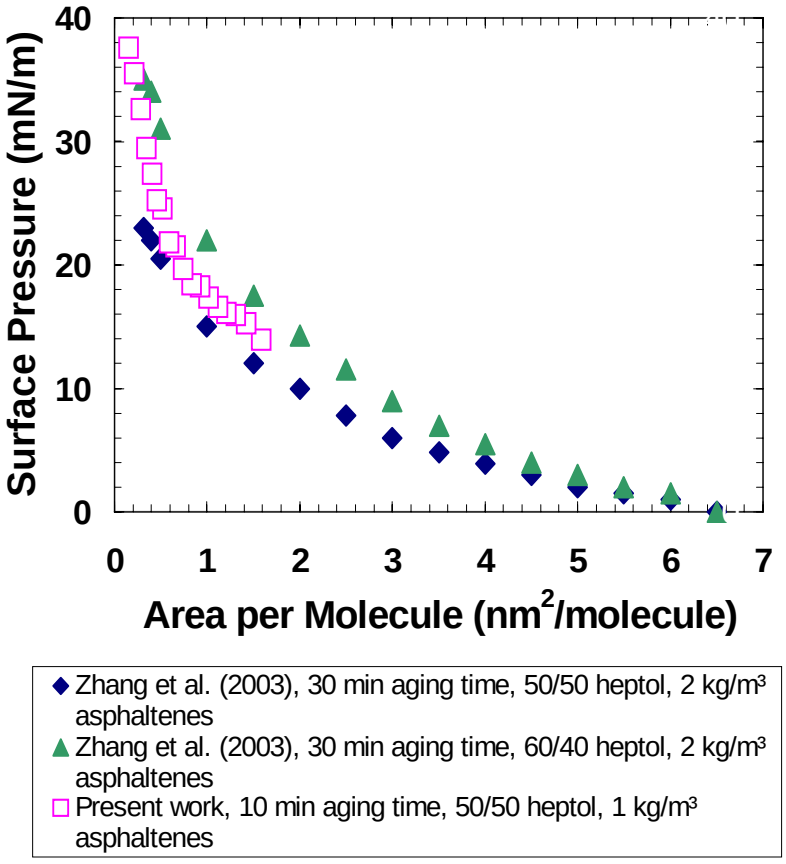

Figure 3.9 Comparison of surface pressure isotherms of asphaltene films with similar Zhang et al. (2003) Langmuir trough experiments.

CHAPTER 4- INTERFACIAL PROPERTIES EVALUATION BY SURFACE PRESSURE ISOTHERMS

This chapter presents the results of "dynamic" surface pressure isotherm studies on film formation and interfacial film properties. The film formation process is evaluated through the changes on film compressibility. The film properties are measured as a function of asphaltene concentrations, solvent compositions, aging times, and temperature.

Surface isotherms of real systems consisting of Athabasca bitumen dissolved at different ratios of heptol mixtures over water are also plotted and are presented in Appendix A. The evaluation of the interfacial properties of these systems is recommended as part of the future work.

4.1 Interfacial Compressibility

One measure of film rigidity is its compressibility. The compressibility of the interfacial film can be expressed analogously to bulk compressibility as follows:

$$c_I = -\frac{1}{A}\left(\frac{dA}{d\pi}\right)_T = -\left(\frac{d\ln A}{d\pi}\right)_T \qquad \textbf{Eq. 4.1}$$

where c_I is the compressibility of the interfacial film, A the interfacial area and π the surface pressure. The compressibilities can be calculated from the slopes of the surface pressure isotherms.

Figure 4.1 shows two surface pressure isotherms measured for 1 kg/m³ asphaltenes dissolved in pure toluene: (a) with 10 minutes of aging before compression; (b) after 60 minutes of aging. In both cases, the film compressibility is high (approximately 0.2 m/mN) at high film ratios. This region is considered to be a liquid-like interfacial phase, here denoted “Phase 1”. In Figure 4.1a, the film remained in Phase 1 at least until the droplet became very small and the measurement became invalid (high scatter region). In Figure 4.1b, the film experienced a phase change at a film ratio of 0.28. The compressibility decreased fivefold to 0.047 m/mN. This solid-like or rigid phase was termed, “Phase 2”. A similar reduction in compressibility was observed whenever an apparent interfacial phase change took place. In almost all cases, further contraction leads to crumpling of the interface; that is, the compressibility is reduced to zero. Similar phase change behaviour including a film fracture observation was reported by Nordli et al. (1990).

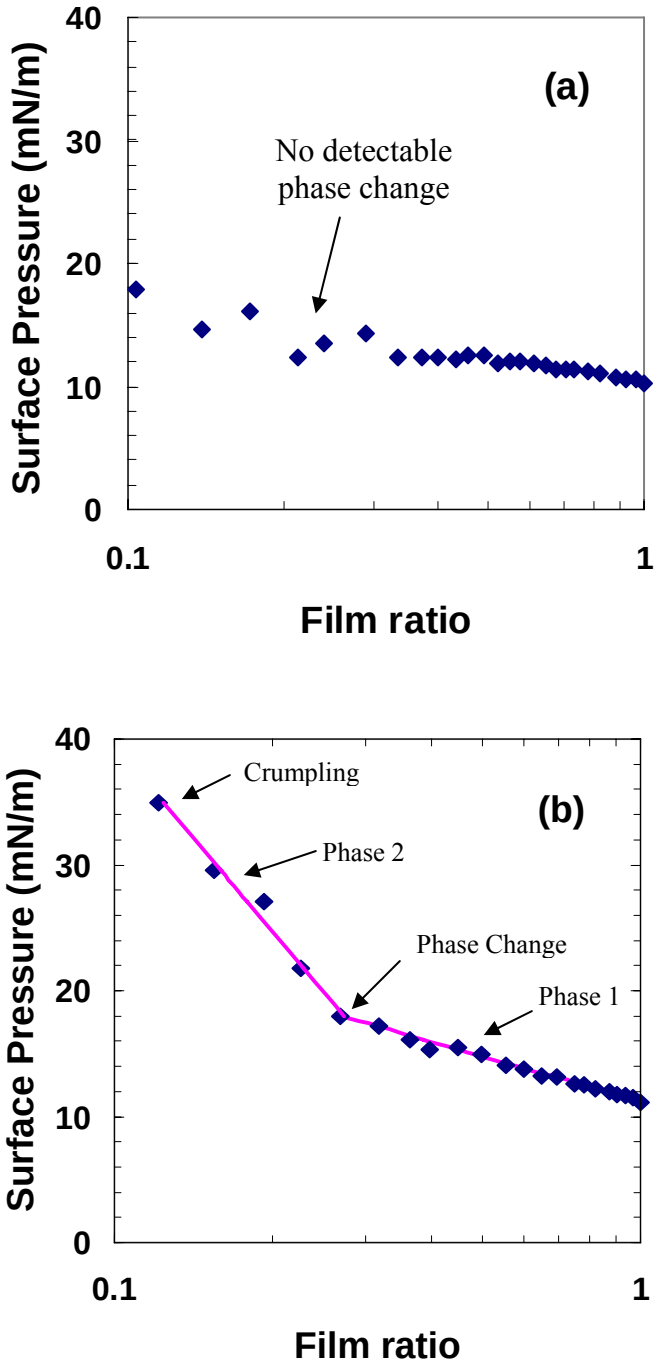

Figure 4.1 Detection of low compressibility film formation in semilog coordinates for a) 1 kg/m³ asphaltenes in pure toluene at 10 min of aging time and 23 °C b) 1 kg/m³ asphaltenes in pure toluene at 60 min of aging time and 23 °C.

Of relevance to emulsion stability is how much compression must occur before the low compressibility and zero compressibility films appear. If little compression is required, only a small amount of coalescence can occur before the low compressibility film appears and inhibits further coalescence. Therefore, the film ratio at which the incompressible film appeared was determined from the change in slope on the surface pressure isotherms. The film ratio at which the crumpling occurred is always the point at the lowest reported film ratio shown for a given isotherm. The Phase 1 and Phase 2 compressibilities as well as the film ratios at which the phase changed and at which crumpling occurred are listed in Tables 4.1 to 4.3 for all the experiments performed in this work.

In this work, a reproducibility analysis was performed with a confidence interval of 90% for all measurements. Details can be found in Appendix B. The Phase 1 compressibilities vary from the reported value on average by ±0.246 m/mN, ±0.073 m/mN and ±0.071 m/mN for pure toluene, 25/75 heptol and 50/50 heptol systems, respectively. On average, the Phase 2 compressibilities vary from the reported value by ±0.032 m/mN, ±0.024 m/mN and ±0.028 m/mN for pure toluene, 25/75 and 50/50 heptol systems, respectively.

Phase change film ratios vary from the reported value on average by ±0.077 m/mN, ±0.075 m/mN and ±0.128 m/mN for pure toluene, 25/75 heptol and 50/50 heptol systems, respectively. On average, the crumpling film ratios vary from the reported value by ±0.034 m/mN, ±0.044 m/mN and ±0.078 m/mN for pure toluene, 25/75 heptol and 50/50 heptol systems, respectively.

Note that this apparent compressibility is not a true thermodynamic property because the number of molecules on the interface is not fixed. In other words, asphaltenes may be free to leave the interface upon compression. A thermodynamically valid compressibility can be measured only when all of the asphaltenes are irreversibly adsorbed. However, the apparent compressibility may be a more useful measure for emulsion stability studies because asphaltenes are not necessarily bound to the interface in an emulsion.

Table 4.1 Interfacial compressibilities, phase change film ratio, and crumpling film ratio for droplets of asphaltenes in toluene surrounded by water at 23°C.

Aging Time (min)	Phase 1 Compressibility (m/mN)	Phase 2 Compressibility (m/mN)	Phase Change Film Ratio	Crumpling Film Ratio
1 kg/m³				
10	0.42	0.037	0.13	0.06
30	0.26	0.040	0.22	0.10
60	0.19	0.047	0.27	0.12
240	0.090	0.050	0.52	0.22
480	0.087	0.052	0.47	0.19
10 kg/m³				
10	0.61	N/A	N/A	N/A
30	0.58	0.044	0.20	0.09
60	0.43	0.024	0.19	0.13
240	0.14	0.043	0.48	0.25
480	0.096	0.047	0.55	0.33
20 kg/m³				
10	0.59	N/A	N/A	N/A
60	0.42	0.034	0.24	0.17
240	0.18	0.040	0.48	0.27
480	0.11	0.037	0.55	0.30

Table 4.2 Interfacial compressibilities, phase change film ratio, and crumpling film ratio for droplets of asphaltenes in 25/75 heptol surrounded by water at 23°C.

Aging Time (min)	Phase 1 Compressibility (m/mN)	Phase 2 Compressibility (m/mN)	Phase Change Film Ratio	Crumpling Film Ratio
1 kg/m³				
10	0.16	0.065	0.23	0.092
30	0.13	0.073	0.41	0.16
60	0.16	0.059	0.47	0.22
240	0.088	0.054	0.52	0.28
480	0.076	0.059	0.73	0.33
10 kg/m³				
10	0.49	N/A	N/A	N/A
30	0.36	0.047	0.19	0.12
60	0.30	0.063	0.32	0.18
240	0.16	0.064	0.48	0.26
480	0.12	0.056	0.60	0.36
20 kg/m³				
10	0.45	0.054	0.17	0.08
30	0.44	0.060	0.22	0.13
60	0.30	0.035	0.24	0.15
240	0.13	0.046	0.43	0.27
480	0.11	0.054	0.62	0.35

Table 4.3 Interfacial compressibilities, phase change film ratio, and crumpling film ratio for droplets of asphaltenes in 50/50 heptol surrounded by water at 23°C.

Aging Time (min)	Phase 1 Compressibility (m/mN)	Phase 2 Compressibility (m/mN)	Phase Change Film Ratio	Crumpling Film Ratio
1 kg/m³				
10	0.13	0.075	0.41	0.094
30	0.12	0.064	0.42	0.16
60	0.11	0.068	0.53	0.19
240	0.051	-	1.00	0.45
480	0.032	-	1.00	0.69
10 kg/m³				
10	0.23	0.074	0.36	0.13
30	0.18	0.061	0.36	0.19
60	0.13	0.065	0.52	0.24
240	0.082	-	1.00	0.39
480	0.042	-	1.00	0.61
20 kg/m³				
10	0.40	0.061	0.28	0.15
30	0.23	0.071	0.43	0.20
60	0.15	0.074	0.54	0.22
240	0.054	-	1.00	0.47

4.2 Effect of Asphaltene Concentration

Figures 4.2 to 4.4 show the surface pressure isotherms of interfacial films of 1, 10, or 20 kg/m³ asphaltenes after 60 minutes of aging at 23°C in toluene, 25/75 heptol and 50/50 heptol, respectively. Asphaltene concentration had relatively little effect on the surface pressure isotherms. In general, for most solvents and aging times, the highest "phase change" film ratio was observed at an asphaltene concentration of 1 kg/m³ and the lowest at 10 kg/m³. In other words, low compressibility films formed more readily at the lowest

concentration considered (1 kg/m³) and less readily at the intermediate concentration of 10 kg/m³. The appearance of rigid skins at more dilute asphaltene solutions were also observed by (Gafonova and Yarranton 2001; Taylor et al. 2002; Yarranton et al. 2000b).

The small effect of asphaltene concentration at these conditions is not surprising. Above 1 kg/m³, an increase in asphaltene concentration does not significantly increase the molecular surface coverage because the interface is almost saturated. The average molar mass of the self-associated asphaltenes does increase. However, as shown by Sztukowski et al. (2003), the area occupied by the self-associated asphaltenes is almost invariant; they simply form thicker interfaces.

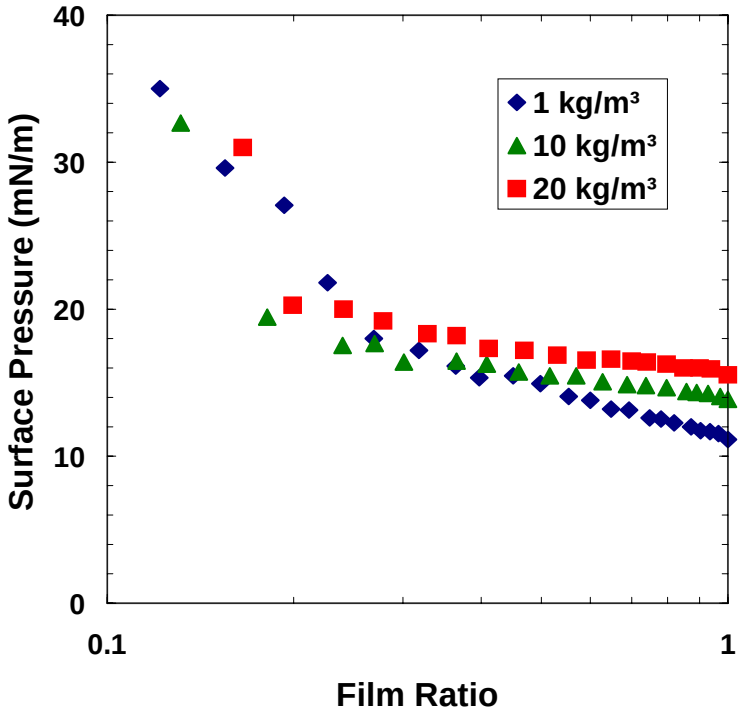

Figure 4.2 Effect of asphaltene concentration on surface pressure isotherms in pure toluene at 60 minute aging time and 23 °C.

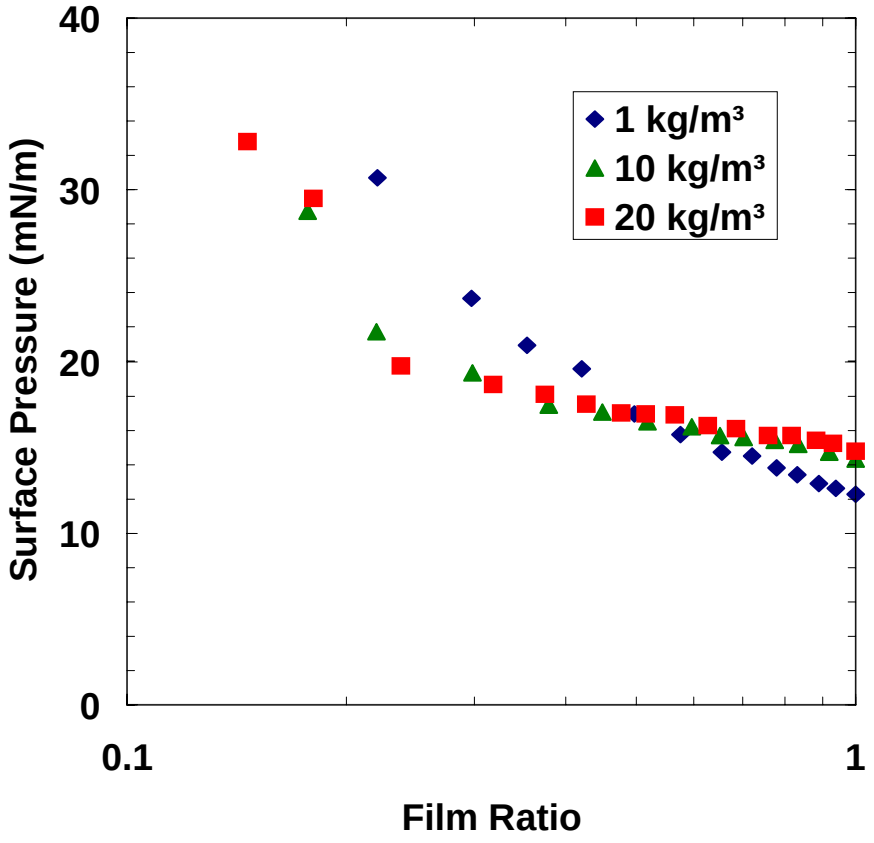

Figure 4.3 Effect of asphaltene concentration on surface pressure isotherms in 25/75 heptol at 60 minute aging time and 23 °C.

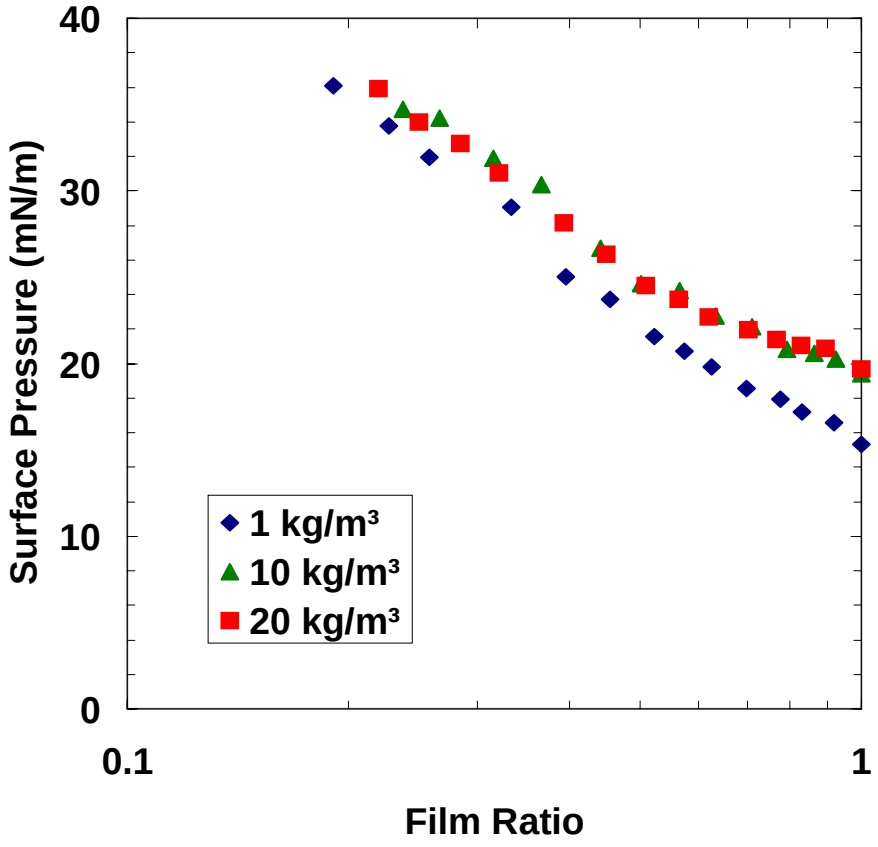

Figure 4.4 Effect of asphaltene concentration on surface pressure isotherms in 50/50 heptol at 60 minute aging time and 23 °C.

4.3 Effect of Solvent

Figures 4.5 to 4.7 show the effect of different solvent systems on surface pressure isotherms of interfacial films of 1,10 and 20 kg/m³ asphaltenes, respectively, after 60 minutes of aging and at 23°C. For most asphaltene concentrations and aging times, there is little difference between the surface pressure isotherms in toluene and 25/75 heptol. However, the films in 50/50 heptol show somewhat lower initial compressibility and form low compressibility films at high film ratios.

Results are consistent with the expected asphaltene behaviour in less aromatic solvents (Taylor et. al., 1992; Mclean and Kilpatrick, 1997; Ese et al., 1998). As the *n*-heptane content increases, the continuous phase becomes a poorer solvent for the asphaltenes and they are more likely to be irreversibly adsorbed. It is the irreversibility of the adsorption that results in incompressible films.

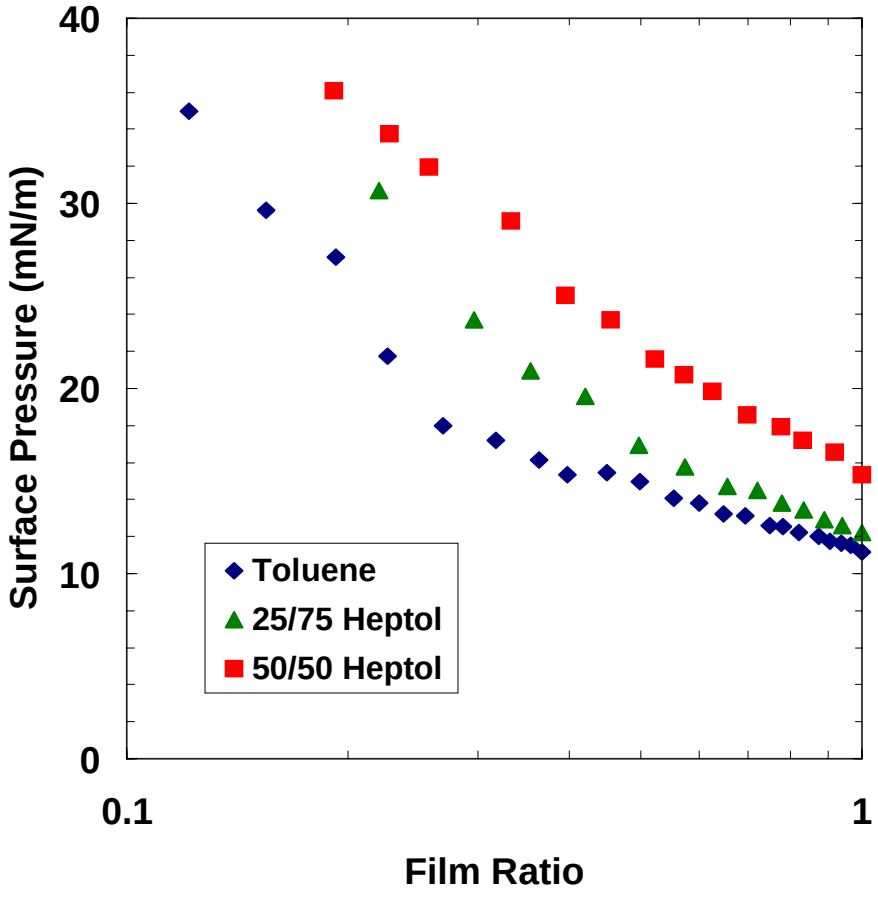

Figure 4.5 Effect of solvent on surface pressure isotherms for 1 kg/m³ asphaltenes after 60 minutes of aging time at 23 °C.

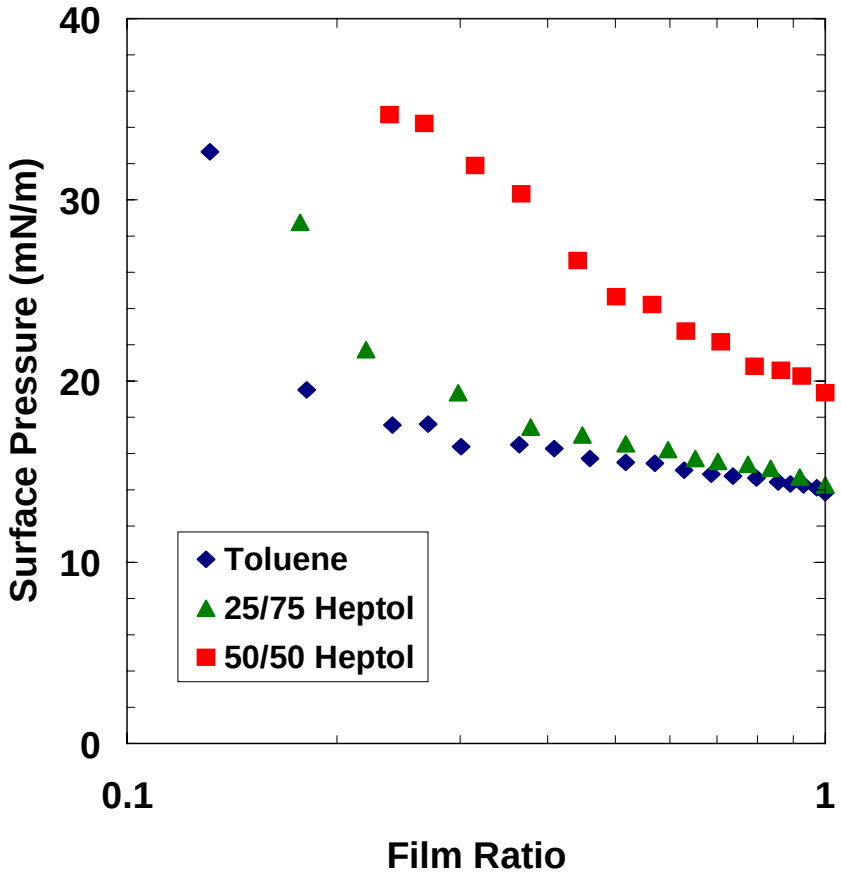

Figure 4.6 Effect of solvent on surface pressure isotherms for 10 kg/m³ asphaltenes after 60 minutes of aging time at 23 °C.

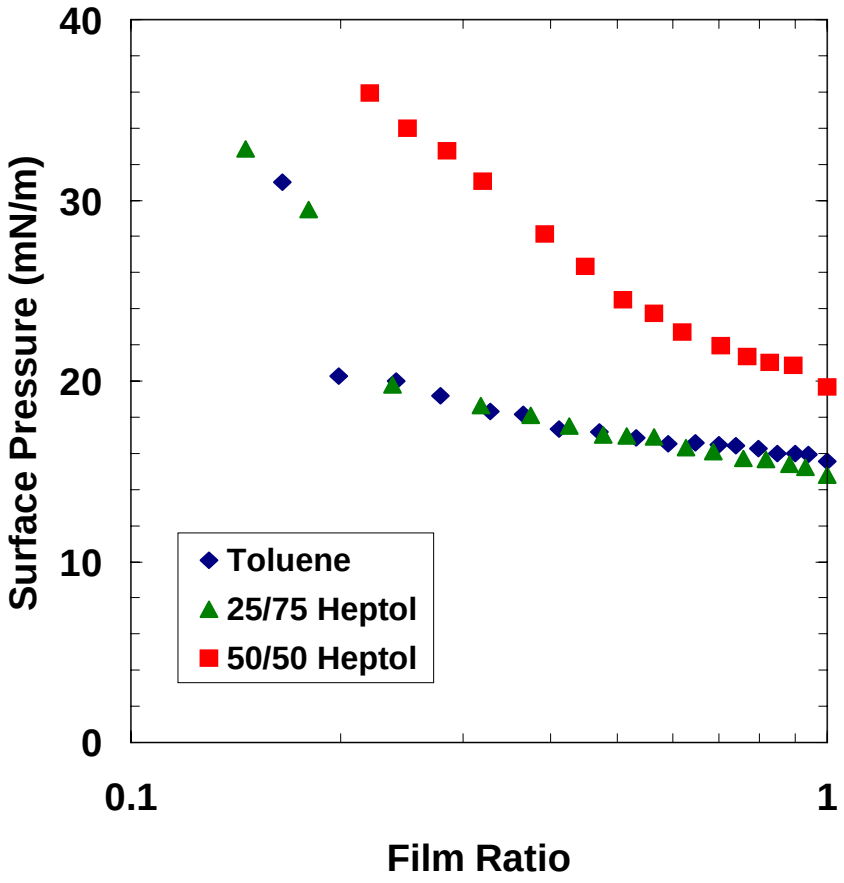

Figure 4.7 Effect of solvent on surface pressure isotherms for 20 kg/m³ asphaltenes after 60 minutes of aging time at 23 °C.

4.4 Effect of Aging Time

Figures 4.8 to 4.10 show the surface pressure isotherms of interfacial films of 1,10 and 20 kg/m³ asphaltenes in toluene after aging from 10 minutes to 8 hours at 23°C, respectively. Film compressibility decreases and higher "phase change" film ratios are observed in all cases with increased aging. The decrease in film compressibility upon aging suggests that a cross-linked network of asphaltenes is gradually established on the interface. The increase in "phase change" film ratio with aging is also shown in Figure 4.11. The significant increase in the "phase change" film ratio in 50/50 heptol solutions is also apparent. Note that the film ratio at which crumpling occurred followed similar trends.

It appears that at low aging time, the film is reversible or nearly reversible but that at higher aging times, at least some of the asphaltenes are irreversibly adsorbed. Freer et al. (2003) and Zhang et al. (2005a) also observed irreversible adsorption of asphaltenes in toluene solutions.

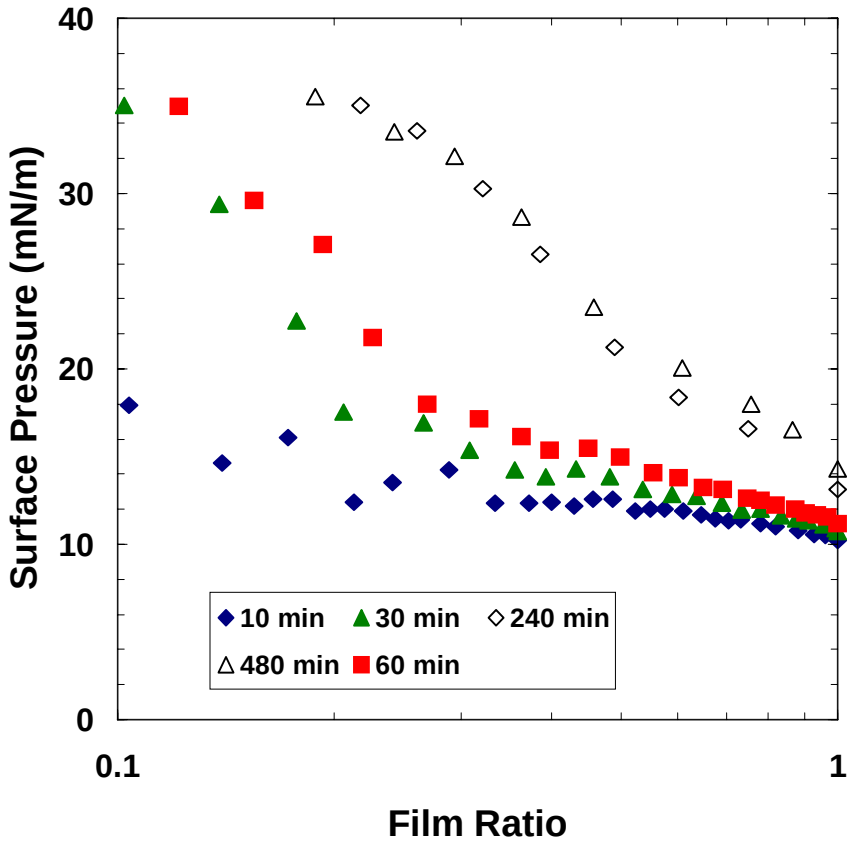

Figure 4.8 Effect of aging time on surface pressure isotherms for 1 kg/m³ asphaltenes on pure toluene at 23 °C.

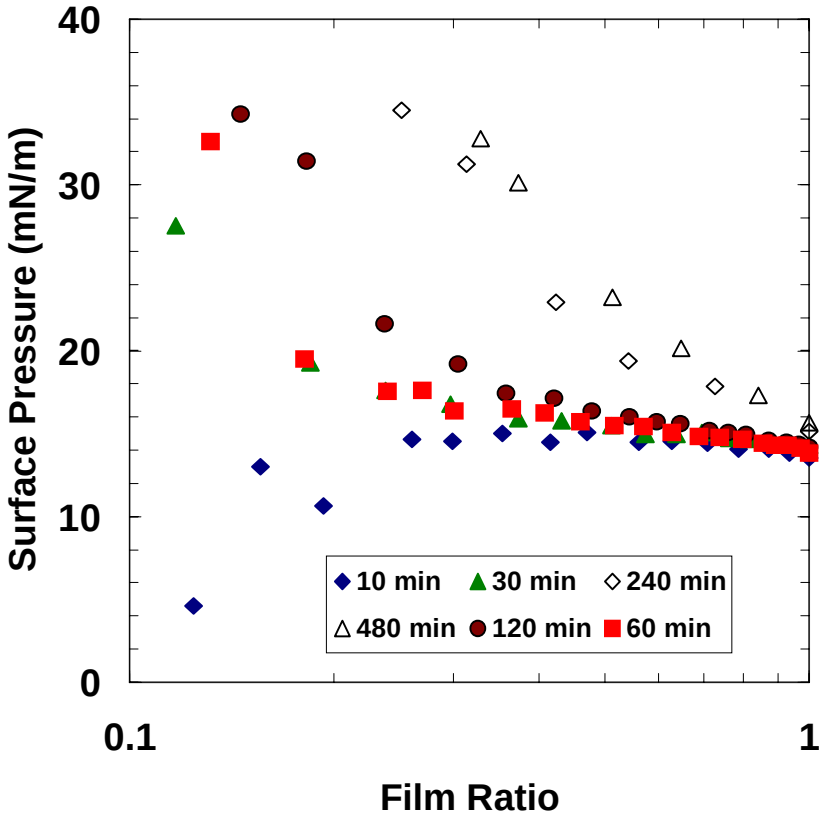

Figure 4.9 Effect of aging time on surface pressure isotherms for 10 kg/m³ asphaltenes on pure toluene at 23 °C.

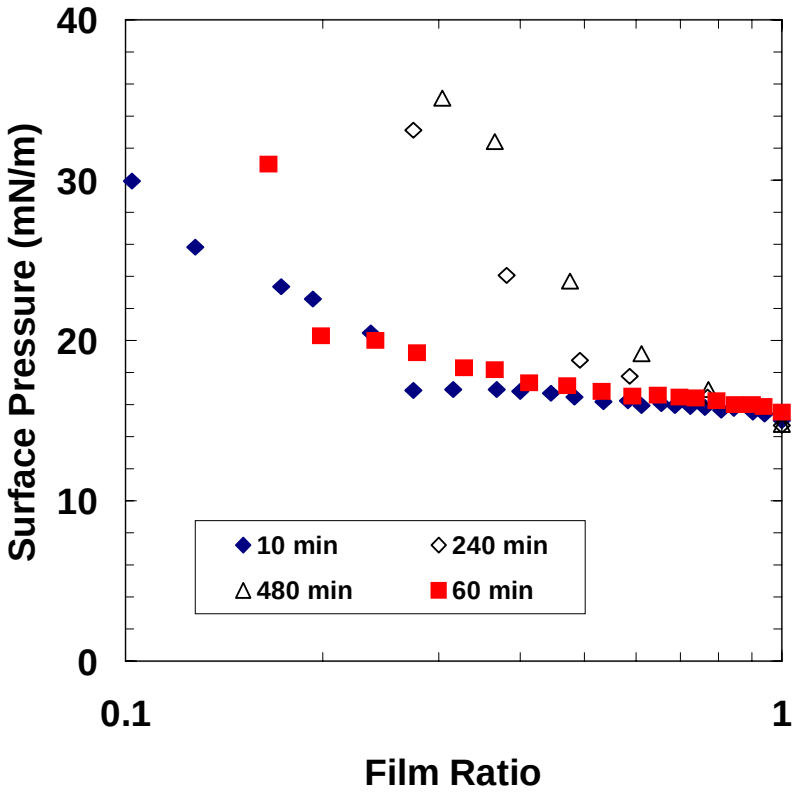

Figure 4.10 Effect of aging time on surface pressure isotherms for 20 kg/m³ asphaltenes on pure toluene at 23 °C.

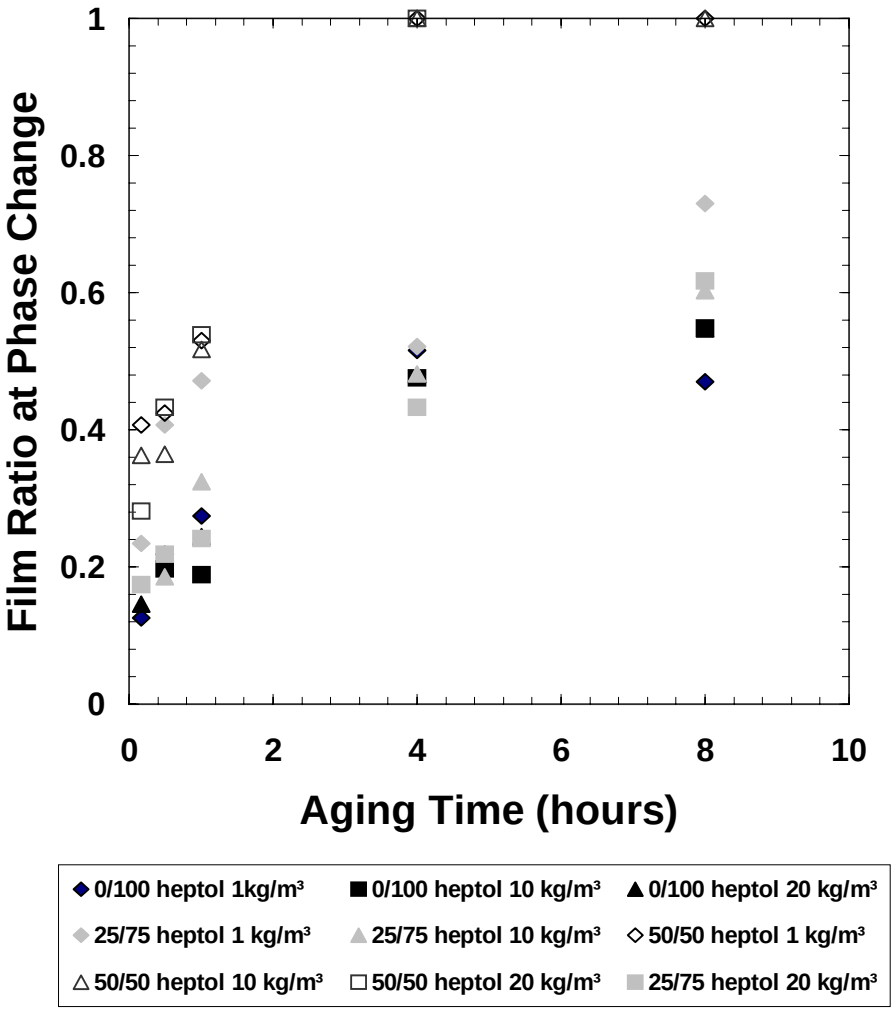

Figure 4.11 Effect of aging on the film ratio at which low compressibility film forms.

4.5 Effect of Temperature

Figure 4.12 shows the effect of temperature on 1 kg/m³ asphaltenes in toluene, 25/75 heptol and 50/50 heptol, at both 23 and 60°C and at aging times of 10 and 60 minutes. An increase in temperature has minor effects on film compressibility. Figures 4.13 and 4.14 illustrate the effect of temperature on 10 kg/m³ and 20 kg/m³ asphaltenes respectively in (a) toluene and (b) 25/75 heptol. At 60 °C the phase change film ratios remain unchanged and a slight decrease in surface pressure occurs regardless of the aging time, shifting the isotherms downwards. This is expected from the decrease in interfacial tension with temperature. The same behaviour is observed for all asphaltene concentrations and solvent cases.

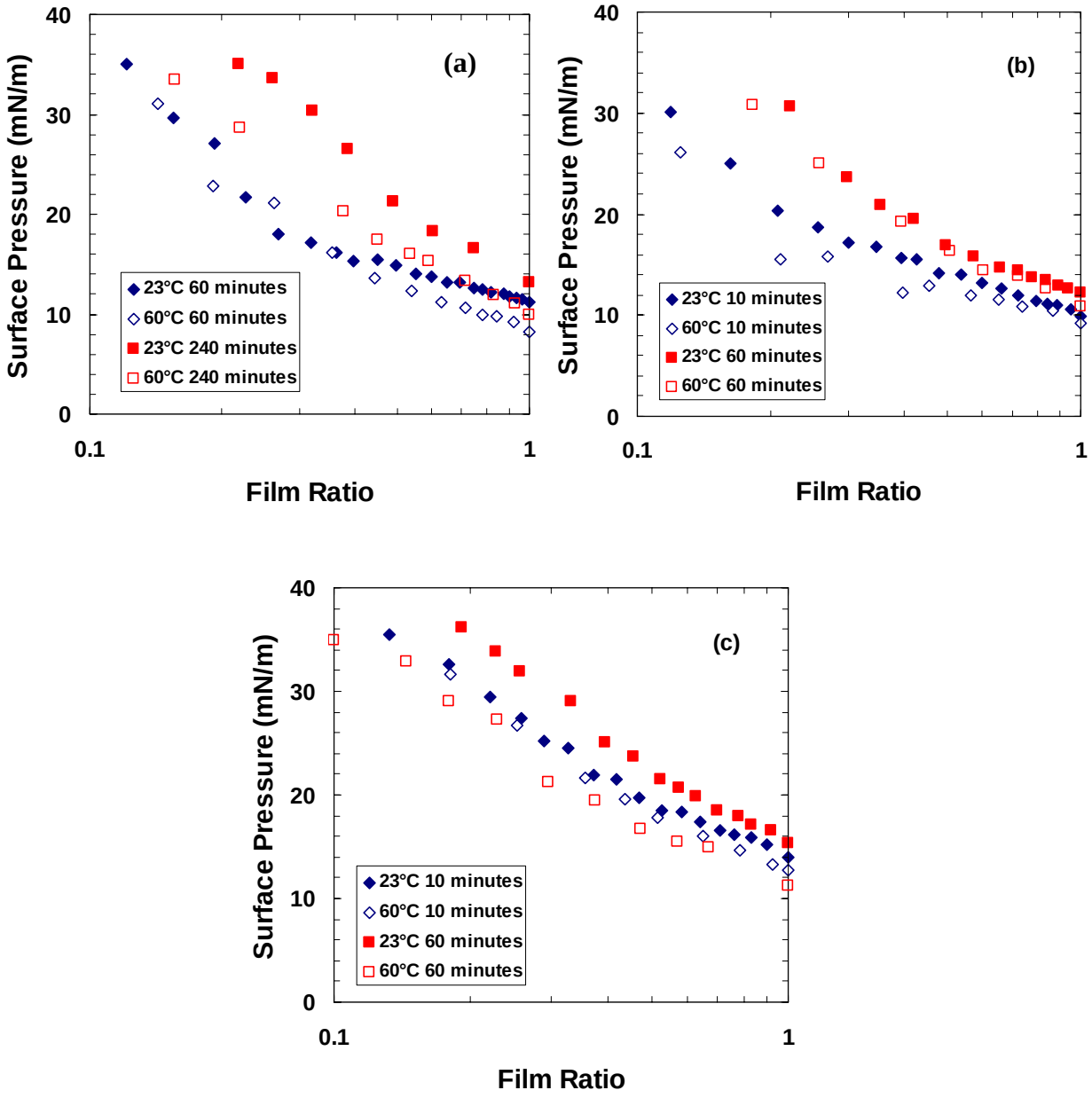

Figure 4.12 Effect of temperature on surface pressure isotherms for 1 kg/m³ asphaltenes in a) toluene, b) 25/75 heptol, c) 50/50 heptol over water at both 23 and 60 °C for different aging times.

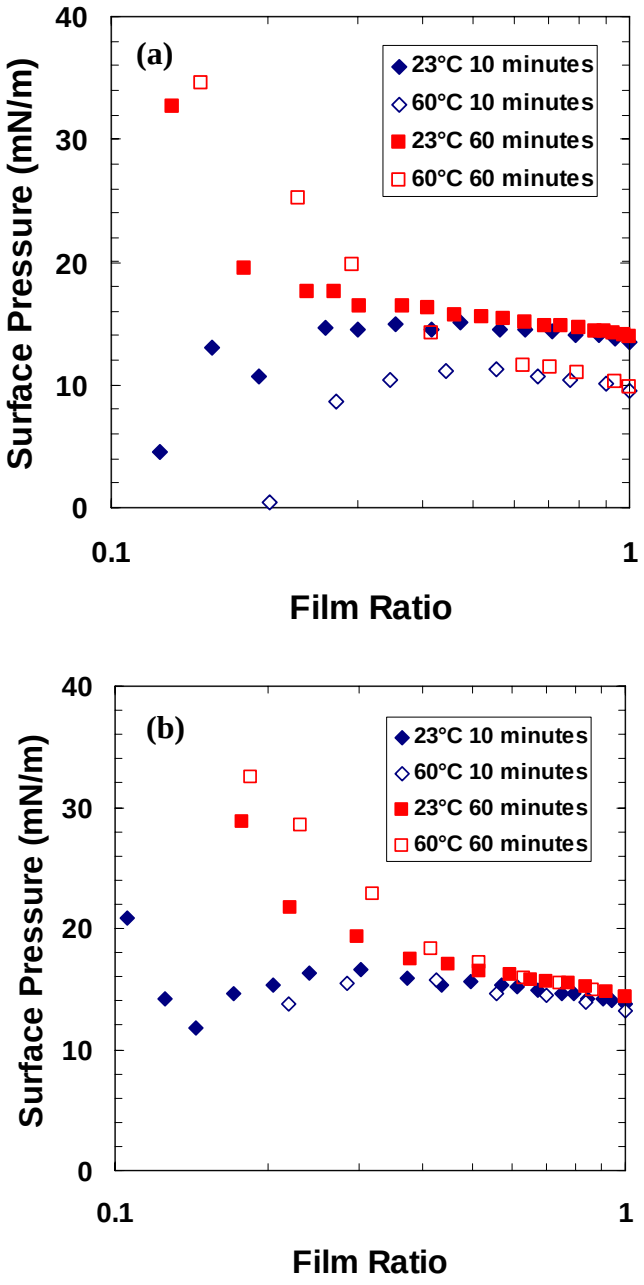

Figure 4.13 Effect of temperature on surface pressure isotherms for 10 kg/m³ asphaltenes in a) toluene, b) 25/75 heptol over water at both 23 and 60 °C for different aging times.

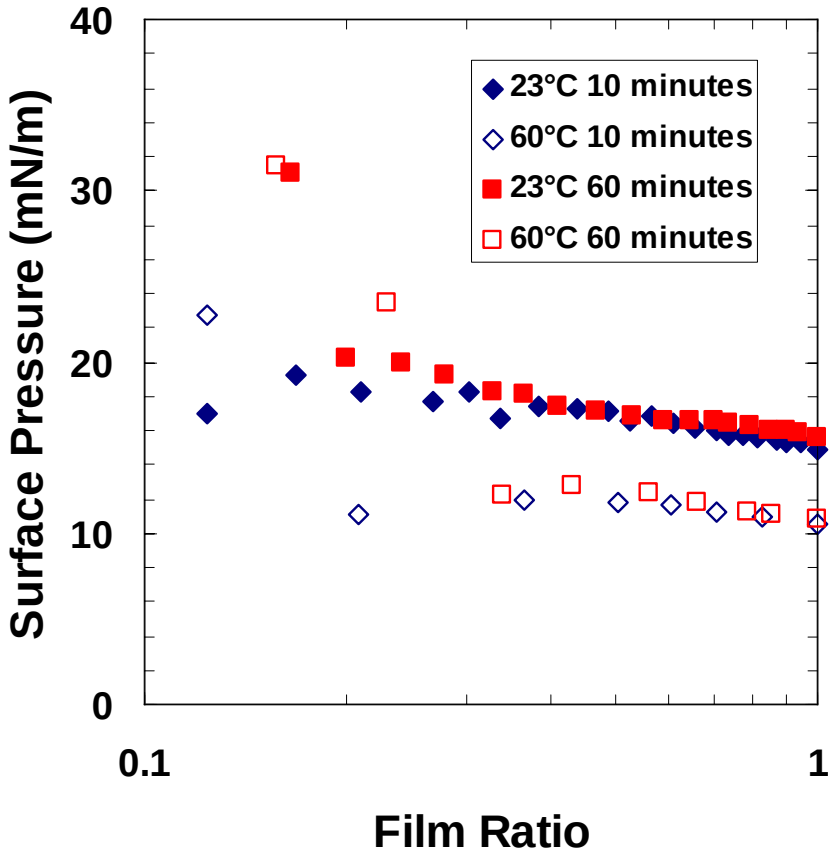

Figure 4.14 Effect of temperature on surface pressure isotherms for 20 kg/m³ asphaltenes in toluene over water at both 23 and 60 °C for different aging times.

CHAPTER 5- COALESCENCE PREDICTION BY INTERFACIAL PROPERTIES

In this chapter, emulsion coalescence rate is predicted from surface pressure isotherm data for asphaltenes in heptol over water. The effect of interfacial compressibility on emulsion coalescence is investigated. The experimental coalescence rate of model emulsions prepared from the same components is assessed from the change in the mean diameter of the emulsion over time at 23 ºC. A correlation between the initial coalescence rate and film compressibility is found. The time dependence of the surface pressure isotherm data is determined; that is, the trends of Phase 1 and Phase 2 compressibilities, the phase change film ratio, and the crumpling film ratio. At each time interval, the film properties are analyzed, and the compressibility is determined. Finally, the change over time in coalescence rate and drop size of the model emulsions at 23 ºC are predicted.

5.1 Coalescence Rate of Model Emulsions

The coalescence rate of the model emulsions is determined from the change in mean diameter of the emulsion over time. The mean diameter was found from previously reported drop size distributions of samples taken at 23 ºC from a settled emulsion after 1.5, 4, 8, 16 or 24 hours of aging. The emulsions were prepared with asphaltenes, toluene, *n*-heptane and water. Data and details on emulsion experiments procedures are found elsewhere (Sztukowski 2005). The drop size distributions and mean diameters considered in this study are reported in Table 5.1.

Table 5.1 Mean Drop Diameters for different aging times and emulsion systems (Sztukowski 2005).

Time (hours)	Mean Diameter (μm)		
	0/100 Heptol	25/75 Heptol	50/50 Heptol
	5 kg/m³		
0	5.1	5.1	5.1
1.5	8.90	7.66	6.49
4		11.79	7.19
8	12.79	12.36	7.73
16	14.74	12.87	7.97
24	15.33	12.82	
	10 kg/m³		
0	5.1	5.1	5.1
1.5	9.14	7.22	5.88
4		10.97	6.70
8	14.37	12.67	7.32
16	16.17	11.26	7.55
24	16.48	11.91	
	20 kg/m³		
0	5.1	5.1	5.1
1.5	7.689	6.087	5.547
4		8.190	6.475
8	14.351	13.660	6.865
16	11.214	14.309	7.870
24	18.499	15.369	

For a concentrated emulsion, such as the settled emulsion phase in these experiments, coalescence depends on the rupture frequency of the interface. Deminiere et al. (1998) showed that, for a monodisperse system, the mean diameter changes with time according to:

$$d\left(\frac{1}{R^2}\right) = -\frac{8\pi}{3}\omega.dt \qquad \textbf{Eq. 5.1}$$

where R is the average drop radius, ω is the rupture rate, and t is time. They also observed the same scaling of $1/R^2$ versus t for polydispersed systems. To calculate the emulsion rupture rate, Equation 5.1 can be rearranged as:

$$\omega = -\frac{3}{8\pi}\left(\frac{d\left(1/R^2\right)}{dt}\right)$$

In Deminiere et al.'s work, there were no aging effects and the rupture rate was constant over time. With the asphaltene systems, the interface becomes more rigid with time and the rupture rate is expected to decrease. Therefore, $1/R^2$ was plotted versus time for emulsions prepared from 5, 10 and 20 kg/m³ asphaltenes in toluene, 25/75 heptol, and 50/50 heptol at 23°C, as shown in Figures 5.1a and 5.2a. A best fit was made to the data (i.e., first order exponential decay function) and the fit equation was then differentiated to find the $\frac{d\left(1/R^2\right)}{dt}$ term. Since the drop radius changes with time, the derivative was calculated for each data point. The rupture rate was determined by substituting the derivative value in the above equation.

The rupture rate at any time is shown in Figures 5.1b and 5.2b. In all cases, the calculated rupture rates decreased exponentially to near zero values after approximately 4 to 8 hours. Note that all of the coalescence experiments were conducted prior to any heating and centrifugation and no free water was observed during the experiments.

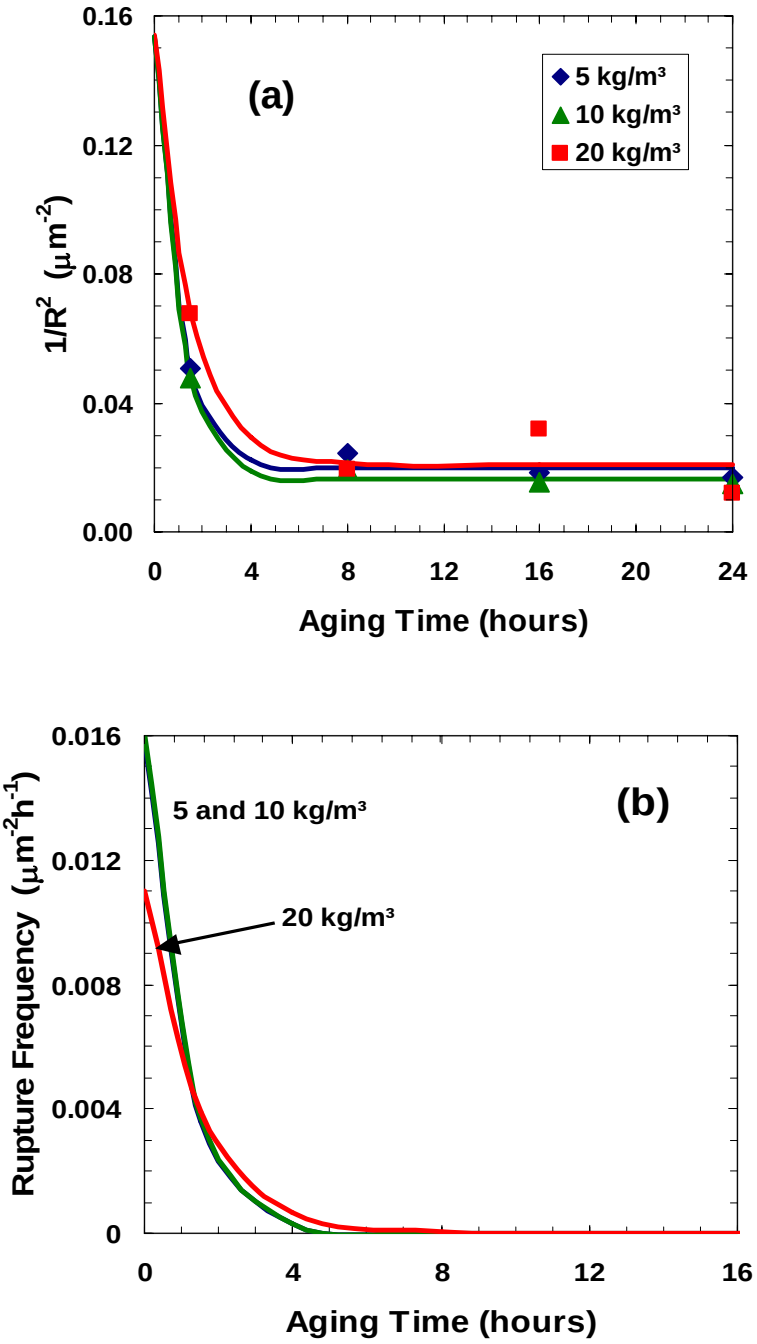

Figure 5.1 Effect of aging time on a) the inverse square of the mean drop diameter and b) the calculated rupture rate for emulsions prepared from water and solutions of asphaltenes in toluene at 23 °C

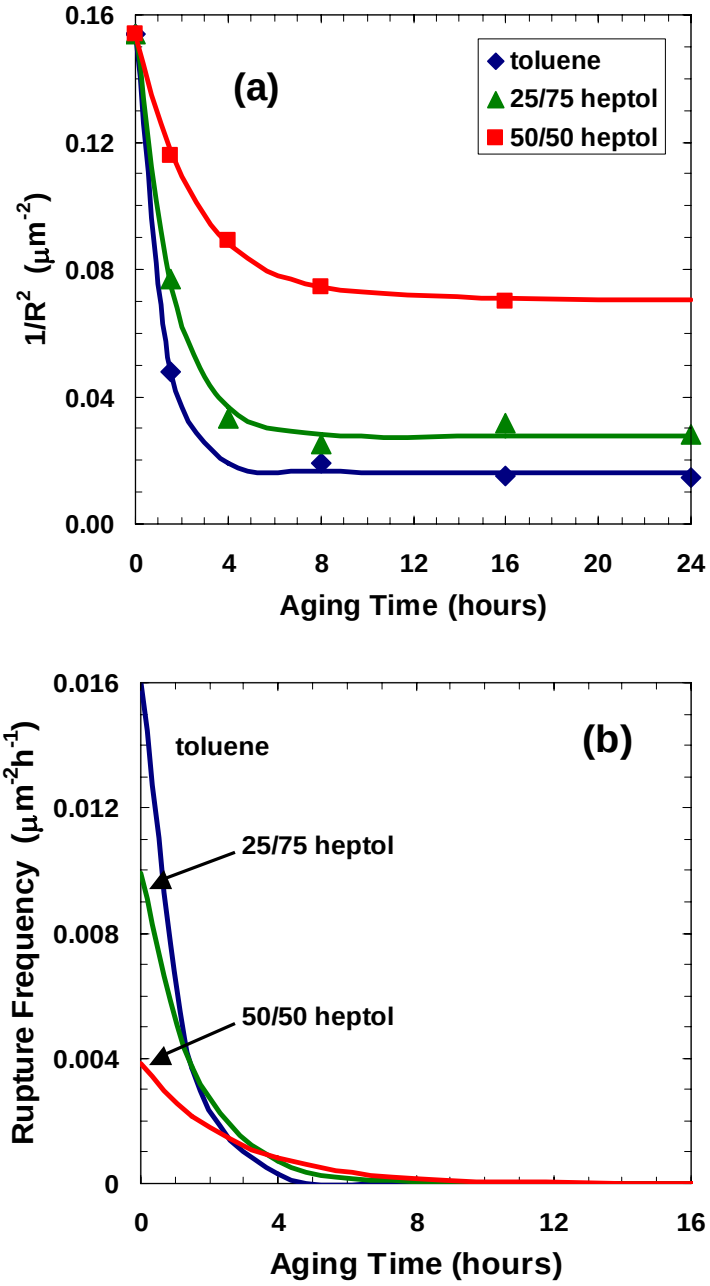

Figure 5.2 Effect of aging time and/or solvent on a) the inverse square of the mean drop diameter and b) rupture rate of emulsions prepared from water and solutions of 10 kg/m³ asphaltenes in heptol at 23 °C.

5.2 Correlation of Coalescence Rate and Interfacial Compressibility

The next step in the prediction was to find a correlation between the experimental coalescence rate and the interfacial compressibility. Recall that, for an emulsion with an irreversibly adsorbed interfacial film, the rupture rate of the settled emulsion depends on the interfacial compressibility. Figure 5.3 shows the initial rupture rate (measured after 1.5 hours of settling) versus the initial interfacial Phase 1 and Phase 2 compressibilities (measured at 60 minutes). The droplet size distributions from which the rupture rates were determined were measured in a previous project and the earliest measurements were taken at 1.5 hours. The compressibility data with the nearest aging time were measured at 60 minutes. The data of Figure 5.3 were then fitted with the following equation:

$$\varpi = 0.0015 \ln(c_I) + 0.0053 \qquad \textbf{Eq. 5.2}$$

where c_I is the interfacial compressibility. The correlation is merely adequate (± 30%) but sufficient to test the hypothesis.

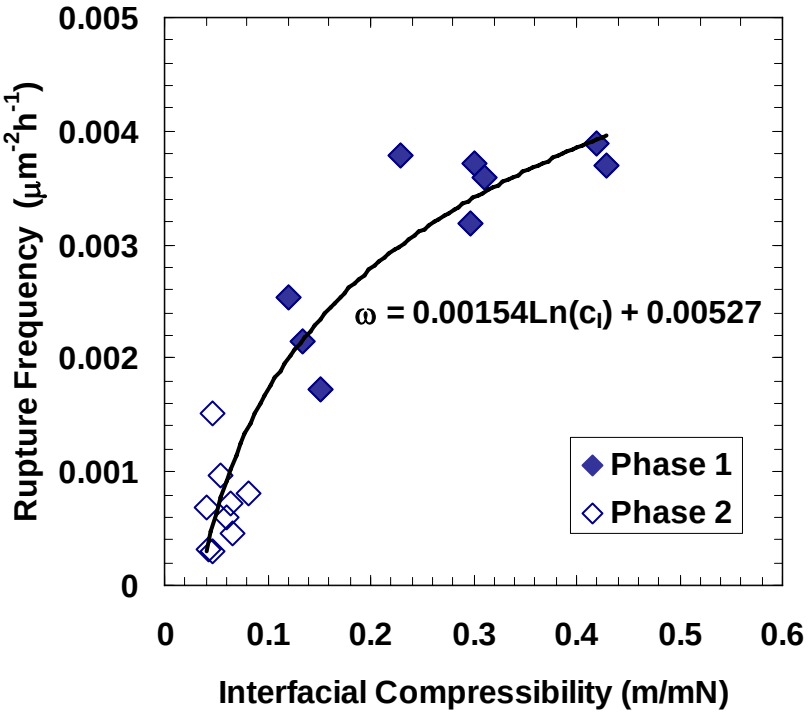

Figure 5.3 Correlation between initial rupture rate (1.5 hours of aging) and initial interfacial compressibility (60 minutes of aging) for 5,10, and 20 kg/m³ asphaltenes in toluene, 25/75 and 50/50 heptol at 23 °C.

5.3 Prediction of Emulsion Coalescence

If we assume that Eq. 5.2 holds at all film ratios and aging times, then the coalescence rate can be predicted with reasonable accuracy as long as the interfacial compressibility can be predicted. To predict the interfacial compressibility of a coalescing emulsion, it is necessary to account for the age of the interface and the film ratio of the interface. To facilitate the calculations, the Phase 1 and Phase 2 compressibilities as well as the film ratios at the phase transition (PR) and crumpling point (CR) were determined from the surface pressure isotherms at different ages (see data in Tables 4.1 to 4.3 in Chapter 4).

The data were plotted versus time and the trends were fitted for each of the systems evaluated in this study. Figures 5.4 and 5.5 show the effect of aging time on both phase transition and crumpling film ratios and the effect of aging time on phase 1 and phase 2 compressibilities, for 20 kg/m³ asphaltenes dissolved in 25/75 heptol at 23 °C.

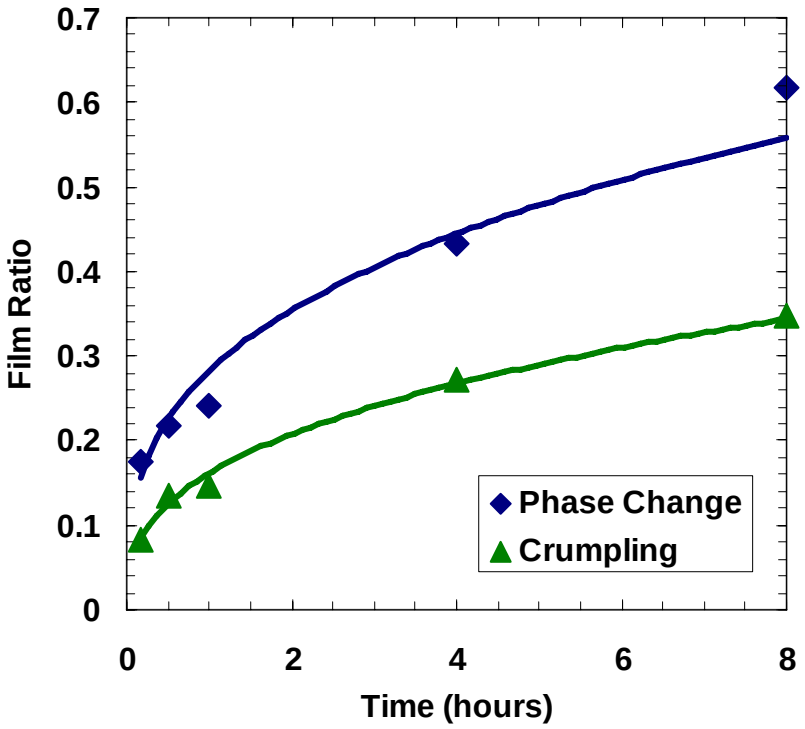

Figure 5.4 Effect of aging time on the phase transition and crumpling film ratios for 20 kg/m³ asphaltenes in 25/75 heptol at 23 °C.

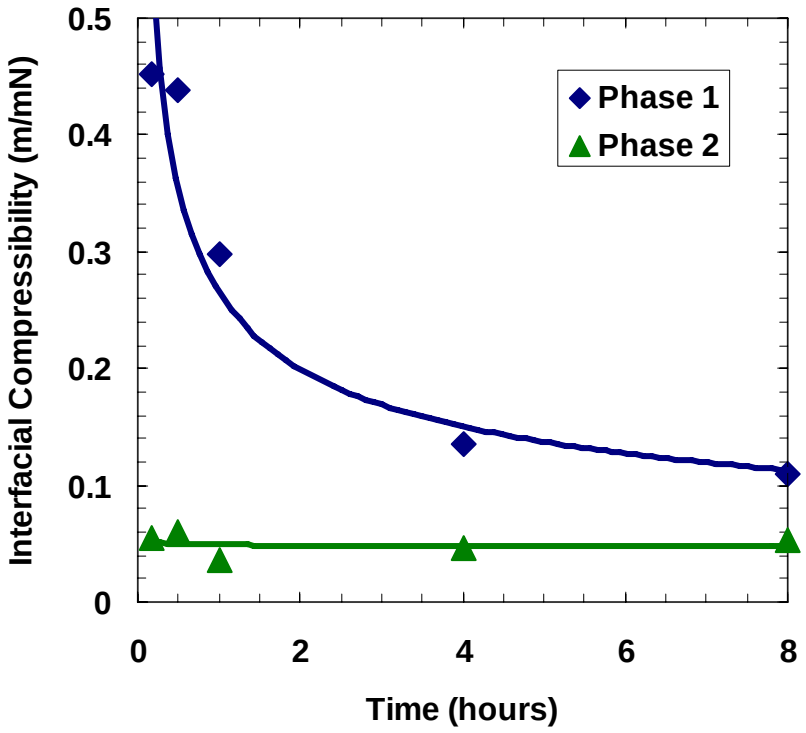

Figure 5.5 Effect of aging time on the Phase 1 and Phase 2 interfacial compressibilities for 20 kg/m³ asphaltenes in 25/75 heptol at 23 °C.

Now, since compressibility depends on the film ratio, which in turn depends on the coalescence rate, a simultaneous solution of compressibility and coalescence rate is required. The prediction method is illustrated conceptually in Figure 5.6. The procedure is outlined below.

Step 1: For any given time. $t_{(n)}$, the phase of the interfacial film is identified using Figure 5.4 and the film ratio at that time, $(A/Ao)_{(n)}$.

Step 2: Once the phase is known, the film compressibility at that time, $c_{I(n)}$, is found from Figure 5.5.

Step 3: The coalescence rate at that time, $\omega_{(n)}$, is then determined from Equation 5.2.

Step 4: The mean drop radius is updated with a rearrangement of Equation 5.1:

$$R_{(n)} = R_{(n-1)} + \left[\frac{1}{\frac{1}{R_{(n-1)}^2} - \frac{8\pi}{3}\omega_{(n)}\Delta t} \right]^{0.5} \qquad \textbf{Eq. 5.3}$$

Step 5: The film ratio is updated. Recall that the total area of the interface of monodisperse droplets is given by:

$$A = \frac{3V}{R} \qquad \textbf{Eq. 5.4}$$

where A is the interfacial area, V is the volume of the dispersed phase, and R is the radius. Hence, the film ratio after some coalescence is given by:

$$\left(\frac{A}{A_o}\right)_{(n)} = \frac{R_o}{R_{(n)}} \qquad \textbf{Eq. 5.5}$$

Step 6: The time is updated using a fixed increment, Δt, typically 0.2 to 0.5 hours. Return to Step 1.

In reality, the droplets are polydisperse and the Sauter mean diameter should be substituted for the mean diameter in Eq. 5.4. However, the droplets were assumed to be monodisperse in the model. Also note that the initial mean radius could not be measured directly but a value of 5 μm was found to provide the best fit of the early time data.

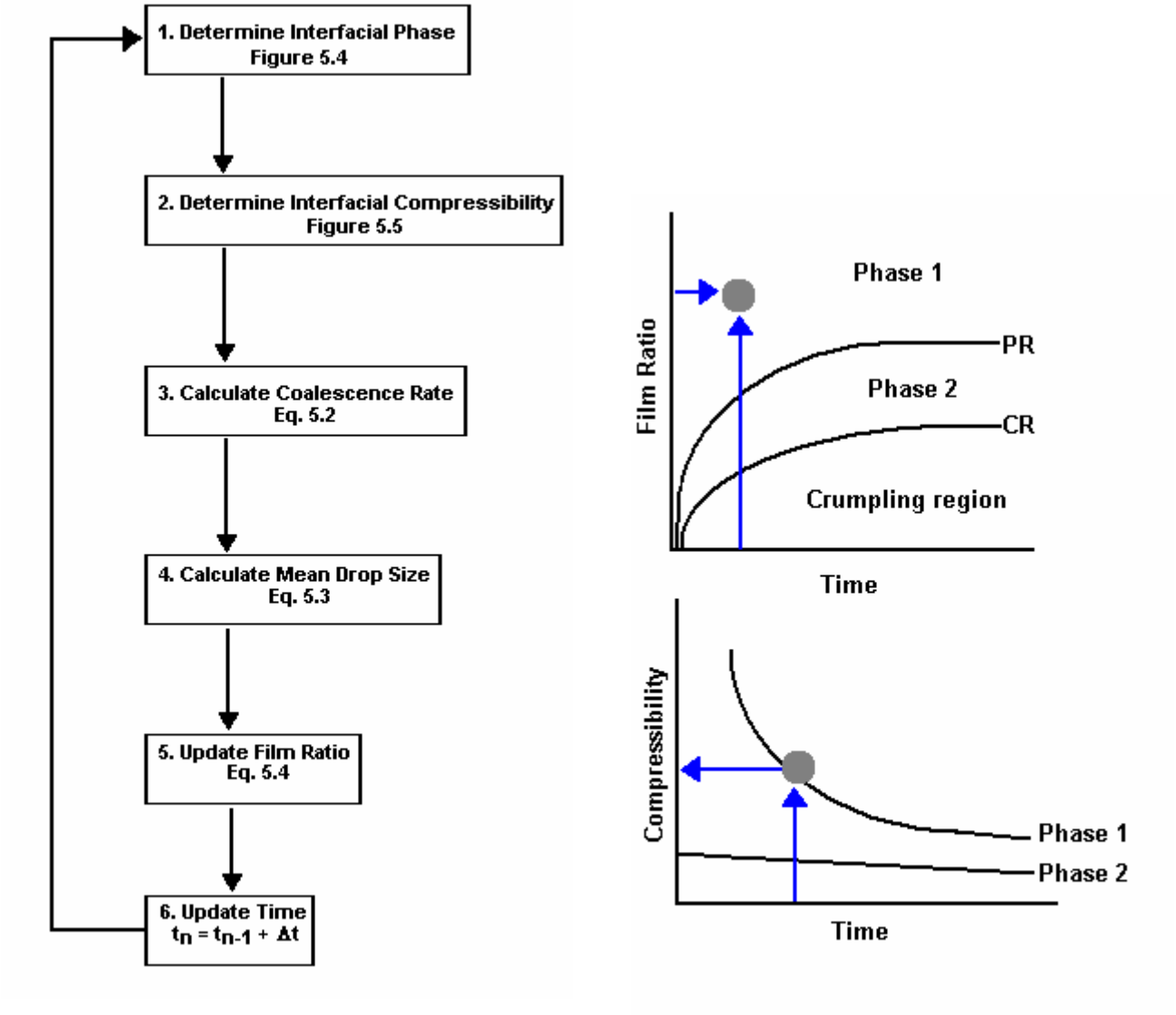

Figure 5.6 Schematic of the procedure to determine the interfacial compressibility and coalescence rate of an emulsion with an irreversibly adsorbed interfacial film.

Figures 5.7 (a) and (b) show the predicted interfacial compressibility and mean drop diameter for an emulsion prepared from water and 20 kg/m³ asphaltenes in 25/75 heptol, respectively. In Figure 5.7 (a), the interfacial compressibility experiences a progressive reduction with time, as the interface ages and undergoes compression. As the time increases, the phase transition is reached and the compressibility drops dramatically. After this stage, a constant low compressibility is observed, corresponding to phase 2 compressibility. In this stage, the film has become very incompressible and coalescence is negligible. Eventually, the crumpling point is reached and the compressibility decreases to zero.

A comparison between the predicted change in mean drop diameter over time and the experimental drop size values is presented in Figure 5.7 (b). The predicted mean diameter is within the experimental error of the measured diameter (approximately ± 2 μm). In the first eight hours, the interfacial film is compressible and a rapid increase in drop diameter is observed with time. At approximately 8 hours, the interface reaches the crumpling point and the curve reaches a plateau region in which the diameter remains unchanged. Therefore, it can be concluded that the emulsion coalesces until the film becomes incompressible.

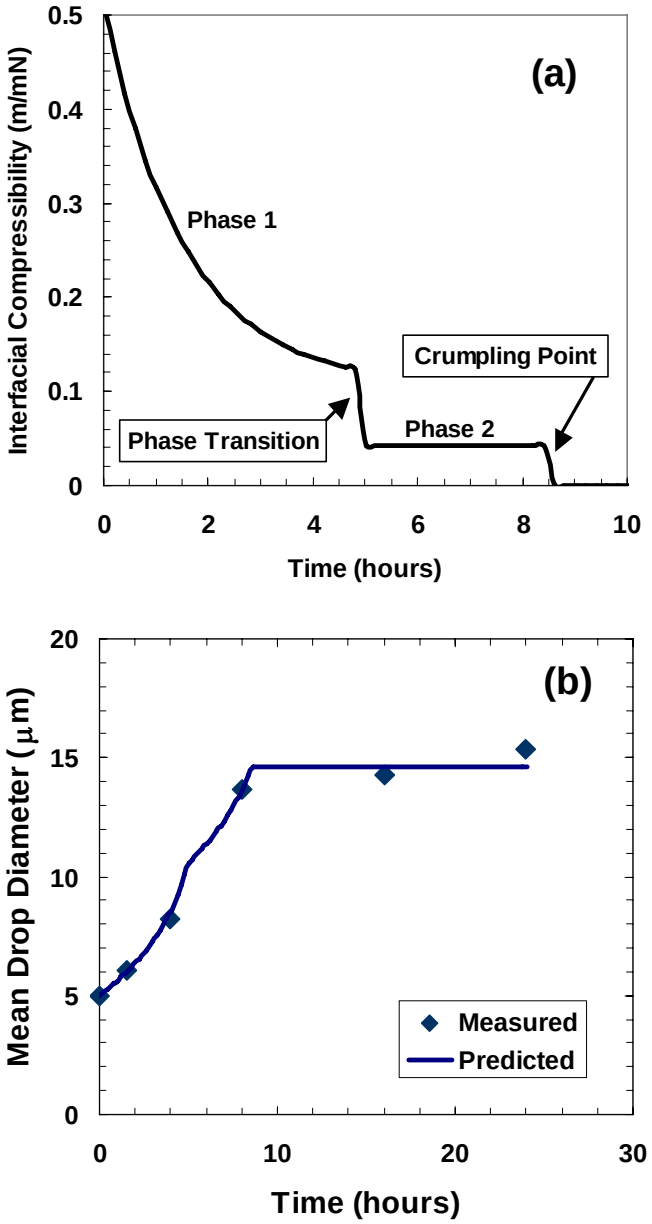

Figure 5.7 Predicted change in interfacial compressibility (a) and mean droplet diameter (b) of a coalescing emulsion prepared from water and a solution of 20 kg/m³ asphaltenes in 25/75 heptol at 23 °C.

The predicted change in mean diameter for emulsions prepared from the different solvents and at asphaltene concentrations of 20, 10, and 5 kg/m³ (Figures 5.8, 5.9, and 5.10, respectively) also matched the measured values within experimental error. Note that the film properties were not measured at 5 kg/m³. The properties measured at 1 and 10 kg/m³ were averaged to model the coalescence rate at 5 kg/m³.

The prediction results show that for all asphaltene concentrations, the transition to a lower compressibility phase occurs more rapidly for 50/50 heptol mixtures as expected with a higher fraction of the poorer solvent. As a result, the mean drop diameter hardly changes with time for 50/50 heptol systems. This result indicates that the well known increase in emulsion stability of water-in-crude oil emulsions with the addition of an aliphatic solvent (Gafonova and Yarranton 2001) is caused by a reduction of the film compressibility.

The film compressibility and emulsion coalescence rates do not vary significantly with the asphaltene concentration. It is likely that the interface is saturated with asphaltenes at concentrations at and above 5 kg/m³, consistent with previous observations (Sztukowski and Yarranton 2005).

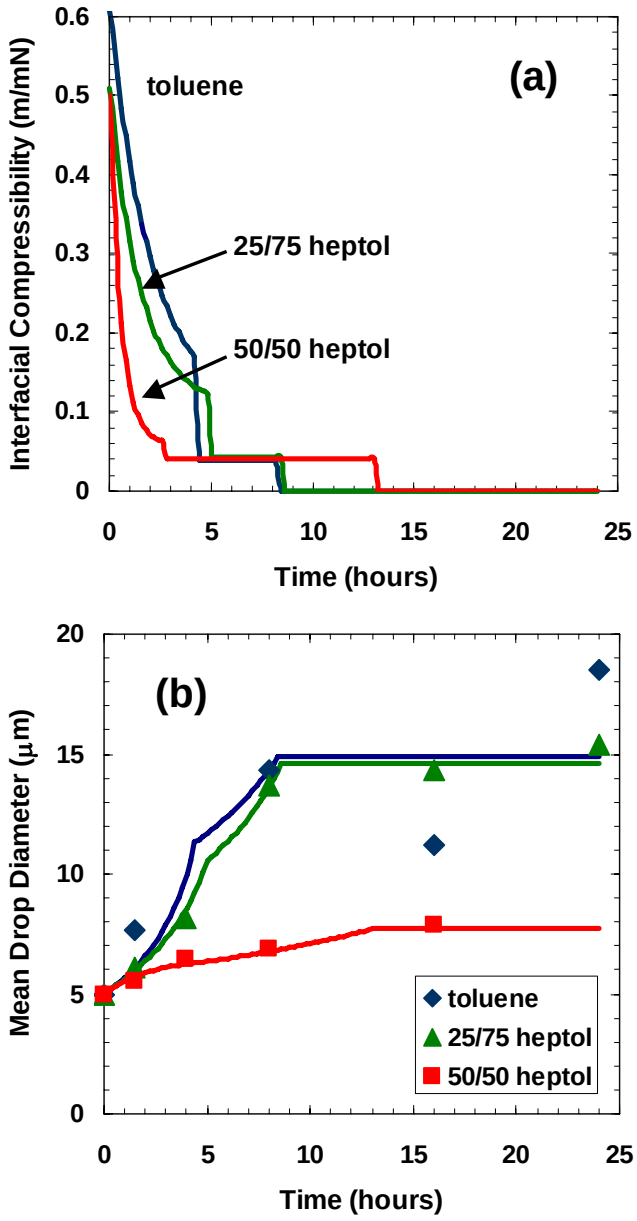

Figure 5.8 Predicted change in interfacial compressibility (a) and mean droplet diameter (b) of a coalescing emulsion prepared from water and a solution of 20 kg/m³ asphaltenes in toluene, 25/75 heptol and 50/50 heptol at 23 °C.

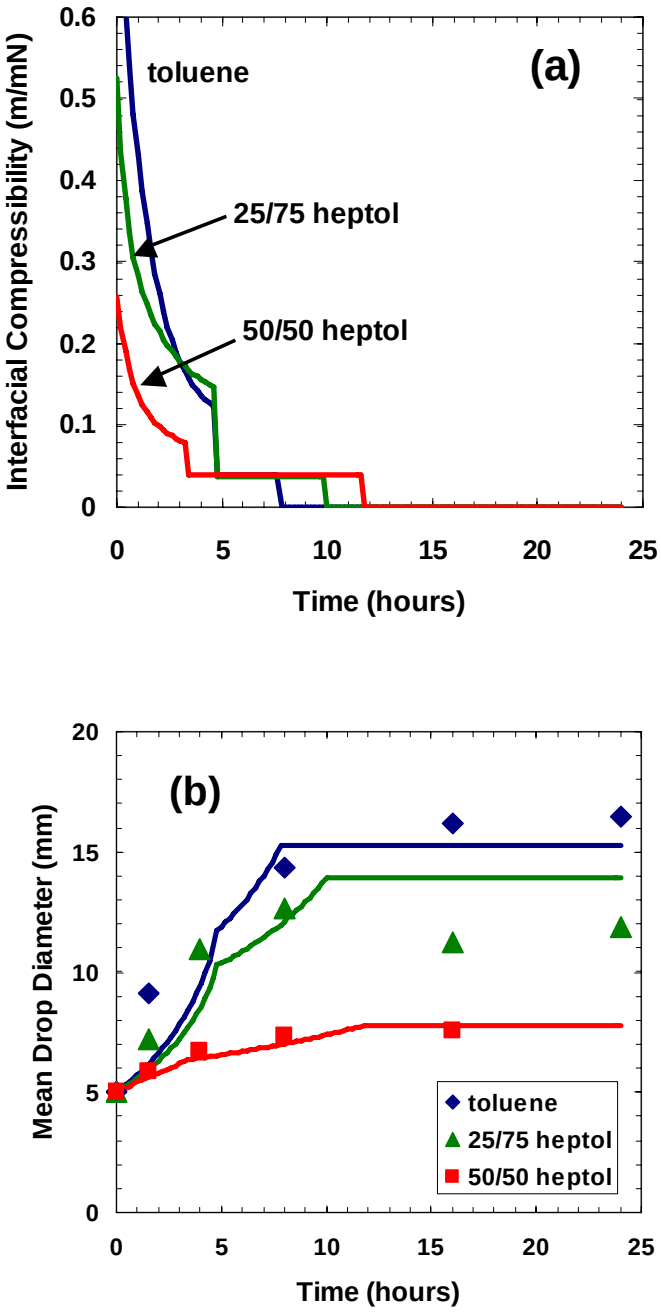

Figure 5.9 Predicted change in interfacial compressibility (a) and mean droplet diameter (b) of a coalescing emulsion prepared from water and a solution of 10 kg/m³ asphaltenes in toluene, 25/75 heptol and 50/50 heptol at 23 °C.

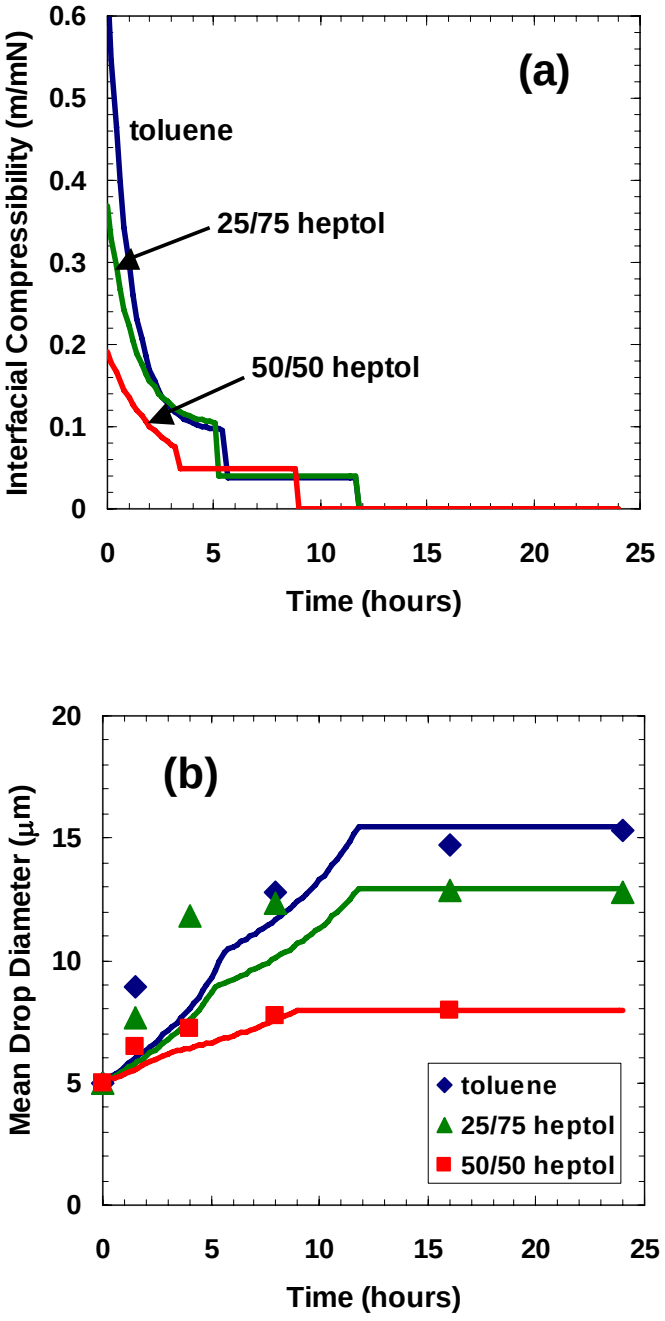

Figure 5.10 Predicted change in interfacial compressibility (a) and mean droplet diameter (b) of a coalescing emulsion prepared from water and a solution of 5 kg/m³ asphaltenes in toluene, 25/75 heptol and 50/50 heptol at 23 °C.

CHAPTER 6- CONCLUSIONS AND RECOMENDATIONS

The main objectives of this work were to investigate the properties of asphaltenic films at the oil-water interface using surface pressure isotherms and to relate emulsion coalescence to film compressibility. The conclusions from this study and recommendations for future work are presented below.

6.1 Thesis Conclusions

Surface Pressure Isotherms

1. Surface pressure isotherms indicated that the compressibility of interfacial films decreased monotonically with a reduction in the area of these films. In most cases, as the interface was compressed, the interfacial film underwent an apparent phase change from a high compressibility phase to a low compressibility phase. The compressibility of the second phase was typically 5 times lower than the first phase. Upon further compression, the interface crumpled; that is, the compressibility was reduced to zero.

2. The change of film compressibility with time is an indication of irreversible asphaltene adsorption at the interface. As the molecules become more tightly packed, the compressibility is reduced until it becomes incompressible and crumples. If the adsorption were reversible, the compressibility would stay constant because the adsorbed molecules would desorb when compressed.

3. The compressibility of the film at any film ratio is reduced as the film ages and as the *n*-heptane fraction in the heptol increases. The decrease in film compressibility upon aging suggests that a cross-linked network of asphaltenes is gradually established on the interface. It is shown that increasing the aliphatic solvents content of the continuous phase increases the film rigidity. Aliphatic solvents are poorer solvents for asphaltenes and therefore the asphaltenes become irreversibly adsorbed more readily in these solvents.

4. Asphaltene temperature has little effect on the compressibility of the films. For all evaluated systems, the phase change film ratio for 23 °C is not significantly different from that at 60 °C. This behaviour is similar to that of a bulk liquid undergoing compression far from the critical point.

5. Surface pressure isotherms did not change significantly at different asphaltene concentrations for all solvent systems and aging times. It appears that at asphaltene concentrations above 1 kg/m^3, the interface is saturated with asphaltene molecules forming interfacial films with similar properties. It was observed that low compressibility films formed more readily at the lowest concentration considered (1 kg/m^3) and less readily at the intermediate concentration of 10 kg/m^3.

Coalescence Prediction from Interfacial Properties

1. It is possible to predict emulsion coalescence from film properties. Emulsion coalescence was assessed from the change of mean drop diameter over time of an emulsion prepared from water and mixtures of asphaltenes and heptol. The change in mean diameter was predicted from the film compressibility which was a function of aging time and the film ratio. A deviation of approximately ± 2 μm was found between the predicted mean diameter and the measured mean diameter.

2. Coalescence rate is reduced by a decrease in the compressibility of the film, as shown by the prediction results. For an irreversibly adsorbed asphaltenic film at the oil-water interface, the compressibility of the film is reduced as the film is compressed. Coalescence decreases the surface area, compressing the film, increasing the resistance to further compression, and therefore inhibiting coalescence.

3. Increased film rigidity and reduced coalescence result in more stable emulsions. Emulsion stability can be explained by means of coalescence behaviour. Coalescence is limited at higher aging times and higher *n*-heptane heptol fractions. At low aging times, there may not be sufficient time for a rigid film to establish itself and the compressibility is high and coalescence is fast. Therefore, emulsions destabilize before the rigid film is formed. At higher *n*-heptane content in the bulk phase, the asphaltenes molecules do not leave the interface as their solubility in the bulk solvent is reduced. Consequently, asphaltenes contribute to

strong network formation on the interface, acting as a mechanical barrier to coalescence and therefore more stable emulsions can be expected.

6.2 Recommendations for Future Work

Although this work provided a better understanding on the formation of asphaltenic interfacial films, their properties and their role in stabilizing emulsions, much information is still unknown. The following are some recommendations for future research in the area of crude oil emulsions:

1. Of interest to emulsion stability is to study the effect of chemical demulsifiers on the interfacial properties of model systems by surface pressure isotherms and to determine their role in destabilizing water-in-oil emulsions. A comparison of the effect of different demulsifiers on interfacial compressibility and emulsion stability considering the effect of changing operational conditions such as temperature, solvent chemistry, aging time and asphaltene concentration, is strongly recommended for industrial applications.

2. This work showed that emulsion coalescence can be predicted from interfacial properties for systems of asphaltenes and heptol mixtures over water. Coalescence prediction models considering demulsifiers performance would be of use in designing effective emulsion treatments for the oil industry.

3. As shown by the literature, resins adsorb at the water/oil interface and interact with asphaltenes, changing the interfacial properties. However, details on how this interfacial interaction occurs remains unclear. Since most crude oils containing asphaltenes also contain resins, it is recommended to investigate the effect of adding resins on film properties as well as in coalescence prediction.

4. So far in this study, surface pressure isotherms were measured for real systems consisting of diluted Athabasca bitumen with heptol mixtures at different ratios. The next step in this investigation is to evaluate interfacial properties and to predict emulsion coalescence for these systems.

5. Finally, only asphaltenes extracted from Athabasca bitumen were examined for this work. In order to generalize the results, it is necessary to investigate other crude oils from various locations.

REFERENCES

Agrawala, M., and Yarranton, H. W. (2001). "An asphaltene association model analogous to linear polymerization." *Industrial & Engineering Chemistry Research*, 40(21), 4664-4672.

Akbarzadeh, K., Ayatollahi, S., Moshfeghian, M., Alboudwarej, H., and Yarranton, H. W. (2004a). "Estimation of SARA fraction properties with the SRK EOS." *Journal Of Canadian Petroleum Technology*, 43(9), 31-39.

Akbarzadeh, K., Dhillon, A., Svrcek, W. Y., and Yarranton, H. W. (2004b). "Methodology for the characterization and modeling of asphaltene precipitation from heavy oils diluted with n-alkanes." *Energy & Fuels*, 18(5), 1434-1441.

Alboudwarej, H., Beck, J., Svrcek, W. Y., Yarranton, H. W., and Akbarzadeh, K. (2002). "Sensitivity of asphaltene properties to separation techniques." *Energy & Fuels*, 16(2), 462-469.

Aske, N., Orr, R., and Sjoblom, J. (2002). "Dilatational elasticity moduli of water-crude oil interfaces using the oscillating pendant drop." *Journal Of Dispersion Science And Technology*, 23(6), 809-825.

Backes, H. M., Ma, J. J., Bender, E., and Maurer, G. (1990). "Interfacial tensions in binary and ternary liquid-liquid systems." *Chemical Engineering Science*, 45(1), 275.

Bauget, F., Langevin, D., and Lenormand, R. (2001). "Dynamic surface properties of asphaltenes and resins at the oil-air interface." *Journal Of Colloid And Interface Science*, 239(2), 501-508.

Deminiere, B., Colin, A., Calderon, F. L., and Bibette, J. (1998). *Modern Aspects of Emulsion Science*, The Royal Society of Chemistry, Cambridge, UK.

Evdokimov, I. N., Eliseev, N. Y., and Akhmetov, B. R. (2003). "Initial stages of asphaltene aggregation in dilute crude oil solutions: studies of viscosity and NMR relaxation." *Fuel*, 82(7), 817-823.

Fan, T., Wang, J., and Buckley, J. S. "Evaluating Crude Oils by SARA Analysis." Tulsa, OK, United States, 883.

Freer, E. M., and Radke, C. J. (2004). "Relaxation of asphaltenes at the toluene/water interface: Diffusion exchange and surface rearrangement." *Journal Of Adhesion*, 80(6), 481-496.

Freer, E. M., Svitova, T., and Radke, C. J. (2003). "The role of interfacial rheology in reservoir mixed wettability." *Journal Of Petroleum Science And Engineering*, 39(1-2), 137-158.

Gafonova, O. V., and Yarranton, H. W. (2001). "The stabilization of water-in-hydrocarbon emulsions by asphaltenes and resins." *Journal Of Colloid And Interface Science*, 241(2), 469-478.

Gray, M. R. (1994). *Upgrading Petroleum Residues and Heavy Oils*, Marcel Dekker, New York.

Heimenz, P. C., and Rajagopalan, R. (1997). *Principles of Colloids and Surface Chemistry*, Marcel Dekker, Inc., New York.

Hepler, L. G. a. H., Chu. (1989). *AOSTRA Technical Handbook on Oil Sands, Bitumens and Heavy Oils*, Alberta Oil Sands Technology and Research Authority, Edmonton, Alberta.

Hiemenz, P. C., and Rajagopalan, R. (1997). *Principles of colloid and surface chemistry*, Marcel Dekker, New York.

Hirasaki, G. J., Miller, C. A., Jiang, T., Moran, K., and Fleury, M. (2006). "Emulsion Stability and Coalescence by NMR Diffusion and Profile Measurements." Oil Sands 2006, Edmonton, Alberta.

Horvath-Szabo, G., Masliyah, J. H., Elliott, J. A. W., Yarranton, H. W., and Czarnecki, J. (2005). "Adsorption isotherms of associating asphaltenes at oil/water interfaces based on the dependence of interfacial tension on solvent activity." *Journal of Colloid and Interface Science*, 283(1), 5-17.

Jafari, M. (2005). "Interfacial Rheology of Asphaltenes in Water-in-Hydrocarbon Emulsions," MSc. Thesis, University of Calgary, Calgary.

Jeribi, M., Almir-Assad, B., Langevin, D., Henaut, I., and Argillier, J. F. (2002). "Adsorption kinetics of asphaltenes at liquid interfaces." *Journal Of Colloid And Interface Science*, 256(2), 268-272.

Jones, T. J., Neustadter, E. L., and Whittingham, K. P. (1978). "Water-In-Crude Oil Emulsion Stability And Emulsion Destabilization By Chemical Demulsifiers." *Journal Of Canadian Petroleum Technology*, 17(2), 100-108.

Kokal, S. (2005). "Crude-oil emulsions: A state-of-the-art review." *Spe Production & Facilities*, 20(1), 5-13.

Kumar, K., Nikolov, A. D., and Wasan, D. T. (2001). "Mechanisms of stabilization of water-in-crude oil emulsions." *Industrial & Engineering Chemistry Research*, 40(14), 3009-3014.

Li, B., and Fu, J. (1992). "Interfacial tensions of two-liquid-phase ternary systems." *Journal of Chemical and Engineering Data*, 37(2), 172-174.

Lyklema, J. (2005). *Fundamentals of Interface and Colloid Science*, Elsevier Ltd.

McLean, J. D., and Kilpatrick, P. K. (1997). "Effects of asphaltene solvency on stability of water-in-crude-oil emulsions." *Journal Of Colloid And Interface Science*, 189(2), 242-253.

Mitchell, D. L., and Speight, J. G. (1973). "Solubility of Asphaltenes in Hydrocarbon Solvents." *Fuel*, 52(2), 149.

Moschopedis, S. E., Fryer, J. F., and Speight, J. G. (1976). "Investigation Of Asphaltene Molecular-Weights." *Fuel*, 55(3), 227-232.

Murgich, J., Abanero, J. A., and Strausz, O. P. (1999). "Molecular recognition in aggregates formed by asphaltene and resin molecules from the Athabasca oil sand." *Energy & Fuels*, 13(2), 278-286.

Nellensteyn, F. J. (1938). *The Science of Petroleum, The Colloidal Structure of Bitumens*, Oxford University Press.

Nordli, K. G., Sjoblom, J., Kizling, J., and Stenius, P. (1991). "Water-In-Crude Oil-Emulsions From The Norwegian Continental-Shelf.4. Monolayer Properties Of The Interfacially Active Crude-Oil Fraction." *Colloids And Surfaces*, 57(1-2), 83-98.

Peramanu, S., Pruden, B. B., and Rahimi, P. (1999). "Molecular weight and specific gravity distributions for athabasca and cold lake bitumens and their saturate, aromatic, resin, and asphaltene fractions." *Industrial & Engineering Chemistry Research*, 38(8), 3121-3130.

Pfeiffer, J. P., and Saal, R. N. J. (1940). "Asphaltic Bitumen as Colloid System." *The Journal of physical chemistry*, 44(2), 139-149.

Rogacheva, O. V., Rimaev, R. N., Gubaidullin, V. Z., and Khakimov, D. K. (1980). "Investigation Of The Surface-Activity Of The Asphaltenes Of Petroleum Residues." *Colloid Journal Of The Ussr*, 42(3), 490-493.

Schramm, L. (1992). *Emulsions. Fundamentals and Applications in the Petroleum Industry*, American Chemical Society, Washington, DC.

Schramm, L. (2005). *Emulsions, Foams, and Suspensions Fundamentals and Applications*, Wiley-VCH Verlag GmbH & Co. KGaA, Weinheim.

Sheu, E. Y., Detar, M. M., Storm, D. A., and Decanio, S. J. (1992). "Aggregation And Kinetics Of Asphaltenes In Organic-Solvents." *Fuel*, 71(3), 299-302.

Speight, J. G. (1978). *Structure of petroleum asphaltenes - current concepts*.

Speight, J. G. (1999). *The chemistry and technology of petroleum*, Marcel Dekker, New York.

Speight, J. G., Wernick, D. L., Gould, K. A., Overfield, R. E., Rao, B. M. L., and Savage, D. W. (1985). "Molecular-Weight And Association Of Asphaltenes - A Critical-Review." *Revue De L Institut Francais Du Petrole*, 40(1), 51-61.

Spiecker, P. M., Gawrys, K. L., and Kilpatrick, P. K. (2003). "Aggregation and solubility behavior of asphaltenes and their subfractions." *Journal Of Colloid And Interface Science*, 267(1), 178-193.

Strausz, O. P., Mojelsky, T. W., and Lown, E. M. (1992). "The Molecular-Structure Of Asphaltene - An Unfolding Story." *Fuel*, 71(12), 1355-1363.

Strausz, O. P., Mojelsky, T. W., Lown, E. M., Kowalewski, I., and Behar, F. (1999). "Structural features of Boscan and Duri asphaltenes." *Energy & Fuels*, 13(2), 228-247.

Sun, T. L., Zhang, L., Wang, Y. Y., Peng, B., Zhao, S., Li, M. Y., and Yu, J. Y. (2003). "Dynamic dilational properties of oil-water interfacial films containing surface active fractions from crude oil." *Journal Of Dispersion Science And Technology*, 24(5), 699-707.

Sztukowski, D. M. (2005). "Asphaltene and Solids-Stabilized Water-in-Oil Emulsions," PhD. Thesis, University of Calgary, Calgary.

Sztukowski, D. M., Jafari, M., Alboudwarej, H., and Yarranton, H. W. (2003). "Asphaltene self-association and water-in-hydrocarbon emulsions." *Journal Of Colloid And Interface Science*, 265(1), 179-186.

Sztukowski, D. M., and Yarranton, H. W. (2005). "Rheology of asphaltene - Toluene/water interfaces." *Langmuir*, 21(25), 11651-11658.

Taylor, S. D., Czarnecki, J., and Masliyah, J. (2002). "Disjoining pressure isotherms of water-in-bitumen emulsion films." *Journal Of Colloid And Interface Science*, 252(1), 149-160.

Taylor, S. E. (1992). "Resolving Crude-Oil Emulsions." *Chemistry & Industry*(20), 770-773.

Ting, P. D., Hirasaki, G. J., and Chapman, W. G. (2003). "Modeling of asphaltene phase behavior with the SAFT equation of state." *Petroleum Science And Technology*, 21(3-4), 647-661.

Wang, J. X., and Buckley, J. S. (2001). "A two-component solubility model of the onset of asphaltene flocculation in crude oils." *Energy & Fuels*, 15(5), 1004-1012.

Weast, R. C. (1984). *CRC Handbook of Chemistry and Physics*, Chemical Rubber CO., Boca Raton, Florida.

Xia, L. X., Lu, S. W., and Cao, G. Y. (2004). "Stability and demulsification of emulsions stabilized by asphaltenes or resins." *Journal Of Colloid And Interface Science*, 271(2), 504-506.

Yarranton, H. W. (2005). "Asphaltene self-association." *Journal Of Dispersion Science And Technology*, 26(1), 5-8.

Yarranton, H. W., Alboudwarej, H., and Jakher, R. (2000a). "Investigation of asphaltene association with vapor pressure osmometry and interfacial tension measurements." *Industrial & Engineering Chemistry Research*, 39(8), 2916-2924.

Yarranton, H. W., Hussein, H., and Masliyah, J. H. (2000b). "Water-in-hydrocarbon emulsions stabilized by asphaltenes at low concentrations." *Journal of Colloid and Interface Science*, 228(1), 52-63.

Yarranton, H. W., and Masliyah, J. H. (1996a). "Gibbs-Langmuir model for interfacial tension of nonideal organic mixtures over water." *Journal of Physical Chemistry*, 100(5), 1786-1792.

Yarranton, H. W., and Masliyah, J. H. (1996b). "Molar mass distribution and solubility modeling of asphaltenes." *Aiche Journal*, 42(12), 3533-3543.

Yarranton, H. W., and Masliyah, J. H. (1997). "Numerical Simulation of Ostwald Ripening in Emulsions." *Journal of Colloid and Interface Science*(196), 157-169.

Yaws, C. L. (1999). *Chemical Properties Handbook*, McGraw-Hill.

Yen, T. F. (1974). "Structure of petroleum asphaltene and its significance." *Energy Sources*, 1(4), 447.

Yeung, A., Dabros, T., Czarnecki, J., and Masliyah, J. (1999). "On the interfacial properties of micrometre-sized water droplets in crude oil." *Proceedings Of The Royal Society Of London Series A-Mathematical Physical And Engineering Sciences*, 455(1990), 3709-3723.

Yeung, A., Dabros, T., and Masliyah, J. (1998). "Does equilibrium interfacial tension depend on method of measurement?" *Journal of Colloid and Interface Science*, 208(1), 241-247.

Zaki, N., Schorling, P. C., and Rahimian, I. (2000). "Effect of asphaltene and resins on the stability of water-in-waxy oil emulsions." *Petroleum Science And Technology*, 18(7-8), 945-963.

Zhang, L. Y., Lawrence, S., Xu, Z. H., and Masliyah, J. H. (2003a). "Studies of Athabasca asphaltene Langmuir films at air-water interface." *Journal Of Colloid And Interface Science*, 264(1), 128-140.

Zhang, L. Y., Lopetinsky, R., Xu, Z. H., and Masliyah, J. H. (2005a). "Asphaltene monolayers at a toluene/water interface." *Energy & Fuels*, 19(4), 1330-1336.

Zhang, L. Y., Xu, Z. H., and Mashyah, J. H. (2003b). "Langmuir and Langmuir-Blodgett films of mixed asphaltene and a demulsifier." *Langmuir*, 19(23), 9730-9741.

Zhang, L. Y., Xu, Z. H., and Masliyah, J. H. (2005b). "Characterization of adsorbed athabasca asphaltene films at solvent-water interfaces using a Langmuir interfacial trough." *Industrial & Engineering Chemistry Research*, 44(5), 1160-1174.

APPENDIX A- DILUTED BITUMEN ISOTHERM RESULTS

This section contains the results of surface pressure isotherms for diluted bitumen systems. The effect of different bitumen to solvent dilution ratios, aging times and solvent mixtures on surface pressure isotherms are shown in the graphs below. The evaluation of the interfacial properties of these systems is recommended as part of the future work.

A.1. Effect of Bitumen Dilution

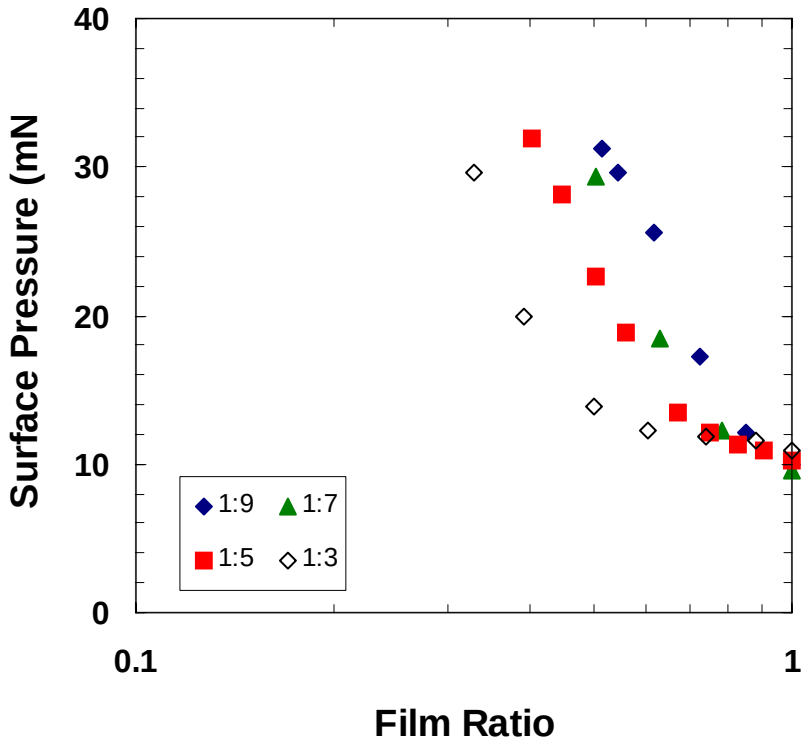

Figure A.1 Effect of bitumen dilution with pure toluene on surface pressure isotherms after 60 minutes of aging time at 23 °C.

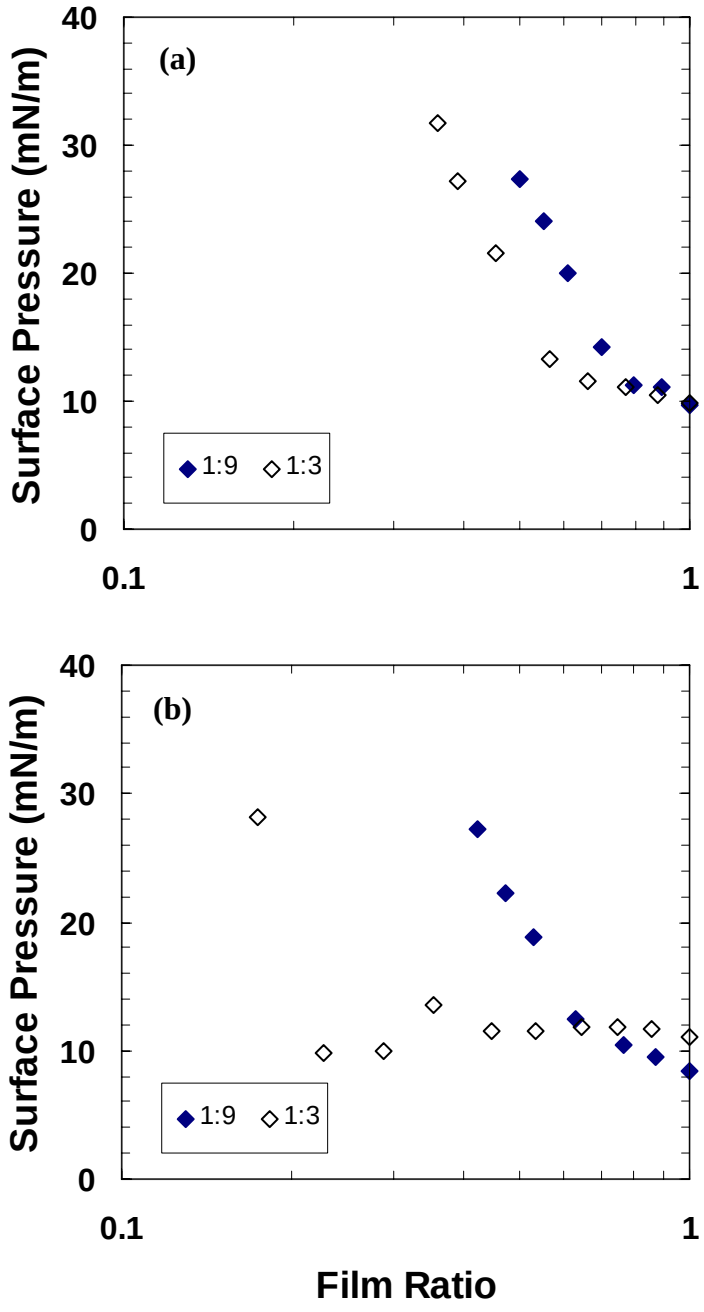

Figure A.2 Effect of dilution on bitumen dissolved with 25/75 heptol on surface pressure isotherms after: (a) 60 minutes and (b) 30 minutes of aging time, at 23 °C.

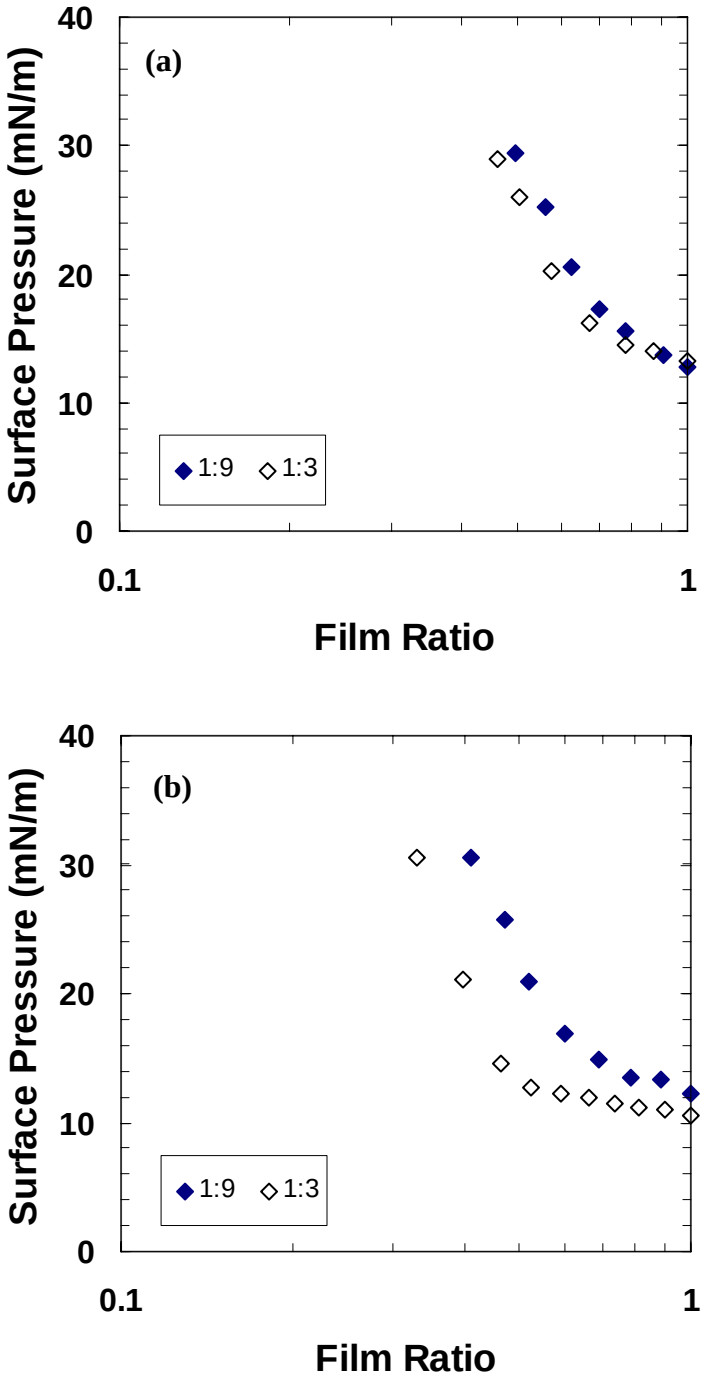

Figure A.3 Effect of dilution on bitumen dissolved with 50/50 heptol on surface pressure isotherms after: (a) 60 minutes and (b) 30 minutes of aging time, at 23 °C.

A.2. Effect of Aging Time

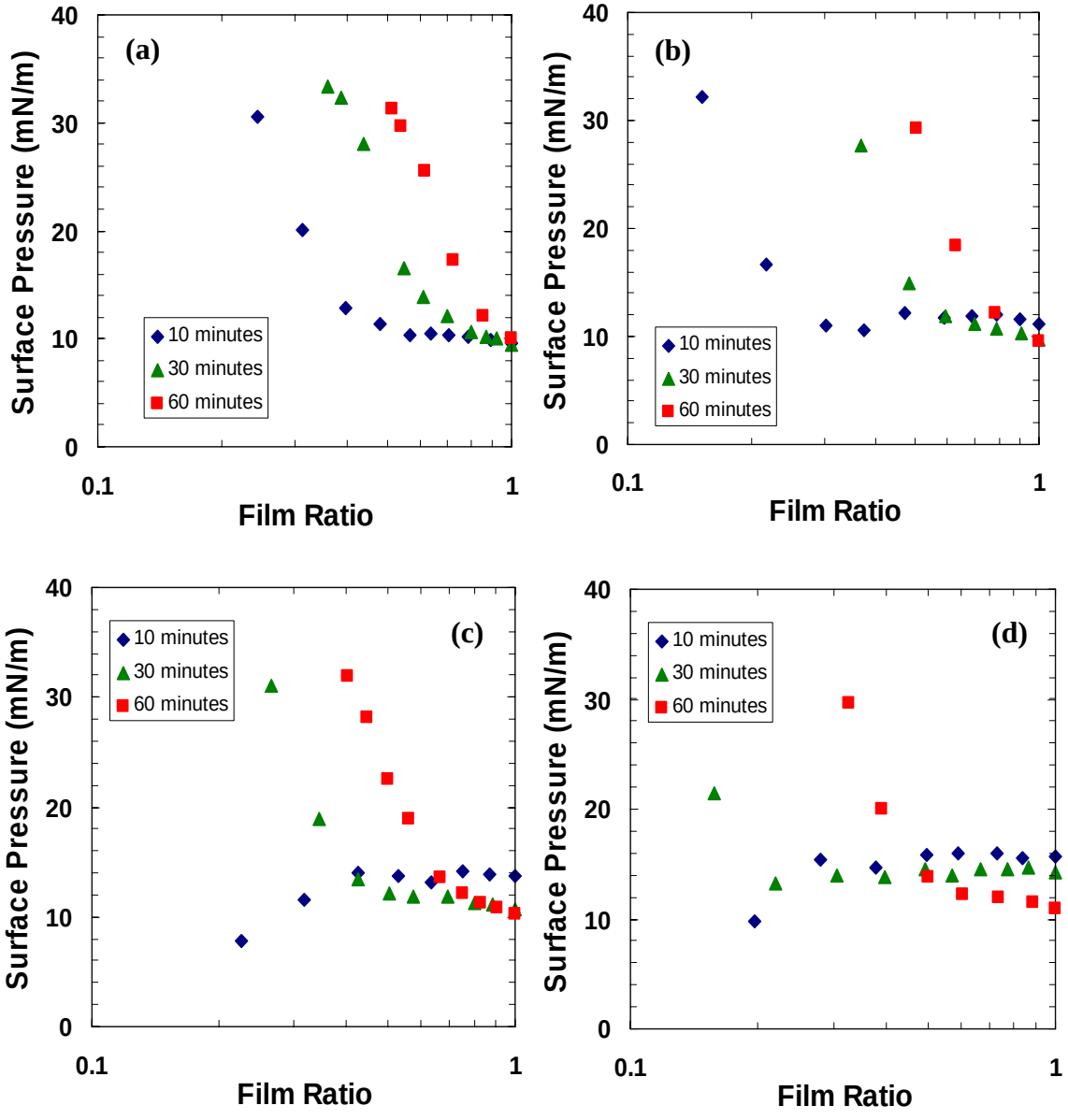

Figure A.4 Effect of aging time on surface pressure isotherms for different bitumen to solvent ratios, dissolved in pure toluene at 23 °C: (a) 1:9, (b) 1:7, (c) 1:5, (d) 1:3.

A.3. Effect of Solvent

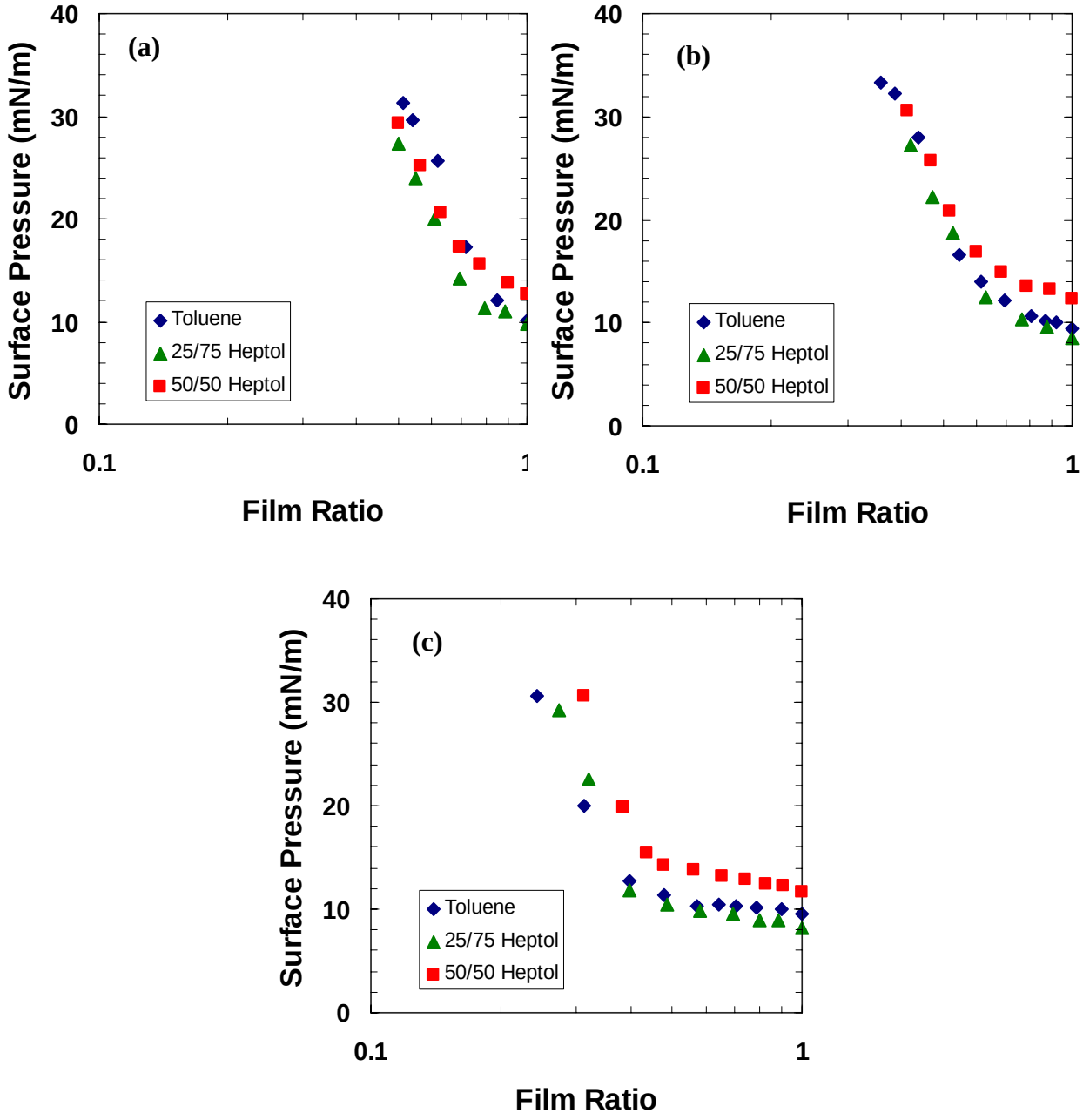

Figure A.5 Effect of solvent on surface pressure isotherms for 1:9 bitumen to solvent ratio at 23 °C, after: (a) 60 minutes, (b) 30 minutes and (c) 10 minutes of aging time.

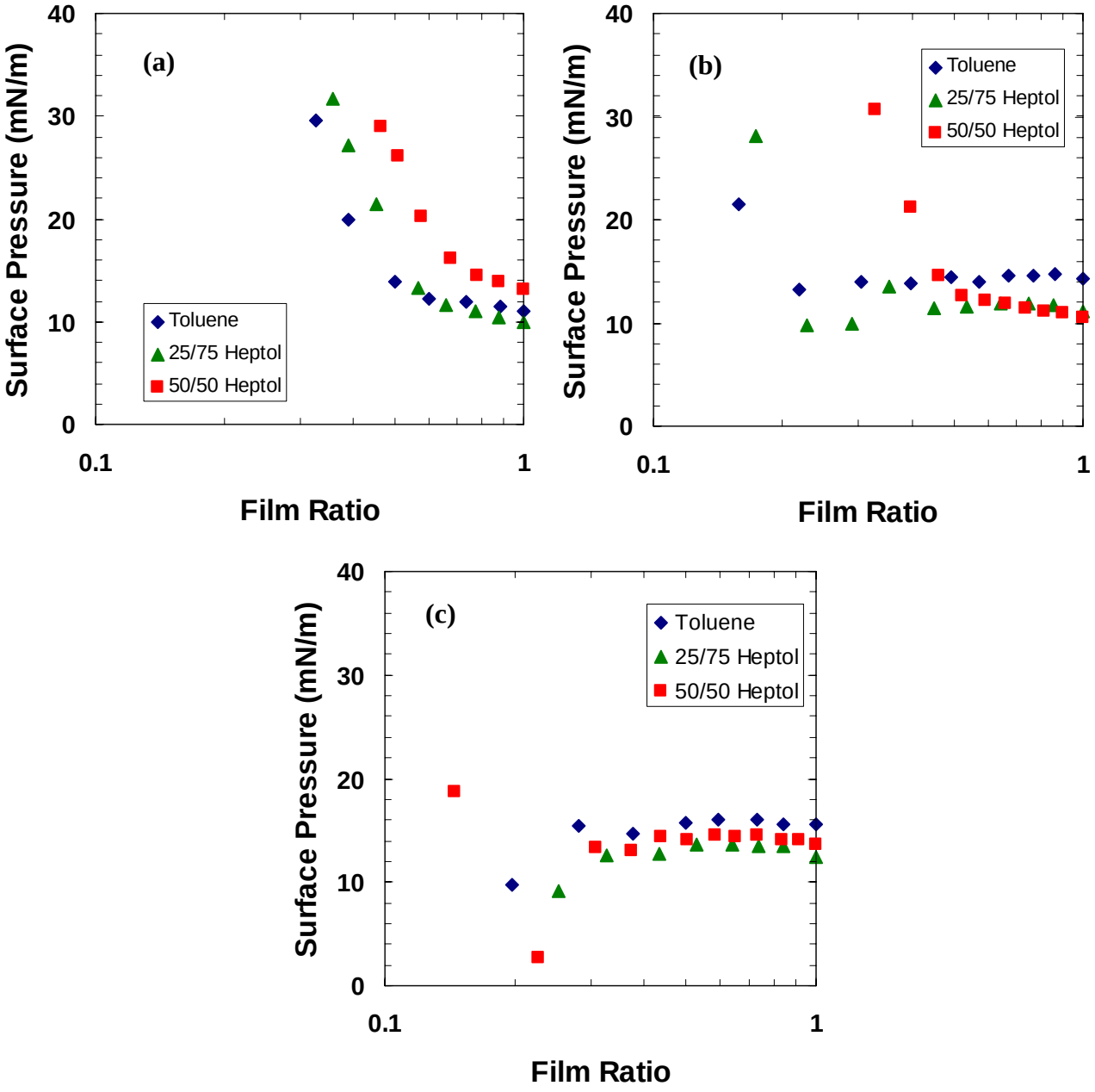

Figure A.6 Effect of solvent on surface pressure isotherms for 1:3 bitumen to solvent ratio at 23 °C, after: (a) 60 minutes, (b) 30 minutes and (c) 10 minutes of aging time.

APPENDIX B- REPRODUCIBILITY ANALYSIS

Reproducibility analyses for phase 1 and phase 2 interfacial compressibilities, phase change film ratio and crumpling film ratio measurements are presented in this appendix. For repeat measurements made at one experimental condition, confidence intervals are established based on the standard deviations of sets of repeated measurements. A 90% confidence interval was used for the assessment of error for all types of experiments.

The mean of several measurements is defined as:

$$\bar{x} = \frac{1}{n}\sum_{i=1}^{n} x_i \qquad \textbf{Eq. B.1}$$

where n is the number of data points, x_i is the measured data point. The standard deviation (s) is given by:

$$s = \sqrt{\left(\frac{1}{n-1}\sum_{i=1}^{n}\left(x_i - \bar{x}\right)^2\right)} \qquad \textbf{Eq. B.2}$$

The statistical distribution used for determining the confidence interval is the t-distribution. The confidence interval is given by:

$$\bar{x} - t_{(\alpha/2,\nu)}\frac{s}{\sqrt{n}} \le \mu \le \bar{x} + t_{(\alpha/2,\nu)}\frac{s}{\sqrt{n}} \qquad \textbf{Eq. B.3}$$

where μ is the correct mean, $n = \nu$-1 and α = 1- (%conf/100). In the current work, a confidence interval of 90% is utilized in all error analyses. Therefore, $\alpha = 0.1$.

B.1. Interfacial Tension

A sample interfacial tension error analysis was conducted by Jafari (2005). An approximately average absolute error of ± 0.6 mN/m was reported.

B.2. Phase 1 Compressibility

Tables B.1, B.2 and B.3 show the reproducibility analyses results for phase 1 compressibility of interfaces consisting of asphaltenes dissolved in pure toluene, 25/75 heptol and 50/50 heptol over water, respectively. Different asphaltene concentrations and aging times were taken into account. According to the results, 20 kg/m^3 asphaltenes in pure toluene and 10 minutes of aging time measurements had the highest absolute error of ± 0.712 m/mN for a confidence interval of 90%. On average, absolute errors of ± 0.246 m/mN, ± 0.073 m/mN and ± 0.071 m/mN were found for pure toluene, 25/75 heptol and 50/50 heptol systems, respectively.

Table B.1 Reproducibility analysis for phase 1 compressibility data in pure toluene with a confidential interval of 90%.

Time (min)	# Data	Mean (m/mN)	Standard deviation	± Error (m/mN)
1 kg/m^3				
30	2	0.249	0.004	0.020
60	2	0.205	0.010	0.046
20 kg/m^3				
10	2	0.542	0.159	0.712
60	2	0.308	0.046	0.207

Average absolute error = ± 0.246 m/mN

Table B.2 Reproducibility analysis for phase 1 compressibility data in 25/75 heptol with a confidential interval of 90%.

Time (min)	# Data	Mean (m/mN)	Standard deviation	± Error (m/mN)
1 kg/m^3				
10	3	0.147	0.016	0.028
30	2	0.135	0.007	0.032
10 kg/m^3				
30	2	0.386	0.014	0.063
60	2	0.293	0.027	0.120
20 kg/m^3				
30	2	0.398	0.083	0.370
60	2	0.292	0.014	0.065

Average absolute error = ± 0.073 m/mN

Table B.3 Reproducibility analysis for phase 1 compressibility data in 50/50 heptol with a confidential interval of 90%.

Time (min)	# Data	Mean (m/mN)	Standard deviation	± Error (m/mN)
1 kg/m^3				
10	2	0.017	0.013	0.060
60	2	0.107	0.0002	0.001
10 kg/m^3				
10	2	0.218	0.012	0.054
60	2	0.135	0.018	0.081
20 kg/m^3				
10	2	0.378	0.034	0.154
60	2	0.135	0.016	0.073

Average absolute error = ± 0.071 m/mN

B.3. Phase 2 Compressibility

The reproducibility analysis results for phase 2 compressibility of interfaces consisting of asphaltenes dissolved in pure toluene, 25/75 heptol and 50/50 heptol over water at different asphaltene concentrations and aging times are summarized in Tables B.4, B.5 and B.6, respectively. For example, the phase 2 compressibility absolute error for 1 kg/m³ asphaltenes dissolved in pure toluene at 30 minutes of aging time is 0.040 ± 0.011 m/mN. On average, absolute errors of ± 0.032 m/mN, ± 0.024 m/mN and ± 0.028 m/mN were found for pure toluene, 25/75 heptol and 50/50 heptol systems, respectively, for a confidence interval of 90%.

Table B.4 Reproducibility analysis for phase 2 compressibility data in pure toluene with a confidential interval of 90%.

Time (min)	# Data	Mean (m/mN)	Standard deviation	± Error (m/mN)
1 kg/m^3				
30	2	0.041	0.002	0.011
60	2	0.040	0.012	0.056
20 kg/m^3				
10	2	0.029	0.016	0.027
60	2	0.070	0.019	0.032

Average absolute error = ± 0.032 m/mN

Table B.5 Reproducibility analysis for phase 2 compressibility data in 25/75 heptol with a confidential interval of 90%.

Time (min)	# Data	Mean (m/mN)	Standard deviation	± Error (m/mN)
1 kg/m^3				
10	3	0.073	0.008	0.014
30	2	0.070	0.004	0.017
10 kg/m^3				
30	2	0.039	0.002	0.007
60	2	0.063	0.0004	0.002
20 kg/m^3				
30	2	0.051	0.012	0.053
60	2	0.043	0.011	0.051

Average absolute error = ± 0.024 m/mN

Table B.6 Reproducibility analysis for phase 2 compressibility data in 50/50 heptol with a confidential interval of 90%.

Time (min)	# Data	Mean (m/mN)	Standard deviation	± Error (m/mN)
1 kg/m^3				
10	2	0.080	0.007	0.031
60	2	0.068	0.0003	0.001
10 kg/m^3				
10	2	0.084	0.014	0.062
60	2	0.068	0.003	0.015
20 kg/m^3				
10	2	0.063	0.004	0.016
60	2	0.068	0.010	0.043

Average absolute error = ± 0.028 m/mN

B.4. Phase Change Film Ratio

The reproducibility analyses for the phase change film ratios of interfaces consisting of asphaltenes dissolved in pure toluene, 25/75 heptol and 50/50 heptol over water at different asphaltene concentrations and aging times are summarized in Tables B.7, B.8 and B.9, respectively, for a confidence interval of 90%. As indicated in Table B.7, for any asphaltene concentration and aging time, the phase change film ratio varies on average by ± 0.077. Similarly, according to Tables B.8 and B.9, the phase change film ratio varies on average by ± 0.075 and ± 0.128, respectively.

Table B.7 Reproducibility analysis for phase change film ratio data in pure toluene with a confidential interval of 90%.

Time (min)	# Data	Mean	Standard deviation	± Error
1 kg/m^3				
30	2	0.225	0.012	0.055
60	2	0.273	0.018	0.081
20 kg/m^3				
10	2	0.212	0.018	0.031
60	2	0.226	0.083	0.140

Average absolute error = ± 0.077

Table B.8 Reproducibility analysis for phase change film ratio data in 25/75 heptol with a confidential interval of 90%.

Time (min)	# Data	Mean	Standard deviation	± Error
1 kg/m^3				
10	3	0.336	0.091	0.154
30	2	0.403	0.010	0.043
10 kg/m^3				
30	2	0.182	0.017	0.076
60	2	0.332	0.006	0.028
20 kg/m^3				
30	2	0.219	0.001	0.006
60	2	0.266	0.032	0.143

Average absolute error = ± 0.075

Table B.9 Reproducibility analysis for phase change film ratio data in 50/50 heptol with a confidential interval of 90%.

Time (min)	# Data	Mean	Standard deviation	± Error
1 kg/m^3				
10	2	0.394	0.017	0.078
60	2	0.528	0.001	0.007
10 kg/m^3				
10	2	0.385	0.032	0.141
60	2	0.543	0.055	0.243
20 kg/m^3				
10	2	0.287	0.008	0.035
60	2	0.499	0.060	0.266

Average absolute error = ± 0.128

B.5. Crumpling Film Ratio

The reproducibility analyses for the crumpling film ratio of interfaces consisting of asphaltenes dissolved in pure toluene, 25/75 heptol and 50/50 heptol over water at different asphaltene concentrations and aging times are shown in Tables B.10, B.11 and B.12, respectively, for a confidence interval of 90%. As indicated in Table B.10, the measured data points varies on average by ± 0.034 for any asphaltene concentration and aging time. The errors are similar for all other solvent systems, and according to Tables B.11 and B.12, the crumpling film ratio error varies on average by ± 0.044 and ± 0.078, respectively.

.

Table B.10 Reproducibility analysis for crumpling film ratio data in pure toluene with a confidential interval of 90%.

Time (min)	# Data	Mean	Standard deviation	± Error
1 kg/m^3				
30	2	0.103	0.001	0.003
60	2	0.134	0.018	0.081
20 kg/m^3				
10	2	0.144	0.030	0.051
60	2	0.077	0.001	0.002

Average absolute error = ± 0.034

Table B.11 Reproducibility analysis for crumpling film ratio data in 25/75 heptol with a confidential interval of 90%.

Time (min)	# Data	Mean	Standard deviation	± Error
1 kg/m^3				
10	3	0.119	0.034	0.057
30	2	0.158	0.002	0.008
10 kg/m^3				
30	2	0.114	0.005	0.021
60	2	0.185	0.011	0.049
20 kg/m^3				
30	2	0.129	0.008	0.036
60	2	0.161	0.021	0.094

Average absolute error = ± 0.044

Table B.12 Reproducibility analysis for crumpling film ratio data in 50/50 heptol with a confidential interval of 90%.

Time (min)	# Data	Mean	Standard deviation	± Error
1 kg/m^3				
10	2	0.100	0.008	0.034
60	2	0.194	0.005	0.021
10 kg/m^3				
10	2	0.152	0.031	0.137
60	2	0.257	0.028	0.125
20 kg/m^3				
10	2	0.144	0.009	0.042
60	2	0.237	0.024	0.107

Average absolute error = ± 0.078